University of Kentucky
UKnowledge

University of Kentucky Doctoral Dissertations

Graduate School

2008

SELECTIVE REGULATION OF CARDIOMYOCYTE SIGNALING BY RGL2

Leah M. Allen
University of Kentucky, lmallen80@gmail.com

Right click to open a feedback form in a new tab to let us know how this document benefits you.

Recommended Citation

Allen, Leah M., "SELECTIVE REGULATION OF CARDIOMYOCYTE SIGNALING BY RGL2" (2008). *University of Kentucky Doctoral Dissertations*. 631.
https://uknowledge.uky.edu/gradschool_diss/631

This Dissertation is brought to you for free and open access by the Graduate School at UKnowledge. It has been accepted for inclusion in University of Kentucky Doctoral Dissertations by an authorized administrator of UKnowledge. For more information, please contact UKnowledge@lsv.uky.edu.

ABSTRACT OF DISSERTATION

Leah M. Allen

The Graduate School

University of Kentucky

2008

SELECTIVE REGULATION OF CARDIOMYOCYTE SIGNALING BY RGL2

ABSTRACT OF DISSERTATION

A dissertation submitted in partial fulfillment of the
requirements for the degree of Doctor of Philosophy in the
College of Pharmacy
at the University of Kentucky

By
Leah M. Allen
Lexington, Kentucky

Director: Dr. Steven R. Post, Associate Professor of Pharmaceutical Sciences

Lexington, Kentucky
2008

Copyright © Leah M. Allen 2008

ABSTRACT OF DISSERTATION

SELECTIVE REGULATION OF CARDIOMYOCYTE SIGNALING BY RGL2

A key cardiovascular signaling molecule involved in both physiologic and pathologic regulation of cardiomyocytes is the small molecular weight G-protein, Ras. Differential effects of Ras are mediated by multiple effector molecules, including the RalGEFs which activate Ral. Studies performed in cardiomyocytes have indicated a role for Ral in cardiac hypertrophic signaling and the RalGEF family member, Rgl2, was shown to specifically interact with Ras in the heart. Therefore, I hypothesized that Rgl2 was an important Ras effector that would regulate cardiomyocyte signaling.

To elucidate the potential importance of Rgl2 in regulating cardiomyocyte signaling, a gain-of-function approach was utilized in which NRVMs were infected with an adenovirus to increase Rgl2 expression. Using this approach, I found that Rgl2 increased Ral-GTP levels, Ras-GTP levels, and PI3-kinase-Akt signaling, but decreased ERK phosphorylation. Overall, my results suggest a model in which Rgl2 disrupts Ras-Raf and Ras-RasGAP interaction to decrease ERK phosphorylation and increase Ras-GTP, respectively. Furthermore, Rgl2-induced Ral activation promotes the enhanced PI3-kinase-Akt signaling. The physiologic consequence of Rgl2 signaling is difficult to predict, but the increase in PI3-kinase-Akt signaling would be expected to promote cardiomyocyte survival and enhance cardiac function, both of which are characteristic of physiologic hypertrophy.

KEYWORDS: Rgl2, Ras, Signal transduction, Cardiomyocyte, Insulin

Leah Allen

7-17-08

SELECTIVE REGULATION OF CARDIOMYOCYTE SIGNALING BY RGL2

By

Leah M. Allen

Dr. Steven Post
Director of Dissertation

Dr. Janice Buss
Director of Graduate Studies

7-17-08

RULES FOR THE USE OF DISSERTATIONS

Unpublished dissertations submitted for the Doctor's degree and deposited in the University of Kentucky Library are as a rule open for inspection, but are to be used only with due regards to the rights of the authors. Bibliographical references may be noted, but quotations or summaries of parts may be published only with the permission of the author, and with the usual scholarly acknowledgments.

Extensive copying or publication of the dissertation in whole or in part also requires the consent of the Dean of the Graduate School of the University of Kentucky.

A library that borrows this dissertation for use by its patron is expected to secure the signature of each user.

Name	Date

DISSERTATION

Leah M. Allen

The Graduate School

University of Kentucky

2008

SELECTIVE REGULATION OF CARDIOMYOCYTE SIGNALING BY RGL2

DISSERTATION

A dissertation submitted in partial fulfillment of the
requirements for the degree of Doctor of Philosophy in the
College of Pharmacy
at the University of Kentucky

By
Leah M. Allen
Lexington, Kentucky

Chair: Dr. Steven R. Post, Associate Professor of Pharmaceutical Sciences

Lexington, Kentucky

2008

Copyright © Leah M. Allen 2008

ACKNOWLEDGEMENTS

Similar to the saying “it takes a village to raise a child”, it takes a community to support, guide, and shape a scientist…

I would like to begin by thanking my mentor, Dr. Steven Post, for his continuous guidance throughout my graduate studies. He has spent countless hours editing my writing and presentations while educating me on the scientific process. Dr. Post has also greatly shaped the scientist that I have become and for that, I am grateful. I would also like to thank the members of my dissertation committee: Dr. Janice Buss, Dr. Ming Gong, and Dr. Todd Porter who have guided my project with their wise insights. Their technical expertise, scientific knowledge, and support has been invaluable. I would also like to thank Dr. Kenneth Campbell for serving as my outside examiner.

I owe Dr. Ginell Post a huge thank you for welcoming me into her lab and giving me such a wonderful experience as an undergraduate. I am certain beyond a doubt that without her support and enthusiasm for research, I would not have come to graduate school. I also wish to thank Ginell Post for her continued support and guidance throughout my graduate studies.

It is my pleasure to thank previous lab members Liquin Du, Dejan Nikolic, and Stuart Rice for setting a superb example with their professionalism and scientific skill. I would like to specifically thank Dejan Nikolic for teaching me many of the common Post lab techniques and for helping me immensely with the immunostaining studies.

I could not have asked for a better group of people to work with than the members of the Post lab that I have had the privilege of knowing in the last couple of years. They have provided a supportive network in which I have gotten the chance to flourish as a scientist. I would like to thank Cecelia Gass not only for her advanced technical expertise, but also for her ability to kindly guide and calm us even at stressful moments when something has gone awry and an experiment seems doomed to fail. It is my pleasure to thank Dr. Brad Blunt for being such a wonderful lab partner. Having another trainee on the Rgl2 project that I could speak with greatly aided in my scientific development. I would like to thank Lindsay Calderon for her friendship and help around the lab. I am confident that a fantastic career awaits this bright, kind-hearted, young lady. I owe Jill Cholewa a thousand “thank you’s” for her help in the lab as well as her friendship. Without Jill’s camaraderie, I never would have completed this journey to my doctorate. She was a bright light in the darkest of times…

Last but not least, I would like to thank my family and friends whose unrelenting support and understanding helped me to complete this process. I would specifically like to thank Alexis Dufilho, Miranda Beam, Jenny Smith, Yolanda Williams, Kedra Cyrus, and Abby Ho whose support was continuous throughout my graduate career. I would be nothing without my family whose encouragement has motivated and strengthened me in all of my endeavors. My father and mother, Tom and Carla Allen, have set an outstanding example with their strong work ethic and morals. I would also like to thank my sister and brother-in-law, Crystal Allen-Daniels and Nathan Daniels, as well as my grandparents (Tom and Ivee Allen as well as Frank and Alice Burks) who help me and inspire me every day. With my family’s love I know that I can do anything.

TABLE OF CONTENTS

ACKNOWLEDGEMENTS……………………..……………………………………..……… iii

LIST OF TABLES……………………………………………..…………...............viii

LIST OF FIGURES……………………………………...…………………............ix

LIST OF FILES……………………………………………..……………................xi

ABBREVIATIONS & DEFINITION OF TERMS……………………………………….…. xii

SECTION I. BACKGROUND AND INTRODUCTION…...……………….......................1

- Cardiovascular Disease and Heart Failure……………………………………..… 1
- Cell Signaling……………………………………………………………………..…. 1
- The Small G-Protein Superfamily ……………………………….........................2
- The Ras Family of Small G-Proteins………………………………………..….. 4
  - Members and Their Functions………………………………..……... 4
  - Ras Activation and Signaling…………………………………..…..... 5
  - Ras Functions in Cardiac Physiology and Pathology…….…………….……7
- Ras Effector Signaling and Functions in the Heart………………………….....9
  - PI3-Kinase-Akt……………………………………………………………....9
  - Raf-MEK-ERK……………………………………………………..….11
  - Ral Guanine Nucleotide Exchange Factors (RalGEFs)……………..……..12
- Ral Activation and Signaling……………………………………..………. 13
- Models for Studying Cardiovascular Signaling…………………..………14
- Statement of the Problem………………………………………..…...15

SECTION II. METHODS……………………………………...............................23

- Reagents and Lysis Buffers ……….. 23
  - Antibodies..23
  - General Chemicals/Reagents.. 23
  - Pharmacological Agents for Cell Treatments...23
  - Tissue Culture... 24
  - Western Blotting Reagents…...…………….. 24
  - Lysis Buffers.……………………………………………………..…. 24
- Primary Myocyte Isolation and Culture……………………………………. 24
- Adenoviral Infection and Agonist Treatment of Cardiomyocytes……………..……25

Ral and Ras Activation Assays………………………………………………..……………. 25
Immunohistochemistry of Adenoviral Infected NRVMs………………….………….. 25
Immunoprecipitation…………………………………………………………..……… 26
Maintenance and Transfection of HEK-293 cells……………………….………26
Immunoblotting…………………………………………………………………..………27
Statistical Analysis………………………………………………………….……...27

SECTION III. RESULTS…………….……………………………………...……….........30
Adenoviral-mediated Expression of Rgl2 in Cardiomyocytes…..……….…………30
AdRgl2 Increases Rgl2 Expression in NRVMs……………………………... 30
Infection Efficiency of NRVMs Infected with AdRgl2……..………………………30
Increased Rgl2 Expression Induces Ral Activation …………………………...31
Effect of Increased Rgl2 Expression on Signaling Cascades in NRVMs................31
Increased Rgl2 Expression Induces Ras Activation…………………………...32
Increasing Rgl2 Expression Decreases ERK1/2 Activation………….……...32
Increased Rgl2 Expression Enhances PI3-kinase-Akt Activity……………….33
Effect of Increased Rgl2 Expression on Ras-induced Signaling Cascades…..…..33
Effect of Rgl2 on Receptor Tyrosine Kinase Signaling in Cardiomyocytes……..... 34
Increasing Rgl2 Expression Alters Insulin-induced Kinase Activation..……. 34
Rgl2 Expression Alters Kinase Activation Induced by Neuregulin-1…......... 36
Rgl2 Enhances Insulin Receptor Activation…...36
Potential Mechanism(s) for Rgl2-dependent Modulation of RTK Signaling in Cardiomyocytes………………………………..…………………………………...37
Crosstalk between ERK and Akt Does Not Account for the Rgl2-mediated Changes in Kinase Activation ……......................................37
Inhibiting Ras Activity Mimics Rgl2-mediated Inhibition of RTK-induced ERK1/2 Phosphorylation in Cardiomyocytes…………………...……38
Activation of Ral Mimics Rgl2-mediated Enhancement of Akt Phosphorylation in HEK-293 Cells…………………………………………........39

SECTION IV. DISCUSSION……………………………………………………………..… 66
Summary...…………….……………………………………………….…………… 74
Limitations…………………………………..……………………………………75
Future Studies………….…………………………………………………………76

SECTION V. REFERENCES……………………........................……….……………….....79
SECTION VI. APPENDIX 1: Protocols………………………………......…………………....90
SECTION VII. VITA..……………… ………………………….…………………...………… 112

LIST OF TABLES

Table 1.1. Small G-protein families..........17
Table 2.1. Antibodies used in the studies..........29

LIST OF FIGURES

Figure.1.1. The small molecular weight G-protein activation cycle……………………..……16

Figure.1.2. G-protein crosstalk. …………………………………………………………...... 18

Figure 1.3. Receptor tyrosine kinase (RTK)-mediated Ras activation..…………….….….. 19

Figure 1.4. Ras-induced activation of effector molecules... 20

Figure 1.5. Ras-mediated activation of PI3-kinase-Akt signaling....................................21

Figure 1.6. Ras-mediated activation of Raf-MEK-ERK signaling....................................22

Figure 2.1. Rgl2 adenoviral vector…………………………………………………………...28

Figure 3.1. Titer-dependent Rgl2 expression in NRVMs. …………………………….…… 41

Figure 3.2. Infection efficiency of AdRgl2 in NRVMs……………………………………… 42

Figure 3.3. Increased Rgl2 expression induces Ral activation. ….………………………. 43

Figure 3.4. Increased Rgl2 expression induces Ras activation....................…………… 44

Figure 3.5. Increased Rgl2 expression inhibits ERK1/2 phosphorylation
in a titer dependent manner………………………………………………….... 45

Figure 3.6. Increased Rgl2 expression enhances PI3-kinase activity………..................46

Figure 3.7. Increased Rgl2 expression enhances Akt activity. …………………………… 47

Figure 3.8. Rgl2 differently regulates Ras-induced signaling. .……………………………. 48

Figure 3.9. Dose-dependence of Rgl2-mediated changes in insulin signaling................ 49

Figure 3.10. Time-dependence of Rgl2-mediated changes in insulin signaling...............50

Figure 3.11. Rgl2 inhibits insulin-induced ERK1/2 phosphorylation…………………….51

Figure 3.12. Rgl2 enhances insulin-induced PI3-kinase activity. …………………………52

Figure 3.13. Rgl2-mediated enhancement of insulin-induced Akt
phosphorylation is PI3-kinase-dependent..…………………………….………53

Figure 3.14. Rgl2 enhances insulin-induced Akt activity. …………………………………54

Figure 3.15. Rgl2-mediated enhancement of insulin-induced GSK3-β
phosphorylation is PI3-kinase-dependent……………………………………..55

Figure 3.16. Rgl2 inhibits neuregulin-induced ERK1/2 phosphorylation..…………………56

Figure 3.17. Rgl2 enhances neuregulin-induced PI3-kinase activity.…...………………… 57

Figure 3.18. Rgl2-mediated enhancement of neuregulin-induced Akt
phosphorylation is PI3-kinase-dependent.……..…..................................... 58

Figure 3.19. Rgl2 Increases IR-β Expression and Activation. ……………….................59

Figure 3.20. Enhanced Akt phosphorylation does not inhibit ERK1/2
phosphorylation in cardiomyocytes..……………………………………………60

Figure 3.21. ERK1/2 inhibition does not enhance Akt phosphorylation in cardiomyocytes……………………………………………………………….. 61

Figure 3.22. Dominant-negative Ras (DNRas) mimics Rgl2-mediated inhibition of ERK1/2..………………………………………………………………62

Figure 3.23. Rgl2-mediated Enhancement of Akt is not dependent on Ras……………..63

Figure 3.24. Rgl2 and Ral have no effect on ERK1/2 phosphorylation in transfected HEK-293 cells……………………………………………………….. 64

Figure 3.25. RalV23 mimics Rgl2-mediated enhancement of insulin-induced Akt phosphorylation in transfected HEK-293 cells……………………………. 65

Figure 4.1. Model of Rgl2-mediated regulation of cardiomyocyte signaling..…………..... 78

LIST OF FILES

Leah_Allen_Dissertation_2008.pdf

ABBREVIATIONS & DEFINITION OF TERMS

AdNull	Empty vector adenoviral control
AdRgl2	Rgl2 adenovirus
CAAX	Lipid binding motif
CDC25	GEF domain for exchanging GDP to GTP on G-proteins
ErbB	Receptor tyrosine kinase activated by Neuregulin
GAP	GTPase Activating Protein
GEF	Guanine nucleotide Exchange Factor
GPCR	G-protein coupled receptor
GSK3-β	Glycogen Synthase Kinase-3β
HA	Hemagglutinin epitope tag (encoded by the virally expressed Rgl2)
HEK-293	Human embryonic kidney-293 cell line
Ins	Insulin
IR	Insulin Receptor (receptor tyrosine kinase)
LY-294002	Pharmacological PI3-kinase inhibitor
NRG	Neuregulin-1
NRVM	Neonatal Rat Ventricular Myocyte
PD-98059	Pharmacological MEK inhibitor
PDK	Phosphoinositide-Dependent Kinase (activates Akt)
PE	Phenylephrine
PI	Phosphoinositide
PIP3	Phosphatidylinositol 3,4,5-P3
PLD	Phospholipase D
pMT2	Transfection vector control
pTyr	Phosphorylated tyrosine residue
RalBP1	Ral Binding Protein-1
RalGEF	Guanine nucleotide Exchange Factor specific for Ral
RalV23	Constitutively active Ral mutant
RasN17 / DNRas	Dominant-negative Ras mutant
RasV12	Constitutively active Ras mutant
RBD	Ras binding domain
Rgl2	RalGEF-like factor-2
RTK	Receptor Tyrosine Kinase

SH2	Src Homology-2 Domain (phospho-tyrosine binding domain)
SH3	Src Homology-3 Domain (bind proline-rich regions)
SOS	Son-Of-Sevenless (a RasGEF)
WGA	Wheat Germ Agglutinin
Wort	Wortmannin (Pharmacological PI3-kinase inhibitor)

Ras Effector Signaling Cascades:

PI3-kinase-Akt-GSK3β

Raf-MEK-ERK

Rgl2-Ral-RalBP1/PLD

SECTION I: BACKGROUND AND INTRODUCTION

Cardiovascular Disease and Heart Failure

Heart failure is a progressive condition in which the heart progressively loses its ability to adequately supply blood to the body. The most recent statistics from 2003 indicate that 5 million Americans are living with heart failure and this value is expected to double by the year 2030 as the “baby boomer” generation ages [1, 2].

Heart failure develops as a result of prolonged stress which can be caused by numerous conditions including myocardial infarction, valve defects, and hypertension [3]. These conditions initially place stress upon the heart which induces adaptive cardiac hypertrophy. However, over time the stress leads to maladaptive hypertrophy, ventricular dilation, and contractile impairments such as systolic dysfunction [2]. Although much effort has been directed toward understanding the mechanism by which heart failure progresses and developing therapeutic approaches to treat and/or prevent heart failure, there still is no cure available. Because of the limitations of current therapies for heart failure, mortality for heart failure patients is extremely rapid with patients only having a 50% chance of surviving 3 to 5 years after diagnosis [1]. Therefore, additional studies are required to increase understanding of the cellular targets and signals involved in the loss of cardiac function observed in heart failure.

Cell Signaling

Signal transduction relates to the study of ligand-receptor interactions at the plasma membrane and the effect of interactions on cell function [4]. The study of signal transduction, therefore, includes examining what is happening at the cell membrane, the consequent changes in the interactions of proteins within the cell, and the relationship between these changes and cell function. Although the origination of this field of investigation may be difficult to define, many agree that the 1950’s heralded the first important signal transduction studies with the discoveries that phosphorylation may alter protein activity and that receptors which are sequestered at the plasma membrane utilize second messengers (cAMP) to transmit signals into the cell [5, 6]. Following those initial findings, signaling has become a well accepted research field and our knowledge of molecular interactions within the cell as well as specific signaling cascades has greatly increased.

In addition to the role intracellular signals play in normal cell physiology, alterations in signaling cascades are associated with the development of human pathologies including cancer and cardiovascular disease. For example, one of the first mutations found in human cancers was in the tyrosine kinase, Src [7]. The discovery of protein mutations associated with pathologies increased interest in the field of signal transduction as a means of understanding the regulation of cellular processes and developing novel therapeutics. Indeed, focus has already been placed on developing agents to modulate the function of enzymes that either activate or inhibit signaling processes (protein kinases and phosphatases).

The future of signal transduction appears very promising as many predict that targeting these signaling cascades with pharmacological agonists and inhibitors will be a common therapeutic approach in coming years [4]. This idea is, I believe, best illustrated with this quote from Tony Hunter, “From a practical standpoint, one can foresee that the accumulating knowledge about signaling networks and the proteins involved will permit development of potent and specific pharmacological modulators of signaling that can be used therapeutically” [8].

The Small G-Protein Superfamily

G-proteins are characterized by their ability to bind and hydrolyze GTP; i.e. they are proteins that contain catalytic domain that binds and hydrolyzes GTP to GDP and P_i. Two distinct classes of G-proteins exist within the cell, heterotrimeric and monomeric (also called small molecular weight) G-proteins. Heterotrimeric G-proteins are comprised of three subunits: alpha, beta, and gamma which are coupled to receptors at the plasma membrane [9]. Unlike their heterotrimeric counterparts, small molecular weight G-proteins are only 20-40 kD in size and are monomers that move freely throughout the cell – although they typically localize to membranes when in their active state [10, 11]. The primary focus of my dissertation will be the small molecular weight G-proteins and their downstream signaling events. Therefore, for simplicity, monomeric G-proteins will be referred to only as G-proteins. When heterotrimeric G-proteins are mentioned, they will be referred to as such.

The different members of the G-protein superfamily are quite diverse in both structure and function [11]. However, due to their common GTPase function, G-proteins are highly homologous to one another in the GTP/GDP interaction domain and the catalytic domain. Their ability to bind GTP and release GDP is the crucial point in their cycle of activation (**Figure 1.1**). Therefore, the GTP/GDP exchange cycle is controlled by guanine nucleotide exchange factors (GEFs; also known as GDS's for guanine nucleotide dissociation stimulators) and GTPase activating proteins (GAPs) which are specific to each G-protein.

Following induction of an upstream stimulus, specific GEFs act to stabilize the G-protein resulting in the dissociation of GDP and subsequent binding of GTP. This GDP/GTP exchange process is the rate limiting step in the G-protein activation cycle (**Figure 1.1**). GTP binding to a G-protein induces a conformational change that allows interaction of effector molecules with the GTP-bound G-protein. Interaction of an effector with the G-protein results in activation of the effector and often promotes the co-localization of the effector with downstream signaling targets at the plasma membrane. Conversely, an inhibitory stimulus will induce the dissociation of the GEF and the association of specific GAPs with the G-protein to accelerate the G-protein's intrinsic GTPase activity (**Figure 1.1**). The hydrolysis of GTP to GDP results in the release of the effector molecule and the G-protein is effectively returned to its basal state [10, 12].

The small G-protein superfamily consists of more than 100 members (isolated from eukaryotes such as yeast and humans) and is subdivided into five families based upon their protein structure. These subfamilies include the Rab, Ran, Ras, Rho, and Sar1/Arf families (**Table 1.1**) [11]. Members of these families have classically been associated with cellular functions. For example, the Rab and Sar1 families have been implicated in regulating vesicular trafficking within the cell [10, 11]. Ras family members are primarily thought to regulate gene expression. The Rho family is involved in mediating cytoskeletal rearrangement. Lastly, Ran family members have been shown to regulate aspects of cellular proliferation [10, 11].

However, it is now clear that there is substantial overlap between the functions of these different families and crosstalk among different G-protein family members as well as their downstream effectors. For example, Ras (which has been primarily associated with regulating gene expression) is now well known to induce activation of another Ras family member, Ral, by interacting with RalGEF's [13, 14]. Similarly, the Ral effector, RalBP1 (also called RLIP76), was found to contain GAP activity for the Rho family members Rac and Cdc42 (**Figure 1.2**) [15-17].

The Ras Family of Small G-Proteins

Members and Their Functions

The Ras subfamily consists of 8 members as well as their isoforms with Ras and Rap being some of the best studied (**Table 1.1**) [11]. Ras was first discovered by Chien et. al. and Shih et. al. in the late 1970's as the rat sarcoma virus oncogenes: HRas and KRas [18, 19]. The majority of Ras family members are expressed homologously in all tissues with the exception of R-Ras and Rab3A which are mostly isolated to nervous tissues [10]. Ras oncogenes were also found in humans and human cancers in the early 1980's with constitutively active, GTPase deficient Ras mutations later discovered in one-third of all human cancers [20-22].

When activated, Ras and Rap are thought to localize primarily to the plasma membrane via a C-terminal, lipid binding CAAX motif. Not only do both Ras and Rap localize to the plasma membrane, but they also share effectors. Ras and Rap bind members of the Ral-GEF family, Raf, and PI3-kinase (to regulate RalGEF-Ral, Raf-MEK-ERK, and PI3-kinase-Akt cascade signaling) [14, 23, 24]. Despite similarities in localization and effector molecule binding, Ras and Rap may perform differential functions as Rap has been shown to antagonize some effects of Ras. For example, Rap decreases Raf-MEK-ERK signaling (whose activation is classically associated with Ras activation) by inhibiting Raf in a variety of cells including 239T cells, NIH3T3 cells, CHO cells, and mouse embryonic fibroblasts [23]. The ability of Rap to inhibit Raf-MEK-ERK signaling is thought to be due, in part, to the fact that Ras and Rap do not co-localize to the same micro-domains of the membrane. Therefore, Rap may sequester effector molecules away from Ras, to cellular domains where they are unable to interact with their substrates.

Ral is quite different from other Ras family proteins with respect to its subcellular localization and its effector molecules. Although RalGEFs are activated by Ras and Ral may localize to the plasma membrane when activated, the bulk of Ral-GTP is located at vesicular membranes within the cell. Ral also interacts with different effectors, of which RalBP1 and phospholipase D (PLD) are the best characterized [25]. Ral shares the common function of regulating gene expression with other members of the Ras family, but is also associated with regulating vesicular trafficking [26].

Ras Activation and Signaling

A wide variety of upstream stimuli can induce Ras activation, but heterotrimeric G-protein coupled receptors (GPCRs) or receptor tyrosine kinases (RTKs) generally initiate Ras activation. In dividing cells, Ras activation is thought to be primarily mediated by RTKs. As illustrated in **Figure 1.3**, RTKs are activated by growth factors such as insulin, epidermal growth factor (EGF), and insulin-like growth factor (IGF). Upon agonist binding, the receptor will either dimerize or go through a conformational change that allows the receptor to autophosphorylate tyrosine residues within its cytoplasmic domain. Phosphorylation of these residues on the RTK activates the receptor and creates docking sites onto which a variety of adaptor proteins may bind the receptor. These adaptor proteins are also phosphorylated on tyrosine residues by the receptor which creates docking sites for RasGEFs. Other molecules containing phospho-tyrosine binding domains (such as Src Homology-2, SH2) may also bind the receptor's phosphorylated tyrosine residues to serve as docking sites for other signaling molecules that are unable to bind the receptor directly. One such protein, Grb2, may directly bind the receptor in this way so that when complexed with SOS (Son-Of-Sevenless, a RasGEF), it may localize SOS with Ras to induce Ras activation [27].

Binding of agonists such as phenylephrine, angiotensin II, and endothelin I to GPCRs causes a conformational change in the receptor that allows it to act as a GEF for specific heterotrimeric G-proteins inducing the exchange of GDP for GTP on the alpha subunit [9]. Binding of GTP induces the dissociation of the alpha subunit from the beta and gamma subunits and allows the binding of effectors with either the alpha subunit or the beta-gamma complex of the heterotrimeric G-protein.

Specific details by which GPCR activation leads to Ras activation continue to be elucidated. However Gutkind, Luttrell, and colleagues have proposed three mechanisms for GPCR-mediated Ras activation – all of which involve signaling through the beta-gamma subunit of the activated heterotrimeric G-protein [27-29]. One model involves GPCR-mediated transactivation of RTKs; binding of a non-receptor tyrosine kinase such as Src to the beta-gamma subunit localizes it to the plasma membrane where Src is able to phosphorylate tyrosine residues within the cytoplasmic domain of RTKs to induce their activation and, thereby, indirectly induce the activation of Ras [30, 31]. The second model involves GPCR mediated activation of the focal adhesion kinase, Pyk2. GPCR stimulated activation of calcium and PKC signaling leads to the recruitment of Pyk2 to the activated integrin receptor where Pyk2 autophosphorylates its own tyrosine residues to create a binding site for the SH2 domain of Grb2/SOS to induce Ras activation [29]. In the last model, long-term activation of GPCRs induces their internalization which leads to activation of Ras molecules located within the cytoplasm [27].

Regardless of the primary stimulus, the crucial component of Ras activation is its localization with Ras-GEFs, the most well-known of which is SOS. SOS was initially discovered in Drosophila melanogaster as the missing link in the activation of Ras by the RTK, Sevenless [32]. Later, two homologs of SOS, SOS1 and SOS2, were found in mammalian cells. SOS is a ubiquitously expressed, 150 kD protein containing a CDC25 domain through which it catalyzes the release of GDP on Ras so that Ras may bind the far more abundant GTP molecules within the cell [33]. However, Ras activation is not the sole function of SOS as it also contains a Rho-GEF domain through which it activates the Rho family member, Rac. Specificity of SOS function is conferred through interactions at its proline-rich C-terminus where SH3 domain containing adaptor proteins interact with SOS and localize it either to Ras or Rac. The adaptor protein, Grb2, is responsible for localizing SOS to Ras containing areas of the plasma membrane, whereas, E3b1 localizes SOS to Rac [34, 35]. However, SOS is found complexed with Grb2 10-times more frequently than it is found bound to E3b1 in unstimulated cells [35]. Therefore, the majority of SOS is sequestered to await signals for Ras, rather than Rac, activation.

More recently, an alternative model of SOS recruitment to the plasma membrane has been proposed by Zhao and colleagues [36, 37]. Unlike the model described above, this model predicts that SOS may be recruited to the membrane without the help of adaptor proteins. Rather, PLD mediated production of phosphatidic acid (PA) creates a docking site for the SOS PH-domain [36]. Once bound to PA, SOS is able to activate Ras as described above.

Binding of GTP induces a conformational change that activates Ras by allowing Ras interaction with a variety of effector molecules, the best characterized of which include: Raf, PI3-kinase, and members of the Ral-GEF family [38]. All of these effectors interact with Ras via a Ras binding domain (RBD) which is thought to bind within the 100 amino acid sequence effector domain [39]. However, point mutations within the Ras effector domain have indicated that each effector interacts at different points within this domain [40, 41].

As detailed above, Ras is classically thought to activate its effectors (immediate downstream interacting molecules) by localizing them to the plasma membrane where the Ras effectors interact with their own effector molecules. However, theories have emerged more recently suggesting that Ras not only localizes the effector to the plasma membrane, but also induces a conformational change in the effector that does one of three things (**Figure 1.4**). The conformational change could open a site in adaptor molecules to allow docking of the adaptor with its own effectors. A conformational change could also occur within the catalytic domain of enzymatic effectors to enable the catalytic domain to modify downstream effectors. Alternatively, Ras binding could remove a regulatory subunit away from the functional part of the protein to remove an inhibitory stimulus on the Ras effector rather than enabling the functional domain of the effector [39].

Like all small G-proteins, Ras inactivation is brought about by its interaction with a specific GAP - the best known is Ras-GAP, a 120kD protein that contains an N-terminus through which it localizes to the membrane via interaction with receptors and phospholipids. Its catalytic domain is located within the C-terminus. The catalytic domain is primarily responsible for stimulating Ras-GTPase activity and, thereby, converting Ras back to its inactive, GDP-bound form [42].

Ras Functions in Cardiac Physiology and Pathology

Extensive *in vitro* as well as *in vivo* research has begun to elucidate Ras functions in both physiological and pathological conditions. Since its discovery as the rat sarcoma virus oncogene, mutated Ras was recognized as a contributor to cancer signaling. Ras was later found to control normal cell growth, proliferation, differentiation, and survival [43]. More recently, Ras has been implicated in cardiac hypertrophic signaling [44]. However, before discussing the role of Ras in hypertrophic signaling, cardiac development and hypertrophy should be reviewed.

The fetal heart develops through both cellular proliferation (increased cell number) and hypertrophy (increased cell size). However, proliferation of the neonatal cardiomyocytes ends shortly after birth – leaving the cells terminally differentiated. The neonatal myocardium is primarily composed of these terminally differentiated myocytes that cannot re-enter the cell cycle. Therefore, hypertrophy is the principal mechanism by which the heart gains mass as it develops into adulthood, at which time, hypertrophy normally halts [45]. However, hypertrophic growth may resume as an adaptive response to compensate for increased workload or stress placed upon the heart. A number of stressors induce cardiomyocyte hypertrophy in the adult including: hypertension (high blood pressure), cardiac valve dysfunction, ischemic events, genetic mutations of the sarcomeric proteins, exercise, and pregnancy [46]. These conditions initially induce compensated or adaptive hypertrophy, collectively termed physiologic hypertrophy, in which heart function is improved. However, over time, many of these conditions will induce decompensated or maladaptive hypertrophy, collectively termed pathologic hypertrophy, which eventually leads to the development of heart failure.

Numerous agonists induce both cardiomyocyte hypertrophy and Ras activation *in vitro* including, angiotensin II, phenylephrine (PE), endothelin I, and growth factors [44]. The involvement of Ras activation in the hypertrophic response is demonstrated by transient transfection of the constitutively active, GTPase deficient, Ras mutant (RasV12) which induces hypertrophic growth and gene expression in NRVMs [47, 48]. PE induced hypertrophic growth of NRVMs was inhibited by transfection or microinjection of the dominant-negative Ras mutant (RasN17) which preferentially binds GDP so that it may not interact with Ras effector molecules, but competitively blocks endogenous Ras interaction with RasGEFs [48]. Taken together, these results give strong evidence for a role of Ras as a mediator of cardiac hypertrophy in cell culture models.

Ras expression has not only been linked to the development of hypertrophic cardiac growth, but has also been linked to the development of pathologic hypertrophy and heart failure. For example, transgenic mice expressing RasV12 in the myocardium develop an extensive hypertrophic phenotype that is lethal due to a defect in sarcomeric calcium handling [49]. Ras expression is also increased in rat hearts subjected to pressure overload and Ras expression levels are also increased with increasing severity of hypertrophic cardiomyopathy in humans [50, 51]. Thus, data from both animal and cell models demonstrate that Ras is a critical mediator of cardiomyocyte hypertrophy.

Although Ras has been linked to pathologic hypertrophy, several Ras effectors have been implicated in contributing to the development of physiologic hypertrophy – namely Raf-MEK-ERK and PI3-kinase-Akt signaling. Therefore, it is important to understand the signaling mechanisms downstream of Ras and how they, as well as Ras, are regulated in order to understand how Ras signaling switches from inducing cardioprotection to inducing cardiac pathology.

Ras Effector Signaling and Functions in the Heart

PI3-Kinase-Akt

PI3-kinases are a group of ubiquitously expressed kinases that phosphorylate phosphoinositides (PI) at the D3 position of the inositol ring. They are categorized into three separate classes dependent upon the substrates that they act upon and their subunit composition. However, only the class I PI3-kinases have been identified as Ras effectors [52, 53]. Class I PI3-kinases are comprised of a 50 to 100 kD regulatory subunit and an approximately 100 kD catalytic subunit. This class of PI3-kinases is further subdivided by their association with different receptor families into class IA and IB – Class IA is activated by Ras and RTKs while class IB is activated by Ras and GPCRs. This difference in receptor coupling is due to differences in their subunit composition.

Class IA PI3-kinases contain one of the following regulatory subunits: p85 (the most well-known), p55α, p50α, p85β, and p55γ. The regulatory subunit is thought to be responsible for localizing PI3-kinase molecules to the membrane since it contains Src homology-2 domains (SH2), Src homology-3 domains (SH3), and proline-rich domains. SH2 domains directly interact with phosphorylated tyrosine residues on active RTKs and/or their tyrosine phosphorylated substrates. SH3 domains bind proline-rich regions of proteins such as Shc. Proline-rich domains interact with other SH3 containing molecules such as Grb2 and Src [52, 53]. Class I PI3-kinases also contain one of three p110 catalytic subunit isoforms (α, β, or δ) which contain a RBD for interaction with Ras. Conversely, class IB PI3-kinases are composed of the p101 regulatory subunit and a p110γ catalytic subunit that also contains a RBD. In contrast to the class IA regulatory subunits that are able to bind RTKs, p101 contains a heterotrimeric G-protein βγ-subunit binding domain.

Membrane translocation alone appears to be sufficient to induce PI3-kinase activity as the PI3-kinase substrates PI4-P and PI(4,5)P_2 are located at the plasma membrane. This is demonstrated by the ability of membrane targeted PI3-kinase mutants to induce formation of D3 phosphorylated phosphoinositides [54]. Upon translocation to the plasma membrane, PI3-kinase acts on PI4-P and its preferred substrate, PI(4,5)P_2, by phosphorylating the D3 position of each phospholipid to form PI(3,4)P_2 and PI(3,4,5)P_3, respectively.

The best known consequence of PI3-kinase mediated formation of phosphoinositides is the activation of Akt, also known as protein kinase B (PKB). Formation of PI(3,4)P_2 and PI(3,4,5)P_3 allows translocation of the PH domain containing proteins: Akt and phosphoinositide-dependent kinase isoforms (PDK1 and PDK2). Although there is still some controversy surrounding the specific mechanism by which Akt is activated, the leading theory is that colocalization of Akt and PDK2 allows PDK2 to phosphorylate Akt at the Ser473 residue within its C-terminus. This allows PDK1 access to the second phosphorylation site of Akt, Thr308, which is located within its activation loop [55, 56]. Alternative theories about the mechanism by which Akt is phosphorylated at Ser473 include an autophosphorylation event and phosphorylation by other molecules such as PDK1. Regardless, phosphorylation at both the Ser473 and Thr308 site is required for full Akt activation. Once activated, Akt phosphorylates a variety of substrates including GSK3-β, mTOR, and Bad to regulate cellular processes such as metabolism, protein synthesis, and protection from apoptosis [56].

PI3-kinase and Akt have been implicated in the regulation of cardioprotective signaling events because of their ability to promote cardiomyocyte survival and to preserve cardiomyocyte function (**Figure 1.5**). The PI3-kinase-Akt cascade protects from cardiomyocyte death by activating anti-apoptotic signaling cascades as well as inhibiting pro-apoptotic signaling cascades [56]. An example of PI3-kinase-Akt-mediated preservation of cardiomyocyte function is the involvement of PI3-kinase-Akt signaling in the development of physiological hypertrophy [56]. Numerous studies have investigated the functions of PI3-kinase signaling in the myocardium. For example, transgenic mice specifically expressing constitutively active p110α in the heart developed physiologic hypertrophy with improved cardiac function up to one year of age [46, 57]. Furthermore, transgenic mice expressing an inactive, dominant negative, mutant of p110α had blunted cardiac growth during normal development and after exercise [46, 58]. Although unable to develop physiological hypertrophy, these mice were still responsive to pressure overload-induced pathological hypertrophy and their hearts displayed increased dysfunction compared to control. Taken together, these studies indicate that PI3-kinase has a protective effect in the myocardium by participating in signaling that induces physiological cardiac growth and protects from dysfunction associated with pathological stimuli.

Three Akt isoforms have been identified to date; however, only Akt1 and Akt2 are highly expressed in the heart [46]. Although Akt is generally thought to be involved in cardioprotective signaling, recent studies in transgenic mouse models have given evidence for diverse functions of the Akt isoforms. For example, Akt2 is now considered to be a key regulator of glucose homeostasis [59], whereas, Akt1 is thought to have a greater role in the regulation of growth signals and the induction of physiological cardiac hypertrophy [46]. This is evidenced by the fact that Akt1-null mice have decreased body size with a parallel decrease in heart size [60]. Akt1-null mice are also unresponsive to exercise-induced hypertrophy [61]. Conversely, constitutively active Akt1 was found to induce physiological hypertrophy with 2 weeks of expression. However, after 6 weeks, it caused pathological hypertrophy [62]. Thus, the cardioprotective effect of Akt is dependent upon the length of activation (with acute, rather than stable, activity inducing cardioprotection) and may be isoform specific.

Raf-MEK-ERK

In 1993, many research groups identified the serine kinase, Raf, as the first Ras effector molecule [38]. Raf activation is dependent on RBD-mediated interaction with Ras so that Raf may be localized to the plasma membrane [63]. However, membrane localization alone is not sufficient to induce Raf activation as Raf contains a cysteine-rich domain (CRD) that must also interact with Ras to induce a conformational change in Raf that allows its activation by removing CRD-induced inhibition of the catalytic domain [63, 64]. In this way, Ras binding localizes Raf with kinases capable of phosphorylating it and induces a conformational change in Raf that exposes its phosphorylation sites so that Raf may become fully activated. Phosphorylation of one or more residues within the Raf activation loop is thought to be another requirement for its activation. However, the specific Raf phosphorylation sites required for full activation have not yet been elucidated [65, 66]. Activated Raf may then interact with and activate effectors such as MEK (mitogen activated protein kinase/ERK kinase).

The best characterized effect of Raf is initiation of the Raf-MEK-ERK signaling cascade. Once active, Raf induces activation of the serine/threonine kinases, MEK1/2 (also called MKK1/2), by phosphorylating two serine residues on each isoform [43, 64]. Active MEK1/2 then functions to activate the serine/threonine kinase ERK1/2 (also referred to as MAPK1/2 and p44/42) by phosphorylating a threonine residue as well as a tyrosine residue on ERK1/2 (**Figure 1.6**).

Although five ERK1/2 isoforms have been identified to date (ERK1-5); the 44kD, ERK1, and the 42kD, ERK2, remain the best studied. This is due, in part, to ERK1/2 being the first isoforms discovered and also because ERK1/2 are the most highly expressed isoforms in most tissues [67]. Once activated, ERK1/2 phosphorylates a wide variety of substrates including protein kinases, transcription factors, and other signaling proteins to regulate many aspects of cellular physiology including protein synthesis and cell survival [68, 69].

Multiple transgenic mouse models have been developed to study the role of Raf-MEK-ERK signaling in the development of cardiac hypertrophy and these studies have given strong evidence for a key role of the Raf-MEK-ERK cascade in mediating myocardial protection. The first indication that Raf-MEK-ERK signaling was involved in the development of cardiac hypertrophy occurred in 2003 when Bueno et. al. discovered that mice specifically expressing constitutively active MEK in the myocardium developed stable physiological hypertrophy up to 12 months of age [70]. Although transgenic mice expressing a dominant inhibitory mutant of Raf displayed no increased heart size in responsive to pressure-overload (used to induce pathological hypertrophy), 35% of the transgenics died within 1 week following the induction of pressure-overload by transverse aortic constriction due to increased cardiomyocyte apoptosis [64, 71]. No wild-type littermates died in the study. Therefore, Raf signaling is cardioprotective as it protects from cell death due to apoptosis and promotes cardiac function through the development of physiologic hypertrophy.

Another transgenic mouse model with decreased Raf activation in the heart was developed by Yamaguchi et. al. in 2004 [72]. In this model, the Raf gene was specifically disrupted in cardiac tissues and caused mice to develop contractile dysfunction by 10 weeks of age with a parallel development of left ventricular dilation [72]. Furthermore, Yamaguchi's group also found that the mice had increased cardiomyocyte apoptosis at 3-5 weeks of age. Cumulatively, these studies give strong evidence for the role of Raf-MEK-ERK signaling in cardioprotection by preventing apoptotic cardiomyocyte death and by preserving cardiac function under conditions of stress.

Ral Guanine Nucleotide Exchange Factors (RalGEFs)

The RalGEF family is composed of 4 members: Ral-GDP dissociation stimulator (RalGDS), RalGEF-like-1 (Rgl1), Rgl2 (also called Rlf), and Rgl3 (also termed Rgr) [13]. RalGEFs are best known as Ral activators because of their ability to stimulate guanine nucleotide exchange on Ral. RalGDS was the first RalGEF discovered to interact with both Ras and Rap [38, 73]. Further examination of Ras-RalGDS interaction showed that RalGDS only interacts with GTP bound Ras and that the Ras binding domain of RalGDS (RalGDS-RBD) was shown to compete with Raf for Ras binding. Combined, these data gave evidence for RalGDS as a Ras effector molecule. After RalGDS was established as a Ras effector, other RalGEF family members, Rgl1 and Rgl2/Rlf, were soon identified as Ras effectors [38, 74, 75].

As with Raf, interaction with Ras translocates RalGEFs to the plasma membrane where they then interact with their effector, Ral. This was demonstrated by showing that a Rgl2 mutant lacking the RBD, but containing a sequence that targets it to the membrane (CAAX) is able to activate Ral [76]. Similarly, cells expressing a constitutively active Ras mutant have been shown to induce RalGDS translocation to the plasma membrane [74].

RalGEFs contain two functional domains of interest, a Ras binding domain (RBD) and a CDC25-like domain. Like all Ras effectors, RalGEFs interact with Ras and Rap through the RBD. The CDC25-like domain mediates Ral activation. Although all RalGEF family members are able to interact with Ras and to induce Ral activation, there is considerable diversity within the family. For example, Rgl1 only shares approximately 50% homology with RalGDS, Rgl3 is 40% identical to RalGDS, and Rgl2 shares even less homology with RalGDS (approximately 30%) [13]. Therefore, there is the potential that RalGEFs may have other, unique functions. Unlike the other Ras effectors that were discussed earlier, little is known about the role of RalGEF signaling in the heart. The little that is known is dependent upon Ral activation and is discussed further in the "Ral Activation and Signaling" section.

Not all RalGEF function is necessarily dependent on Ral activation as demonstrated by Wolthuis et. al. [76]. When constitutively active Rlf/Rgl2 was transfected into A14 cells, Rgl2 induced activation of the c-fos promoter. However, constitutively active, GTPase deficient Ral (RalV23) did not mimic Rgl2-induced c-fos promoter activation indicating that Rgl2 and its family members may have effectors other than Ral.

Ral Activation and Signaling

Ral is a ubiquitously expressed member of the Ras family of small G-proteins [77]. Two Ral isoforms have been identified, RalA and RalB, which share 85% sequence homology. Similar to Ras, Ral activation is induced by a variety of agonists (including GPCR and RTK ligands) and is active when bound to GTP [13]. Ral is translocated to either the plasma membrane or vesicular membranes where it is activated by a family of guanine nucleotide exchange factors (RalGEFs) that promote its exchange of GDP for GTP [14].

Little is known about Ral-mediated signal transduction or the physiological consequences of its activation. However, the discovery of two Ral effector molecules, Ral Binding Protein-1 (RalBP1) and phospholipase-D (PLD) has given some insight into the potential functions of Ral in signal transduction [77, 78]. RalBP1 has GAP activity for Cdc42 and Rac, G-proteins involved in mediating cytoskeletal rearrangements [17]. Therefore, Ral may negatively regulate these G-proteins to regulate the cytoskeleton [17]. PLD activation has been linked to pro-survival signaling (anti-apoptotic effects and activation of Akt); thus, Ral-mediated activation of PLD could lead to protection from apoptosis [79]. PLD has also been implicated in mediating both endocytosis and exocytosis in many cell types and Ral activation is necessary for exocytosis of the synaptic vesicle in neuronal cells [26, 80, 81]. Together, these results support a role for Ral in regulating cell survival and vesicular trafficking.

A potential role for RalGDS and Ral-GTP in the myocardium was provided by Kawai et. al. in 2003 [82]. In this study, transfection of cardiomyocytes with constitutively active Ral (RalV23) induced hypertrophy and increased sarcomeric actin organization. In addition, stimulation of cardiomyocytes with the hypertrophic agonist, cardiotrophin-1, increased levels of RalGDS mRNA and Ral-GTP in non-transfected cardiomyocytes. In addition, we have previously shown that the hypertrophic agonist, phenylephrine, increases Ral-GTP levels in NRVMs [83]. Together, these *in vitro* data indicate that increased RalGDS and Ral activation might be involved in the hypertrophic response. This notion was supported by the observation that Ral activation was increased in an *in vivo* model of pressure-overload hypertrophy [82]. No studies have examined the signaling pathways activated by these changes in RalGDS expression and RalGDS-Ral activation in cardiomyocytes. Therefore, further studies need to investigate how RalGEFs and Ral alter cardiomyocyte signaling as well as the physiological consequences of their action.

Models for Studying Cardiovascular Signaling

Three different systems have been used to study the myocardium; whole animals, isolated hearts, and cultured cells. Animal studies have the advantage of providing a more complete picture of the integrated functional consequences induced by signaling changes. However, it is difficult to precisely control important environmental factors and dissociate primary from secondary effects in animals. Isolated hearts can be used to provide important information regarding cardiac function. However, there is no way to determine which cells are inducing the functional changes in isolated hearts (i.e. the myocytes themselves or factors from fibroblasts altering myocyte activity). Isolated cardiomyocytes offer many advantages to the aforementioned models because they can be used to elucidate signaling changes within a specific cell type and the extracellular environment of isolated/cultured cardiomyocytes can easily be manipulated by simply changing components of the media [84]. In addition, cardiomyocytes can be transiently transfected or virally infected to alter expression of specific signaling components. For these reasons, cultured cardiac cells were used to study Rgl2 signal transduction in my studies.

The use of cultured cardiac cells was first documented approximately 50 years ago [85]. Since then, many groups have worked to develop the conditions necessary to maintain these cells in culture; thereby, creating the classic model for studying cardiomyocyte signaling (primary neonatal rat ventricular myocyte isolates; NRVMs) [84]. Widely utilized for the last 25 years, NRVMs are a trusted model for studying a host of cardiac characteristics including electrophysiology, signaling, and metabolism [84]. In addition, NRVMs survive in culture for extended periods (weeks) which is sufficient time for studies involving cell transfection/infection. Therefore, NRVMs were used throughout my studies.

Statement of the Problem

Rgl2 is a member of the RalGEF family of Ras effector molecules and was the only member identified to specifically interact with Ras in the heart using a yeast two-hybrid approach [83]. Ras is a key component of cardiovascular signaling because of its involvement in both protective and detrimental signaling in cardiomyocytes in response to cardiac stress [44]. However, the factors that determine which signals will be activated by Ras remain poorly understood.

RalGEFs function to increase Ral activation by stimulating its exchange of GDP for GTP. Although not well studied in the myocardium, RalGEF and Ral activation have been implicated in the development of cardiac hypertrophy [82]. In addition, previous studies have shown that Rgl2 regulates the hypertrophic gene program in cardiomyocytes [83]. However, the consequence of Rgl2 activation on cardiac hypertrophic signaling has not been studied. **Therefore, I hypothesized that Rgl2 is an important Ras effector in the heart that will positively regulate hypertrophic signaling pathways in cardiomyocytes.**

Copyright © Leah M. Allen 2008

Figure 1.1

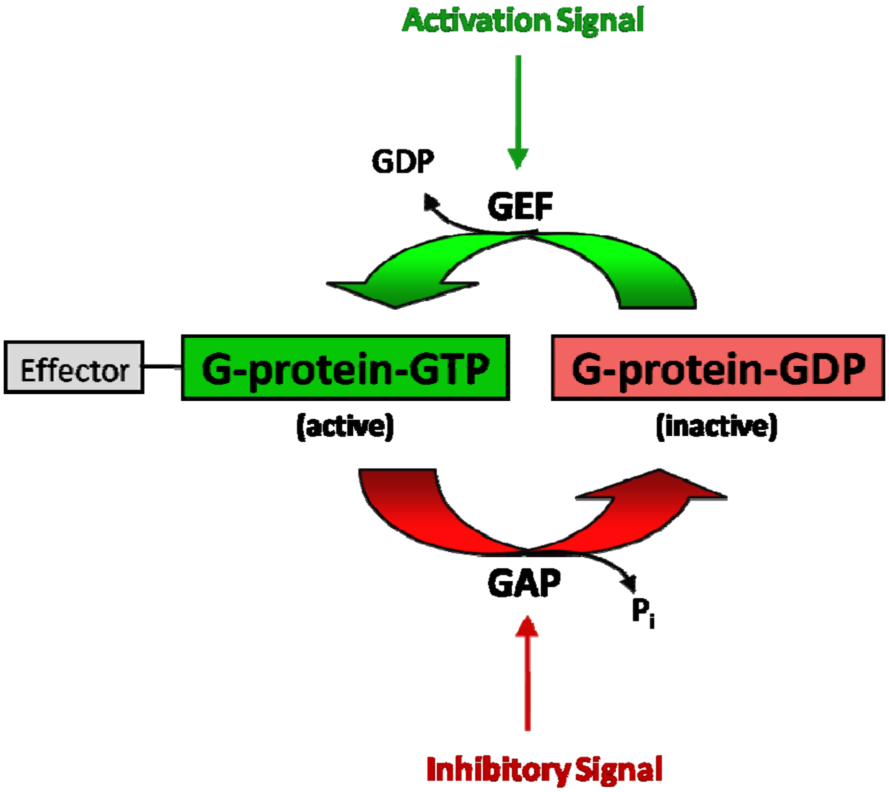
Activation Signal
GDP
GEF
Effector
G-protein-GTP
(active)
G-protein-GDP
(inactive)
GAP
P_i
Inhibitory Signal

The small molecular weight G-protein activation cycle. This figure represents a general representation of the small G-protein activation/inhibition cycle. An upstream stimulus induces G-protein activation by causing a specific GEF for the G-protein to stimulate guanine nucleotide exchange on the G-protein. Once in its active, GTP bound form, the G-protein binds to effector molecules to induce signaling within the cell. The G-protein is then deactivated by a specific GAP which stimulates hydrolysis of the bound GTP and returns the G-protein to its inactive, GDP bound state.

Table 1.1. **Small G-protein families.**

Rab Family		***Ran Family***	***Ras Family***	***Rho Family***	***Sar1/Arf Family***
Rab1A/b	Rab23	Ran	H-Ras	RhoA-E	Arf1
Rab2	Rab24	Gsp1	K-Ras	Rnd3/Rho8	Arf2
Rab3A-D	Rab25	Gsp2	N-Ras	RhoG	Arf3
Rab4	Rab26		R-Ras	RhoH/TTF	Arf4
Rab5A-C	Rab27A/B		M-Ras	Rac1	Arf5
Rab6	Rab28		RalA/B	Rac2	Arf6
Rab7	Rab29		Rap1A/B	Rac3	Sar1a/b
Rab8	Rab30		Rap2A/B	Cdc42	Arl1
Rab9	Rab31		Tc21	Rnd1/Rho6	Arl2
Rab10	Rab32		Rit	Rho1	Arl3
Rab 11A/B	Rab33A/B		Rin	Rho2	Arl4
Rab12	Ypt1		Rad	Rho3	Arl5
Rab13	Sec4		Kir/Gem	Rho4	Arl6
Rab14	Ypt31/Ypt8		Rheb	Yns0	Arl7
Rab15	Ypt32/Ypt9		κB-Ras1		Ard1
Rab16	Ypt51/Vps21		κB-Ras2		Cin4
Rab17	Ypt52		Ras1		
Rab18	Ypt53		Ras2		
Rab19	Ypt6		Rsr1		
Rab20	Ypt7		Yct7		
Rab21	Ypt10				
Rab22	Ypt11				

Figure 1.2

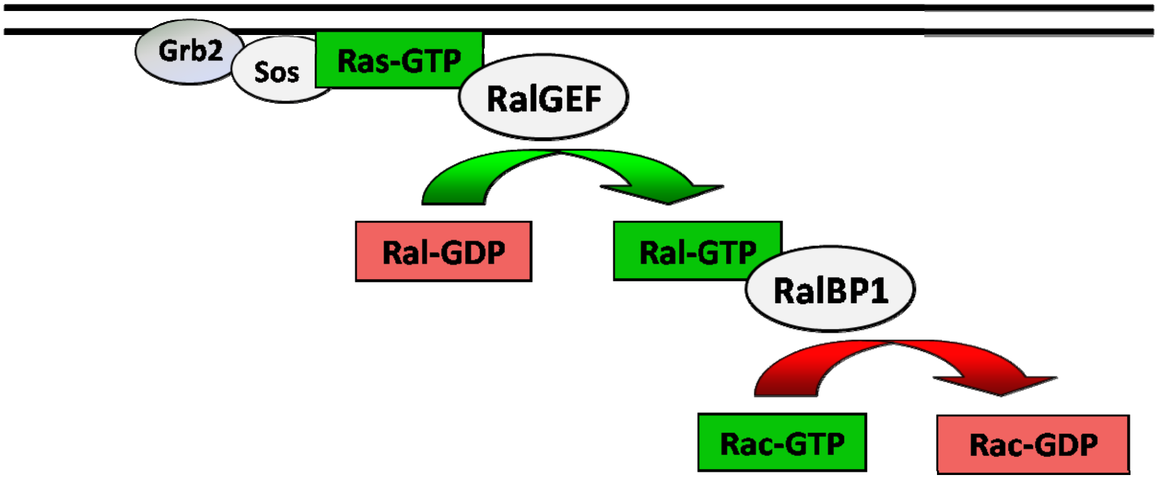
Grb2
Sos
Ras-GTP
RalGEF
Ral-GDP
Ral-GTP
RalBP1
Rac-GTP
Rac-GDP

G-protein crosstalk. G-protein signaling is complicated by the fact that G-proteins can regulate each other. In this example, Ras induces Ral activation by localizing a RalGEF near Ral so that the GEF may induce nucleotide exchange on Ral. GTP-bound, active Ral binds its effector, RalBP1, which has GAP activity for another G-protein, Rac (and Cdc42, not shown).

Figure 1.3

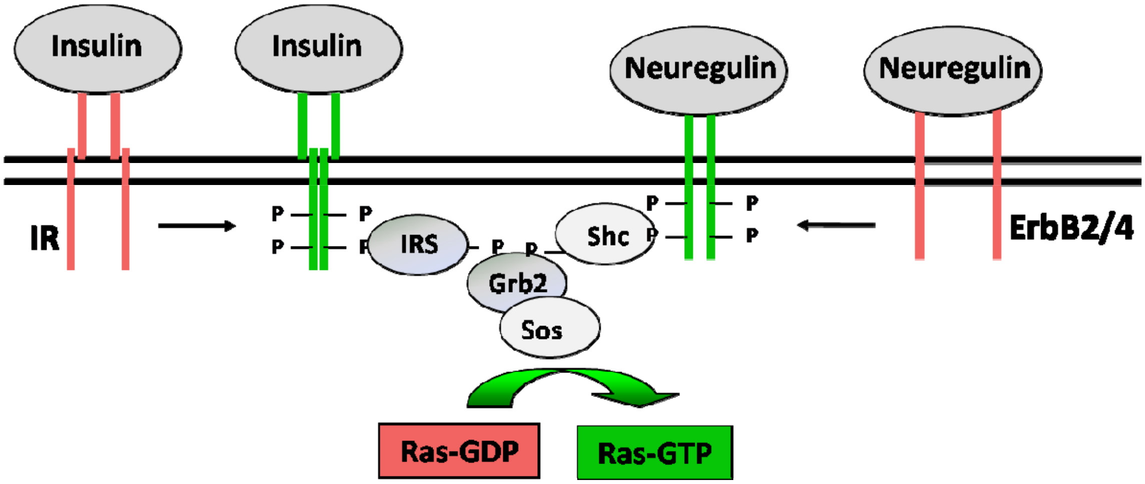

Receptor Tyrosine Kinase (RTK)-mediated Ras activation. Many agonists induce Ras activation. Two RTKs are represented in this illustration. Insulin binding of the insulin receptor (IR) induces a conformational change that allows autophosphorylation of tyrosine residues within the cytoplasmic domain of the IR. Similarly, neuregulin binding the ErbB receptor monomers induces dimerization (ErbB2/3, ErbB2/4, or ErbB4/4) and subsequent tyrosine phosphorylation within the cytoplasmic domains. Phosphorylated tyrosine residues of the receptors serve as docking sites for SH2 domains of effectors such as insulin receptor substrate (IRS) and Shc, which are then also phosphorylated on tyrosine residues by the receptors and allow the docking of other SH2-domain containing molecules such as Grb2. Grb2 forms a complex with the RasGEF, SOS, to localize SOS near the plasma membrane where it then activates Ras.

Figure 1.4

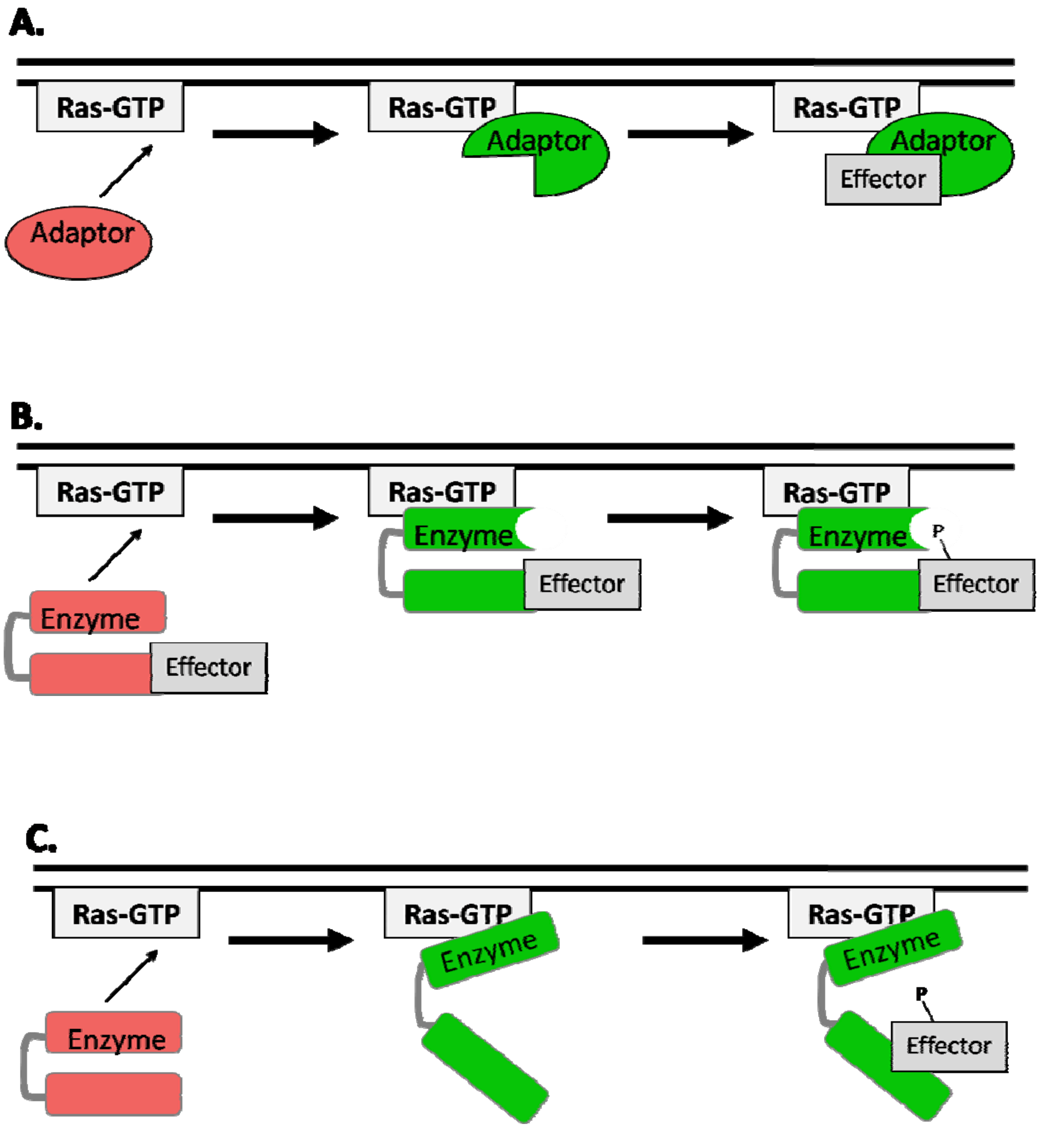
A.
Ras-GTP
Adaptor
Ras-GTP
Adaptor
Ras-GTP
Adaptor
Effector
B.
Ras-GTP
Enzyme
Effector
Ras-GTP
Enzyme
Effector
Ras-GTP
Enzyme
P
Effector
C.
Ras-GTP
Enzyme
Ras-GTP
Enzyme
Ras-GTP
Enzyme
P
Effector

Ras-induced activation of effector molecules. Ras binding can induce many conformational changes in its effectors including: (**A**) opening a site in adaptor molecules to allow docking of effectors, (**B**) activation of the catalytic domain of enzymatic effectors to enable the modification of downstream effectors, or (**C**) dissociation of a regulatory subunit from the catalytic domain on the Ras effector.

Figure 1.5

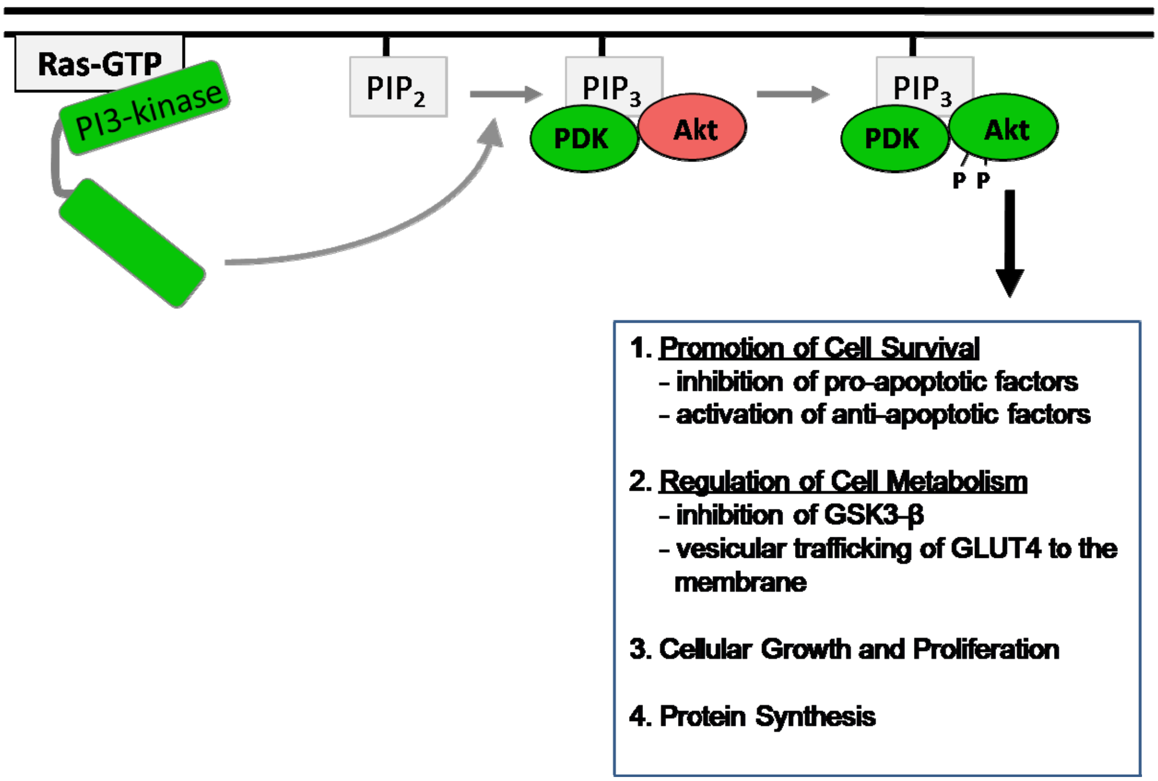

1. Promotion of Cell Survival
   - inhibition of pro-apoptotic factors
   - activation of anti-apoptotic factors

2. Regulation of Cell Metabolism
   - inhibition of GSK3-β
   - vesicular trafficking of GLUT4 to the membrane

3. Cellular Growth and Proliferation

4. Protein Synthesis

Ras-mediated activation of PI3-kinase-Akt signaling. PI3-kinase induces formation of PIP3, a phospholipid that serves as a docking site for PDK1/2 and Akt. PDK1 and PDK2 phosphorylate Akt on two residues (Thr308 and Ser473, respectively). Activation of Akt results in cellular changes that promote cell growth and survival.

Figure 1.6

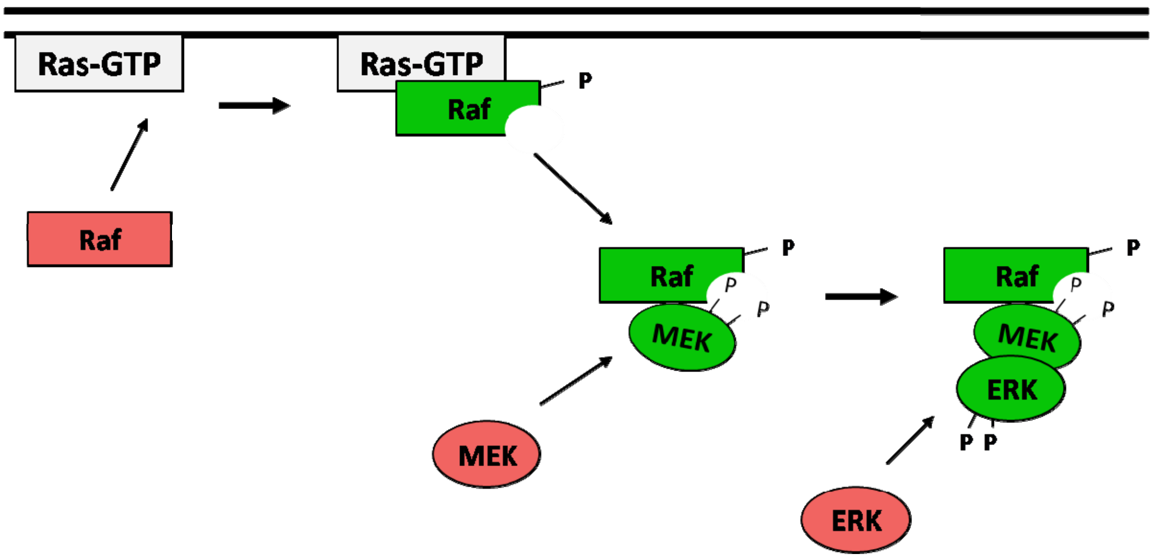
Ras-GTP
Raf
Ras-GTP
Raf
P
Raf
P
P
P
MEK
MEK
Raf
P
P
P
MEK
ERK
P P
ERK

Ras-mediated activation of Raf-MEK-ERK signaling. Raf is activated by binding to Ras and subsequent phosphorylation. Activated Raf may then dissociate from Ras (it has also been hypothesized to remain Ras bound) and activate MEK1/2 by phosphorylating two of their serine residues. Active MEK1/2 functions to activate the serine/threonine kinase ERK1/2 by phosphorylating a threonine residue as well as a tyrosine residue on ERK1/2.

SECTION II. METHODS

Reagents and Lysis Buffers - Reagents used in my studies are divided into the following categories: Antibodies, General Chemicals, Pharmacological Agents, Tissue Culture, and Western Blotting Reagents. Lysis buffer compositions are listed after the reagents.

Antibodies: Agarose conjugated phosphorylated tyrosine (pTyr) antibody was purchased from Cell Signaling. All others are summarized in **Table 2.1**.

General Chemicals/Reagents: Desalting columns were purchased from BIO-RAD. Protease Inhibitor Cocktail was purchased from Calbiochem. Ethylene diamine tetraacetic acid (EDTA), Hepes – no sodium salt, Lysozyme, magnesium chloride ($MgCl_2$), magnesium sulfate ($MgSO_4$), octylglucopyranoside, potassium chloride (KCl), sodium chloride (NaCl), sodium phosphate (NaH_2PO_4), sodium dodecyl sulfate (SDS), Tris base, and Tris hydrochloride (Tris-HCl) were purchased from Fisher. Prolong Antifade Mounting Media was purchased from Invitrogen. Bovine serum albumin (BSA) was purchased from MP Biomedicals. Dialysis bags, glutathione (GSH), and immobilized glutathione agarose beads were purchased from PIERCE. 2-deoxy-d-glucose, Ampicillin, Bradford protein assay, cesium chloride (CsCl), DL-dithiotreitol (DTT), EZ-Mix LB broth base (LB), gelatin, glycerol, igepal, isopropyl β-D-thiogalactopyranoside (IPTG), 2-[N-morpholino]ethane-sulfonic acid (MES), paraformaldehyde (PFA), PBS, Phosphatase Inhibitor Cocktail 1 and 2, Sigma Fast diaminobenzidine (DAB) tablets, Tris-buffered saline (TBS), Tris-buffered saline with tween (TBST), and Triton X-100 were purchased from Sigma. Collagenase type II was purchased from Worthington Biochemical Corporation.

Pharmacological Agents for Cell Treatments: PI3-kinase inhibitors (LY-294002 and Wortmannin; Wort) were purchased from BIOMOL International. The MEK inhibitor (PD-98059) was purchased from Calbiochem. Recombinant human neuregulin-1 (NRG) was purchased from R&D Systems. Insulin isolated from bovine pancreas was purchased from Sigma.

Tissue Culture: Cell culture water was purchased from Cambrex. Trypsin-EDTA was purchased from Cellgro. Dulbecco's Modified Eagle's Medium (DMEM), DMEM without phenol red, fetal bovine serum (FBS), glutamine, Medium-199 (M199), non-heat inactivated FBS, pancreatin, penicillin/streptomycin (Pen/Strep), and sterile phosphate-buffered saline (PBS) were purchased from Gibco. Equine serum (HS) was purchased from Hyclone. TransIT-293 transfection reagent was purchased from Mirius.

Western Blotting Reagents: Criterion XT 12% Bis-Tris precast gels, DC lowry protein assay, Kaleidoscope prestained standards, XT reducing agent, and XT sample buffer were purchased from BIO-RAD. The biotinylated protein ladder was purchased from Cell Signaling. Restore western blot stripping buffer, Supersignal West Pico Stable Peroxide Solution, and Supersignal West Pico Luminol/Enhancer Solution were purchased from Pierce Biotechnology.

Lysis Buffers:

- G-protein lysis buffer – 25 mM Tris-HCl, 40 mM NaCl, 30 mM $MgCl_2$, 1% Igepal, pH 7.5. Protease and phosphatase inhibitor cocktails (10 µl/ ml) were added the day of use.
- MBST/OG – 25 mM MES, 150 mM NaCl, 60 mM Octyglucopyranoside, 1% Triton X-100, pH 6.4. Protease and phosphatase inhibitor cocktails (10 µl/ ml) were added the day of use.
- RIPA buffer – 50 mM Tris-base, 150 mM NaCl, 1% Triton X-100, 0.1% SDS, 1% Glycerol, pH 7.5. Protease and phosphatase inhibitor cocktails (10 µl/ ml) were added the day of use.

Primary Myocyte Isolation and Culture – Neonatal rat ventricular myocytes (NRVMs) were isolated from 1-2 day old Sprague Dawley rats via collagenase digestion; as previously described [83]. To briefly summarize, atria were removed from isolated hearts. Ventricles were then minced, pooled, and cells were separated by incubation in digestion solution containing collagenase type II and pancreatin. Cells were then pre-incubated in plating media (Dulbecco's modified Eagle's medium/Medium 199 (4:1) containing 10% equine serum, 5% fetal bovine serum, and Pen/Strep) for 2 hours at 37°C to allow for attachment of non-myocyte cells. The subsequent NRVM suspension was cultured on a gelatin matrix at 0.3 x 10^6 cells/ml to 0.5 x 10^6 cells/ml and maintained until the day of adenoviral infection.

Adenoviral Infection and Agonist Treatment of Cardiomyocytes – Forty-eight hours after isolation, NRVMs were infected with an adenovirus to increase the expression of wild-type, mouse Rgl2 (AdRgl2; **Figure 2.1**) or with an empty vector control virus (AdNull; provided by Dr. Nancy Webb, University of Kentucky). The use of AdNull as a control was necessary as preliminary results showed that the adenovirus variably affected protein phosphorylation with increasing titer (which is consistent with known effects of the adenovirus). Additionally, the constitutively active RasV12 virus (AdRasV12) and dominant negative RasN17 virus (Ad-DNRas; provided by Dr. Shuang Huang, Medical College of Georgia) was used to alter Ras activity in cardiomyocytes [86]. The cells were typically infected with 90 infectious units per cell (ifu/cell; unless noted otherwise) yielding a transfection efficiency of 70-90%. Twenty-four hours post-infection, cells were incubated in serum-free medium for 4 hours and then treated with 100 nM insulin (Ins), 10 nM neuregulin (NRG), or vehicle before lysis. Some studies required pretreatment with 200 nM wortmannin, 50 μM LY-294002, or 10 μM PD-98059 for 30 minutes prior to agonist stimulation.

Ral and Ras Activation Assays – To assess levels of Ral-GTP and Ras-GTP in NRVMs, cells were lysed in G-protein buffer and assayed for protein concentration. GST fusion proteins that bind specifically to GTP-bound Ral or GTP-bound Ras (GST-RalBP1-BD and GST-Raf-RBD, respectively) were provided by Dr. Douglas Andres (University of Kentucky) and used to determine G-protein activation [83, 87]. Briefly, 500μg lysate protein was incubated with GST-RalBP1-BD or GST-Raf-RBD bound agarose beads for 1 hour at 4°C with gentle rotation. The beads were washed and the bound Ral-GTP or Ras-GTP was separated by 12% SDS-PAGE. Active G-protein was assessed by immunoblotting using antibodies specific for RalA or Ras (BD Biosciences).

Immunohistochemistry of Adenoviral Infected NRVMs – To determine transfection efficiency of the AdRgl2 virus, NRVMs were infected with 90 ifu/cell of AdRgl2 or AdNull. All incubations within this protocol were performed at room temperature unless otherwise noted. Twenty-four hours after infection, cells were fixed with 4% paraformaldehyde for 30 minutes and permeabilized with 0.2% Triton X-100 for 8 minutes. NRVMs were then blocked with 1% BSA in non-phenol red containing DMEM for 30 minutes. This was followed by incubation with rabbit anti-HA antibody (1:200 in 1% BSA; Upstate) for 60 minutes. Cells were then incubated with Alexa Flour-568 Goat anti-rabbit IgG (5 µl/ml in 1% BSA; Invitrogen) and wheat germ agglutinin, a non-specific membrane stain, (WGA; 1:100 in 1% BSA; Invitrogen) for 30 minutes – from this step on, slides were maintained in the dark to protect the fluorophore. Lastly, cells were incubated with DAPI nuclear stain (1 µl per 3 ml in 1% BSA; Invitrogen) for 5 minutes. Coverslips were mounted to the slides using Prolong anti-fade mounting media and slides were stored at 4^{o}C overnight. Images of the stained cells were taken using a Leica TCS SP confocal microscope and the number of cells infected per field was counted manually to determine the percentage of cells infected with this viral titer.

Immunoprecipitation – To assess insulin receptor (IR) activation in NRVMs, cells were lysed in RIPA buffer and assayed for protein concentration. Briefly, 500 µg of whole lysate protein was incubated with an agarose conjugated antibody against phospho-tyrosine (Cell Signaling) at 4^{o}C with gentle rotation for 1 hour. The beads were washed and the bound tyrosine phosphorylated protein (pTyr) was separated by 12% SDS-PAGE. Active IR was assessed by immunoblotting samples, previously incubated with agarose conjugated anti-pTyr, using a polyclonal antibody specific for IR-β (Santa Cruz). Total IR was immunoblotted in whole cell lysates using polyclonal antibodies against IR-β for normalization.

Maintenance and Transfection of HEK-293 cells – Given that some experimental procedures required transfection-mediated rather than adenoviral-mediated gene delivery and that NRVMs are poorly transfected, HEK-293 cells were a necessary component of some experiments. HEK-293 cells were maintained in Dulbecco's modified Eagle's medium (DMEM) supplemented with 10% FBS and Pen/Strep. Once cells were grown to 50% confluence, transfection of DNA for Rgl2, constitutively active Ral (RalV23), or the vector control (pMT2) was performed using the TransIT-293 transfection reagent protocol provided by Mirius. In this protocol, a transfection mixture containing the DNA and transfection reagent was created as follows: 18µl of TransIT-293 transfection reagent was added dropwise to 200 µl serum-free DMEM for every well of a 6-well culture dish that was transfected. This mixture was then incubated at room temperature for 20 minutes followed by addition of 3 µg/well of the appropriate DNA.

After a final 20 minute incubation, 200 µl of the mixture was added dropwise to the cells which were then incubated for 48 hours. Cells were serum starved for 4 hours prior to agonist treatment. Lysates were prepared as described above.

Immunoblotting – Following adenoviral infection and/or pharmacological treatment, whole cell lysates were collected in MBST/OG, RIPA, or G-protein lysis buffer containing protease and phosphatase inhibitors. Lysates were incubated on ice for 30 minutes, centrifuged at 13,000 rpm for 10 minutes, and supernatant used for protein analysis. Protein concentration was determined via the DC Lowry protein assay (BioRad). Equal amounts of lysate protein were combined with reducing sample buffer, heated for 5 minutes, resolved by SDS-PAGE, and transferred to PVDF membrane. The membranes were then blocked with 5% milk, 1% bovine serum albumin (BSA) in tris-buffered saline with tween (TBS/T); the only exception was for membranes probed for phosphorylated tyrosine residues (pTyr) which were blocked with 5% BSA in TBS/T. Membranes were then incubated with various primary antibodies (**Table 2.1**) overnight at 4^{o}C with gentle agitation. The following day, membranes were incubated with the appropriate species specific HRP-conjugated secondary antibody (Cell Signaling) at room temperature for one hour with gentle agitation. Bands were visualized by incubating membranes for in enhanced Super Signal West Pico chemiluminescent substrate (Pierce Biotechnology) for 5 minutes. Bands were visualized and intensity quantified using a Kodak Image Station 4000MM. Unless otherwise noted, phosphorylated kinase was normalized to total kinase and the appropriate statistical analysis was performed for each experiment. All western blot bands pictured in each figure were taken from the same western blot.

Statistical Analysis – Data are presented as the mean ± SEM. Significance between treatment groups was determined by the appropriate t-test for individual comparisons or a Wilcoxon sign-rank test for comparisons of data normalized to AdNull Control followed by one-way ANOVA with the appropriate post-hoc analysis for multiple comparisons. Analyses were completed using GraphPad Prizm software. Results with $p < 0.05$ were considered statistically significant.

**Further information about all methods is provided in Appendix 1.

Copyright © Leah M. Allen 2008

Figure 2.1

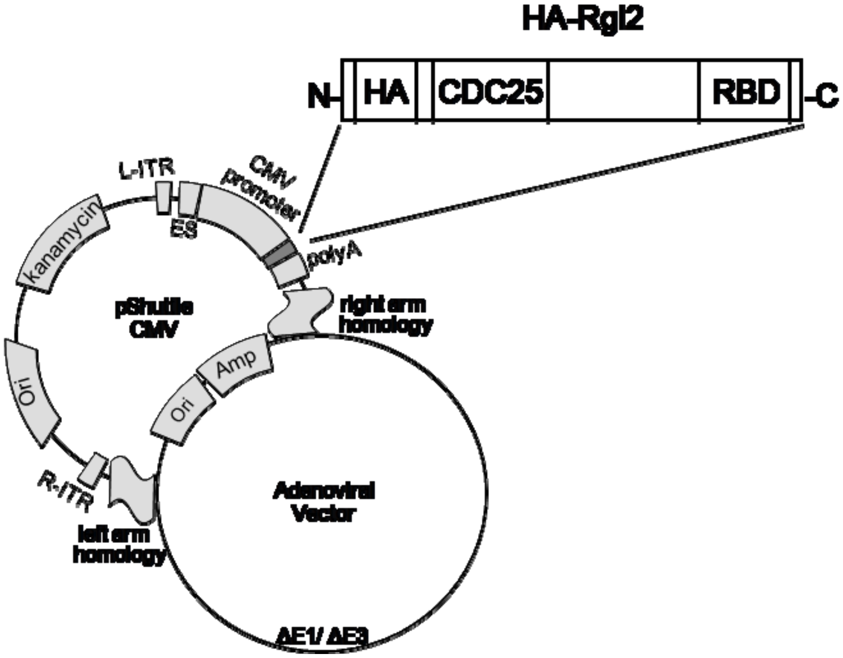
HA-Rgl2
N-
HA
CDC25
RBD
-C
L-ITR
CMV promoter
ES
kanamycin
polyA
pShuttle CMV
right arm homology
Ori
Amp
Ori
R-ITR
left arm homology
Adenoviral Vector
ΔE1/ ΔE3

Rgl2 adenoviral vector. The Rgl2 adenovirus (AdRgl2) was constructed with the AdEasy system developed by Stratagene. In this system, a shuttle vector containing DNA for HA-epitope tagged wild-type Rgl2 was homologously recombined with an adenoviral backbone plasmid. The shuttle vector also contains a CMV-promoter for highly efficient expression, an encapsidation sequence (ES), kanamycin resistance for selection of recombinant adenoviral plasmid, and inverted terminal repeat sequences (L-ITR and R-ITR) which are involved in replication. The adenoviral vector contains most of the adenoviral genome, but lacks the E1 and E3 replication genes as a safety measure. Therefore, the virus is replication difficient in all cells except E1-expressing packaging cells (HEK-293 cells).

Table 2.1. **Antibodies used in the studies.**

Antibody	**Manufacturer**	**Catalog #**	**Dilution**
Actin	Sigma	A2066	1:1000
Akt (tAkt)	Cell Signaling	9272	1:1000
cyclophilin A	Upstate	07-313	1:1000
HA	Santa Cruz	sc-805	1:250
Insulin Receptor β-subunit (IR)	Santa Cruz	sc-711	1:200
p44/42 (tERK1/2)	Cell Signaling	9102	1:1000
Phospho-Akt Ser^{473} (pAkt)	Cell Signaling	9271	1:1000
Phospho-p44/42 Thr^{202}/Tyr^{204} (pERK1/2)	Cell Signaling	9106	1:2000
Phospho-Tyrosine (pTyr)	Cell Signaling	9411	1:1000
RalA	BD Biosciences	R23520	1:5000
Ras	BD Biosciences	610001	1:500
Rgl2 c-54	BD Biosciences	Developed specifically for Dr. Post	1:2500
α-tubulin	Abcam	Ab7291	1:5000

SECTION III. RESULTS

Adenoviral-mediated expression of Rgl2 in Cardiomyocytes

In order to study the effect of Rgl2 on cardiomyocyte signaling, the optimal conditions for use of adenoviral infection to increase expression of Rgl2 in NRVMs were determined. Specifically, I varied the adenoviral titer to maximize the expression and function of Rgl2 in NRVMs.

AdRgl2 Increases Rgl2 Expression in NRVMs

NRVMs were infected with increasing titers (30, 60, or 90 infectious units per cell, ifu/cell) of the empty vector control virus used to control for viral interaction with the cells (AdNull) or the virus to increase Rgl2 expression (AdRgl2) and cell lysates prepared 24 hours after infection. Lysate proteins were quantified and an equal mass of protein (5-20 μg) analyzed by immunoblotting with antibodies for Rgl2, the hemagglutinin (HA) epitope tag encoded by the virally expressed Rgl2, and cyclophilin A as a protein loading control. The intensity of the detected Rgl2 bands was normalized to the intensity of bands from samples infected with the same titer of AdNull virus. HA bands were not quantified because (as expected) no HA was expressed in the AdNull infected NRVMs. As shown in **Figure 3.1**, NRVMs infected with 30 ifu/cell AdRgl2 titer showed increased Rgl2 expression by approximately 40-fold which was increased to 200-fold at a viral titer between 60 and 90 ifu/cell ($p<0.05$). Maximal Rgl2 expression was consistently achieved using a titer of 90 ifu/cell. Higher titers showed no significant increase in Rgl2 protein expression, but toxicity was observed at titers of 240 ifu/cell or higher (unpublished results). Therefore, unless otherwise indicated, a viral titer of no more than 90 ifu/cell was used for all future studies.

Infection Efficiency of NRVMs Infected with AdRgl2

To assess the efficiency with which the AdRgl2 virus induced Rgl2 expression, NRVMs were infected with 90 ifu/cell of AdRgl2 or AdNull, fixed 24 hours post-infection, and immunostained using an Alexa^{568}-labeled antibody to detect the HA-epitope tag on the transfected Rgl2. Cells were also stained with Alexa^{488}-labelled Wheat Germ Agglutinin (WGA) to visualize glycosylated proteins on the plasma membrane of all cells. Confocal images were digitally captured and analyzed to quantify the percentage of

NRVMs expressing HA-Rgl2. As depicted in **Figure 3.2**, all NRVMs in the field were stained green with Alexa^{488} WGA (left panel). Cardiomyocytes expressing the HA-tagged Rgl2 were stained red by the Alexa^{568}-anti-HA (middle panel). Overlaying the two images (right panel), indicated that the vast majority of cells express HA-Rgl2 following infection with 90 ifu/cell AdRgl2 virus. Using these conditions, 70 to 90% of cells are typically infected. Preliminary studies using lower viral titers gave lower infection efficiencies with less than 70% of the cells expressing HA-Rgl2 (unpublished results). This increased infection efficiency paralleled the increased Rgl2 protein expression with increasing viral titer. Therefore, to achieve maximal infection of the NRVMs, a titer of only 90 ifu/cell was used for the majority of my studies. Interestingly, there was partial overlap of HA-Rgl2 with WGA (right panel) indicating that a fraction of Rgl2 is localized to the plasma membrane.

Increased Rgl2 Expression Induces Ral Activation

After determining that 90 ifu/cell AdRgl2 maximally increased Rgl2 protein, I confirmed that the expressed protein was functional. The best characterized function of Rgl2 is its ability to activate Ral. Therefore, the effect of increased Rgl2 expression on Ral activation was determined. Using the infection parameters (90 ifu/cell) described above, NRVMs were infected with AdNull or AdRgl2 and lysates were prepared 24 hours after infection. To assess Ral activation, lysate protein from each sample (500 µg) was incubated for 1 hour with agarose-coupled Ral-BP1-BD, a protein that only interacts with the active, GTP-bound Ral. After incubation with the Ral-BP1-BD beads, active Ral in the sample was isolated by centrifugation and quantified by immunoblotting with a Ral antibody. Cell lysates were analyzed for total Ral protein levels in order to normalize the active Ral to total Ral protein. As a result of this analysis, I found that increasing Rgl2 expression activated Ral 2-fold above basal levels (**Figure 3.3**; p=0.0091). Enhanced Ral activation confirms that the transfected Rgl2 protein is functional.

Effect of Increased Rgl2 Expression on Signaling Cascades in NRVMs

The finding that Rgl2 increases Ral activation indicates that Rgl2 is active in NRVMs following adenoviral infection. Because Rgl2 is activated following its interaction with Ras [76, 83], I studied the effect of increased Rgl2 expression on Ras activation and Ras effector signaling cascades.

Increased Rgl2 Expression Induces Ras Activation

I studied the extent of Ras activation in Rgl2 infected cells using a method similar to that described for examining Ral activity. Cardiomyocytes were infected with 90 ifu/cell AdNull or AdRgl2, followed by cell lysate preparation after 24 hours. To assess Ras activation, equal amounts of lysate protein (500 µg) were incubated with agarose coupled Raf-RBD, a protein that interacts specifically with the active, GTP-bound Ras. After incubating with the Raf-RBD beads, bound Ras-GTP in the sample was isolated by centrifugation and quantified via immunoblot with a monoclonal antibody against Ras. Cell lysates were used to determine total Ras levels so that the intensity of isolated/active Ras that was detected could be normalized to total Ras protein. I found that Ras activation in Rgl2 infected NRVMs was 3-fold above AdNull levels (**Figure 3.4**; $p=0.0023$). Because Rgl2 is thought to interact with Ras at the plasma membrane to become localized with its effector, Ral, this finding is consistent with the finding that Rgl2 was localized to the plasma membrane and that Ral was activated following increased Rgl2 expression.

Increasing Rgl2 Expression Decreases ERK1/2 Activation

Because increased Ras activation was observed in AdRgl2 infected NRVMs, I determined if there was a parallel increase in the activity of Ras effector signaling pathways. The best characterized Ras effector molecules are Raf, PI3-kinase, and the RalGEFs. Data presented above demonstrate that increased Rgl2 expression induces an increase in Ral activation (which precludes the study of endogenous RalGEFs). Therefore, I studied the effect of Rgl2 on Ras signaling by examining the consequence of increased Rgl2 expression on Raf-MEK-ERK and PI3-kinase-Akt signaling.

To study the effect of increased Rgl2 on Raf-MEK-ERK signaling, NRVMs were infected with increasing titers of AdNull or AdRgl2 (30, 60, or 90 ifu/cell), cell lysates prepared, and activation of ERK1/2 was assessed by immunoblotting with antibodies specific for the phosphorylated (activated) kinase. The intensity of the detected phosphorylated protein was normalized to total kinase present in cell lysates and values expressed as fold of AdNull control. As shown in **Figure 3.5**, I found that increasing Rgl2 concentration inhibited ERK1/2 phosphorylation (an index of activation) in a titer-dependent manner and reached a maximal inhibition of 50% compared to AdNull infected cardiomyocytes ($p<0.05$). Thus, increased Rgl2 expression appears to inhibit ERK1/2 activation even though Ras activation was increased.

Increased Rgl2 Expression Enhances PI3-kinase-Akt Activity

To determine if increased Rgl2 expression inhibits activation of other Ras effectors, the effect of Rgl2 on PI3-kinase-Akt signaling was examined. I found that in contrast to its inhibitory effect on ERK1/2 phosphorylation, Rgl2 enhanced PI3-kinase activity, as indexed by Akt phosphorylation on Ser473. Specifically, Rgl2 increased Akt phosphorylation in a titer-dependent manner with a maximal enhancement of approximately 4-fold at 90 ifu/cell (**Figure 3.6A**; $p<0.05$). Inhibiting PI3-kinase with wortmannin (Wort; 200 nM) for 30 minutes abolished the Rgl2-mediated enhancement of Akt phosphorylation indicating that the effect of Rgl2 on Akt phosphorylation was PI3-kinase-dependent (**Figure 3.6B**).

The above data indicate that Rgl2 increases PI3-kinase activation and Akt phosphorylation. As discussed in the introduction, active Akt may then phosphorylate a variety of important substrates, including GSK3-β [56]. GSK3-β was first identified as a regulator of glucose metabolism and more recently as a regulator of apoptosis, protein synthesis, and cardiomyocyte hypertrophy [88-90]. To confirm that Rgl2-mediated enhancement of Akt phosphorylation correlated with a measureable increase in Akt activity, NRVMs were infected with 90 ifu/cell AdNull or AdRgl2 and cell lysates prepared 24 hours after infection. GSK3-β phosphorylation was quantified by immunoblotting using a phospho-GSK3β specific antibody and the amount of phospho-GSK3-β detected was normalized to tubulin (protein loading control). As shown in **Figure 3.7**, Rgl2 increased GSK3-β phosphorylation by 2-fold ($p=0.0168$). Together, these data delineate a Rgl2-PI3-kinase-Akt-GSK3-β pathway in cardiomyocytes which could be mediated by Ras-induced activation of PI3-kinase, indicating that Rgl2 may play a role in regulation of cardiomyocyte metabolism and protein synthesis.

Effect of Increased Rgl2 Expression on Ras-induced Signaling Cascades

I observed an increase in Ras activation in AdRgl2 infected cardiomyocytes as well as Rgl2-mediated differential regulation of Ras effector signaling. However, activation of these effectors (Raf and PI3-kinase) is not exclusive to Ras signaling as they are activated by a variety of signaling molecules. Therefore, I wanted to examine the effect of Rgl2 specifically on Ras signaling. To accomplish this, I expressed a GTPase deficient, constitutively active Ras mutant (RasV12) in NRVMs. Specifically, NRVMs were infected with AdNull, AdNull combined with AdRasV12, or AdRgl2 combined with AdRasV12. Twenty-four hours later, cell lysates were prepared and the activation of

ERK1/2 and Akt assessed as described above. A potential problem associated with dual adenoviral transfection is that one cannot be sure of the percentage of cells infected with both viruses or that the adenoviral-induced transgenes do not alter expression of each other. However, the differential regulation of RasV12 signaling by Rgl2 (discussed below) indicates that a sufficient percentage of NRVMs were infected with both viruses to assess changes in signaling. Furthermore, when Ras expression in cell lysates was assessed by immunoblotting, I found that Ras levels were increased to the same extent in combination with AdNull or AdRgl2.

As shown in **Figure 3.8**, RasV12 expression induced phosphorylation of ERK1/2 (greater than 2-fold) and Akt (greater than 2-fold) as expected. Co-infection with AdRgl2 inhibited ERK1/2 activation induced by RasV12 in a manner that paralleled the inhibition observed in unstimulated cells (**Figure 3.5**). However, increasing Rgl2 expression had no effect on the extent of Akt phosphorylation induced by constitutively active Ras. I speculate that the extremely high level of RasV12-induced Akt phosphorylation precludes detecting any further enhancement by Rgl2.

Effect of Rgl2 on Receptor Tyrosine Kinase Signaling in Cardiomyocytes

Because a supraphysiological activation of Akt was observed in cardiomyocytes expressing RasV12, the effect of Rgl2 on a physiological stimulator of Akt and ERK1/2 was examined. I chose to study the effect of Rgl2 on receptor tyrosine kinase signaling mediated by the insulin and ErbB2/4 receptors. These receptors are expressed in cardiomyocytes and are potent activators of both Raf-MEK-ERK and PI3-kinase-Akt signaling [91].

Increasing Rgl2 Expression Alters Insulin-induced Kinase Activation

To determine if insulin-induced signals were altered by increased Rgl2 expression, I examined the time and concentration-dependence for insulin-induced Akt and ERK1/2 phosphorylation in AdNull and AdRgl2 infected NRVMs. To assess the effect of Rgl2 on insulin-induced Akt phosphorylation, a dose-response experiment was performed in which NRVMs were treated with increasing insulin concentrations (0 to 100 nM) for 10 minutes. As shown in **Figure 3.9**, I found that insulin increased both ERK1/2 and Akt phosphorylation in a dose-dependent manner with a plateau at a 100nM insulin concentration. Rgl2 inhibited insulin-induced ERK1/2 phosphorylation at all concentrations, whereas insulin-induced Akt phosphorylation was increased in AdRgl2 infected NRVMs at all concentrations. Therefore, an insulin concentration of 100 nM was used for additional experiments.

To assess whether changes in insulin-signaling reflected a Rgl2-dependent change in the kinetics of insulin activation and deactivation of signaling pathways, cells were treated with 100 nM insulin for increasing times (0 to 40 minutes). As shown in **Figure 3.10**, Akt phosphorylation in AdNull and AdRgl2 infected NRVMs reached a maximal level after 10 minutes of insulin stimulation. Phosphorylated Akt levels began to decline following 20 minutes of stimulation. The time course for Akt phosphorylation was similar following AdRgl2 infection with the exception that Rgl2 enhanced insulin-induced Akt phosphorylation at all time points. ERK1/2 phosphorylation was also maximally stimulated with 10 minutes of insulin treatment and Rgl2 reduced insulin-induced ERK1/2 phosphorylation at all time points. Based on the observation that insulin-induced signals were maximal at 10 minutes and that AdRgl2 infection did not alter the kinetics of signaling, a time of 10 minutes was chosen for additional experiments.

The effect of Rgl2 on insulin-induced ERK1/2 and Akt phosphorylation (100 nM / 10 min) is summarized in **Figures 3.11-3.13**. Insulin induced a 1.5-fold increase in ERK1/2 phosphorylation as well as a 10-fold increase in Akt phosphorylation. Similar to the effect observed in RasV12 expressing cardiomyocytes, insulin-induced ERK1/2 phosphorylation was reduced by 2-fold in Rgl2 infected NRVMs (**Figure 3.11**; $p<0.05$). However, unlike its effect on Ras signaling, Rgl2 enhanced insulin-induced Akt phosphorylation by 2-fold (**Figure 3.12**; $p<0.0001$). To confirm that enhanced Akt phosphorylation reflected an increase in PI3-kinase activity NRVMs were treated with wortmannin (Wort; 200 nM) or LY-294002 (LY; 50 μM) for 30 minutes prior to the insulin treatment. As shown in **Figure 3.13**, both PI3-kinase inhibitors abolished Akt phosphorylation indicating that PI3-kinase activity is required for Rgl2-mediated enhancement of insulin-induced Akt phosphorylation.

As described above (**Figure 3.7**), Rgl2 enhanced GSK3-β phosphorylation downstream of PI3-kinase-Akt in unstimulated NRVMs. Shown in **Figure 3.14**, Rgl2 similarly enhanced insulin-induced GSK3-β phosphorylation by 1.5-fold ($p<0.05$). Furthermore, the enhancement of GSK3-β phosphorylation by Rgl2 was PI3-kinase-dependent as GSK3-β phosphorylation was decreased by a 30 minute treatment of wortmannin (200 nM) or LY-294002 (50 μM) prior to insulin treatment in AdRgl2 infected NRVMs (**Figure 3.15**). Together, these data illustrate Rgl2-mediated regulation of insulin-induced PI3-kinase-Akt-GSK3-β signaling in NRVMs.

Rgl2 Expression Alters Kinase Activation Induced by Neuregulin-1

Because Rgl2 had the ability to regulate insulin signaling, I determined if this effect was unique to insulin or if Rgl2 would similarly modulate the signaling of another receptor tyrosine kinase (RTK), the ErbB receptors. Neuregulin stimulates ErbB receptors in the heart to aid in cardiac development and to regulate cardiomyocyte hypertrophy and survival [92, 93]. Therefore, neuregulin-1 (NRG) was used to stimulate ErbB signaling in this study. To assess the effect of Rgl2 on NRG-induced signaling, AdNull and AdRgl2-infected NRVMs were treated with 10 nM neuregulin for 10 minutes (determined in preliminary studies to induce maximal activation of both ERK1/2 and Akt), lysates prepared, and kinase activation assessed via immunoblot analysis. The intensities of bands corresponding to the phosphorylated (active) kinase were normalized to total kinase and then normalized to AdNull control. NRG induced ERK1/2 phosphorylation in NRVMs to a similar extent as that induced by insulin (1.5-fold). Although NRG also induced Akt phosphorylation, this effect was less striking than that of insulin as NRG induced only a 5-fold increase in the phosphorylation of Akt whereas insulin induced a 10-fold increase in Akt phosphorylation. Similar to the effects observed with insulin signaling, Rgl2 inhibited NRG-induced ERK1/2 phosphorylation by 2-fold (**Figure 3.16**; $p<0.0001$), but enhanced Akt phosphorylation. Rgl2 appeared to enhance NRG-induced Akt phosphorylation in an additive manner (**Figure 3.17**; $p<0.05$) that was PI3-kinase dependent, as indicated by wortmannin inhibition (**Figure 3.18**).

Rgl2 Enhances Insulin Receptor Activation

Insulin binding to its receptor induces autophosphorylation of the insulin receptor (IR) at tyrosine residues within the cytoplasmic domain of its beta subunits. Phosphorylation at these sites allows for interaction of adaptor molecules such as the insulin receptor substrate (IRS) with the receptor and the subsequent phosphorylation of their tyrosine residues. Tyrosine phosphorylation induces the activation of these adaptor molecules which in turn induce signaling of downstream cascades, including the Ras-Raf-ERK1/2 and PI3-kinase-Akt cascades (**Introduction Figures 1.5 - 1.6**).

Rgl2 synergistically enhanced insulin-dependent Akt phosphorylation, but only additively enhanced neuregulin-induced Akt phosphorylation. One potential explanation for this difference is that Rgl2 could have increased the activation and/or expression of the IR to synergistically increase insulin-induced Akt phosphorylation. Therefore, to determine the effect of Rgl2 on insulin-induced IR activation, NRVMs were infected with

AdNull or AdRgl2 for 24 hours and then treated with 100 nM insulin for 3 minutes. Lysates were collected, lysate protein concentration assessed, and 500 µg of each sample was incubated with agarose conjugated anti-phosphotyrosine (p-Tyr) for 1 hour at $4^{o}C$ with gentle agitation. Following this incubation, samples were immunoblotted with antibodies against IR-β. These values were normalized to total IR-β or the loading control, tubulin, detected in immunoblotted whole cell lysates. Whole cell lysates probed for IR-β were also normalized to tubulin to examine changes in total IR expression levels. As shown in **Figure 3.19**, IR expression and phosphorylation were increased 2-fold following infection with AdRgl2 (p=0.032); indicating that a Rgl2-mediated increase in IR expression corresponds with an increase in IR activation.

Potential Mechanism(s) for Rgl2-dependent Modulation of RTK Signaling in Cardiomyocytes

In this set of experiments, I investigated three potential mechanisms by which Rgl2 may have induced changes in kinase signaling. One set of experiments investigated whether crosstalk between Raf-MEK-ERK and PI3-kinase-Akt was involved in the Rgl2-mediated alterations in cardiomyocyte signaling. The other two sets of experiments investigated the roles of Ras and Ral in Rgl2-mediated regulation of kinase signaling in NRVMs.

Crosstalk between ERK1/2 and Akt Does Not Account for the Rgl2-mediated Changes in Kinase Activation

In some cell systems, activation of the PI3-kinase-Akt pathway inhibits ERK1/2 phosphorylation and vice versa [94, 95]. Therefore, I examined the possibility that crosstalk between these signaling cascades mediated the alterations in RTK signaling that I had previously observed in AdRgl2 infected NRVMs. For these studies, cardiomyocytes infected with either AdNull or AdRgl2 were treated with either 200 nM wortmannin or 10 µM PD-98059 (to inhibit PI3-kinase-Akt or Raf-MEK-ERK signaling, respectively) for 30 minutes prior to treatment with insulin, NRG, or vehicle as control. Another set of cardiomyocytes infected with AdNull or AdRgl2 were not treated with inhibitors prior to agonist stimulation for comparison with the inhibitor treated group. Samples were immunoblotted to determine the effect of pharmacological inhibition on both Akt and ERK1/2 phosphorylation.

If enhanced Akt activity mediated the Rgl2-induced inhibition of ERK1/2, wortmannin should restore ERK1/2 phosphorylation in the Rgl2 control and agonist treated samples. However, wortmannin did not increase ERK1/2 phosphorylation, even though Akt phosphorylation was inhibited as expected (**Figure 3.20**). Because ERK1/2 phosphorylation was not increased by wortmannin, I conclude that a PI3-kinase dependent negative feedback loop was not responsible for the ERK1/2 inhibition observed in cardiomyocytes infected with AdRgl2.

I similarly tested whether Rgl2-mediated inhibition of ERK1/2 enhanced Akt phosphorylation in NRVMs. For this, NRVMs were treated with PD-98059 to inhibit MEK (consequently inhibiting ERK1/2) and the effect on Akt phosphorylation was examined. Although PD-98059 inhibited ERK1/2 phosphorylation as anticipated, it had no effect on Akt phosphorylation in either the Adnull or AdRgl2 infected samples (**Figure 3.21**). Therefore, crosstalk between Raf-MEK-ERK and PI3-kinase-Akt could not explain the changes in kinase signaling induced by Rgl2.

Inhibiting Ras Activity Mimics Rgl2-mediated Inhibition of RTK-induced ERK1/2 Phosphorylation in Cardiomyocytes

Studies have shown that the Ras-binding domains (RBDs) of RalGEF family members have the ability to block Ras interaction with RasGAP and Raf [74, 96]. My result that Rgl2 increases levels of GTP-bound Ras is consistent with decreased coupling of RasGAP to Ras in AdRgl2 infected NRVMs. Furthermore, my finding that Rgl2 inhibits Ras-induced ERK1/2 phosphorylation in AdRgl2 infected NRVMs is consistent with decreased Raf coupling to Ras. To explore the possibility that Rgl2 affects cardiomyocyte signaling by inhibiting Ras-effector interactions, I examined the extent to which a dominant-inhibitory Ras mutant (DNRas; RasN17) mimicked the effects of Rgl2. This DNRas preferentially binds GDP so that it may not interact with Ras effectors and ablates endogenous Ras activation by competitively blocking its interaction with RasGEFs [97]. In these studies, NRVMs were infected with 120 ifu/cell AdNull, 60 ifu/cell AdNull + 60 ifu/cell Ad-DNRas, 60 ifu/cell AdNull + 60 ifu/cell AdRgl2, or 60 ifu/cell AdRgl2 + 60 ifu/cell Ad-DNRas. Twenty-four hours post-infection, cells were treated with 100 nM insulin or 10 nM neuregulin for 10 minutes. Lysates were then collected and samples were analyzed for kinase phosphorylation via immunoblotting. Phosphorylated kinase was normalized to total kinase as described above and all values were subsequently normalized to the appropriate samples not infected with Ad-DNRas to assess changes induced by Ras inhibition (i.e. AdNull + Ad-DNRas treated with insulin was normalized to AdNull alone treated with insulin).

As shown in **Figure 3.22**, expression of DNRas abolished basal (control), insulin-induced, and NRG-induced ERK1/2 phosphorylation in both the AdNull and AdRgl2 infected NRVMs ($p<0.0001$). Therefore, Ras activation plays a fundamental role in Raf-MEK-ERK signaling in cardiomyocytes and that inhibiting Ras-Raf interaction is a plausible mechanism by which Rgl2 may be inhibiting ERK1/2 phosphorylation. As shown in **Figure 3.23**, DNRas had no effect on basal (control), NRG-induced, or Rgl2-mediated enhancement of Akt phosphorylation in cardiomyocytes. However, DNRas decreased insulin-induced Akt phosphorylation by 2-fold in AdNull, but not AdRgl2 infected NRVMs. Thus, other than its role in mediating insulin-induced Akt phosphorylation, Ras activation seems not to play a major role in PI3-kinase-Akt signaling in cardiomyocytes. More importantly, the mechanism by which Rgl2 mediates enhancement of both basal and RTK-induced Akt phosphorylation is Ras-independent.

Activation of Ral Mimics Rgl2-mediated Enhancement of Akt Phosphorylation in HEK-293 Cells

The best characterized function of Rgl2 is its ability to activate Ral and we found that levels of Ral-GTP were increased in cardiomyocytes expressing increased levels of Rgl2. Therefore, I tested the possibility that activation of Ral might mediate Rgl2-induced changes in kinase signaling. My model system was modified for this study because Ral adenoviruses were not accessible and cardiomyocytes are poorly transfected by conventional methods. Therefore, I used HEK-293 cells because they are commonly used for studying signal transduction. Specifically, I transfected HEK-293 cells with DNA for Rgl2, constitutively active Ral (RalV23), or the vector (pMT2) as a control. Forty-eight hours after transfection, HEK cells were treated with 100 nM insulin for increasing times (0 to 30 minutes). This time course was necessary to study the effects of Rgl2 and RalV23 on insulin-induced kinase signaling because insulin has been shown to have a different time of maximal ERK1/2 and Akt phosphorylation in this proliferative cell system [98]. Lysates were then collected and changes in ERK1/2 and Akt phosphorylation evaluated via immunoblotting.

As shown in **Figure 3.24**, ERK1/2 phosphorylation was stimulated with 5 minutes of insulin treatment; however, increased expression of Rgl2 did not alter insulin-induced ERK1/2 phosphorylation in this cell system. Although transfection of Rgl2 did not alter

ERK1/2 phosphorylation, increased expression of Rgl2 enhanced insulin-induced Akt phosphorylation. Moreover, expression of RalV23 mimicked the effect of Rgl2 (**Figure 3.25**); indicating that Rgl2-mediated activation of Ral may induce activation of the PI3-kinase-Akt pathway as described above in NRVMs.

Copyright © Leah M. Allen 2008

Figure 3.1

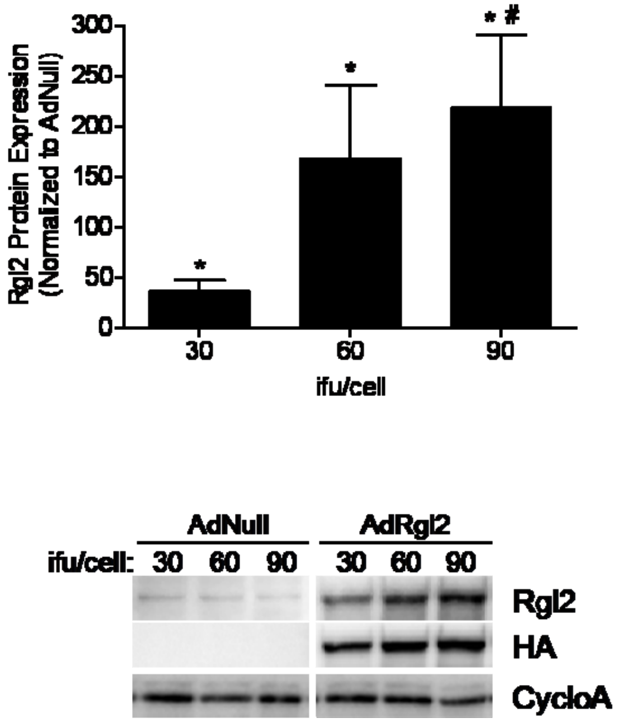

Titer-dependent Rgl2 expression in NRVMs. Neonatal rat ventricular myocytes (NRVMs) were isolated from 2-day-old Sprague-Dawley rats via collagenase digestion. Forty-eight hours after isolation, NRVMs were infected with increasing titers of an adenoviral vector (0 to 90 ifu/cell) to increase expression of HA epitope-tagged Rgl2 (AdRgl2) or with an empty vector (AdNull) used as control. Lysates were collected 24 hours after infection, resolved by SDS-PAGE, and immunoblotted for the HA epitope, total Rgl2, and cyclophilin A (CycloA; protein loading control). The graph represents Rgl2 expression in AdRgl2 infected samples normalized to Rgl2 expression in the AdNull samples infected with the same viral titer. Significance was determined by wilcoxon sign-rank test for comparison to AdNull and one-way ANOVA for comparison of all other groups. Values are expressed as mean ± SEM, n=6-7. $p<0.05$ vs. AdNull (*), vs. 30 ifu/cell AdRgl2 (#)

Figure 3.2

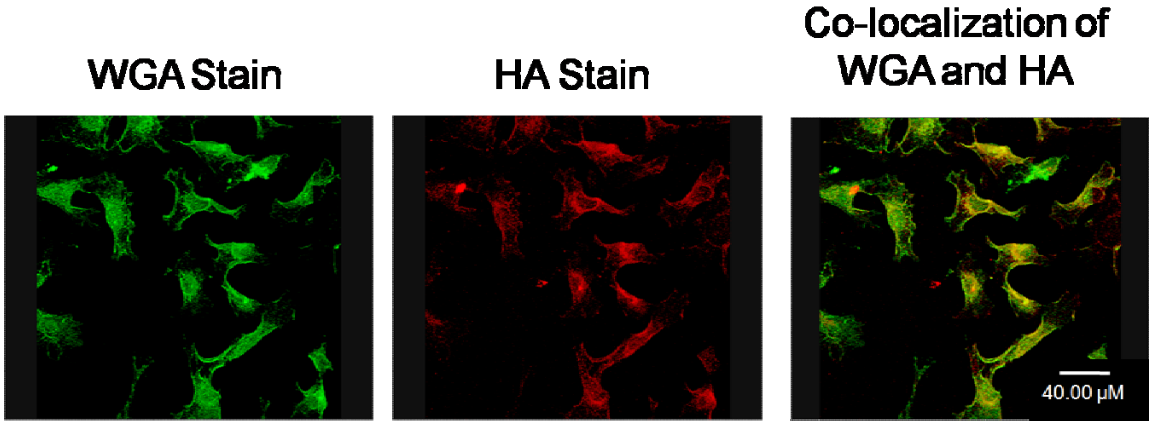

Infection efficiency of AdRgl2 in NRVMs. NRVMs were infected with an adenoviral vector (90 ifu/cell) to increase expression of Rgl2 (AdRgl2) or with an empty vector (AdNull) used as control. Twenty-four hours after infection, cells were fixed with paraformaldehyde and immunostained with Alexa 488 WGA (left panel in green) or with antibodies against the HA-epitope tag encoded by virally expressed Rgl2 (middle panel in red). The right panel represents an overlay of the two stains (yellow). Images of the stained AdRgl2 cells were taken using a Leica TCS SP confocal microscope and the number of cells infected per field counted manually to determine the percentage of cells infected with this viral titer. Infection efficiency of AdRgl2 was examined in 4 independent experiments.

Figure 3.3

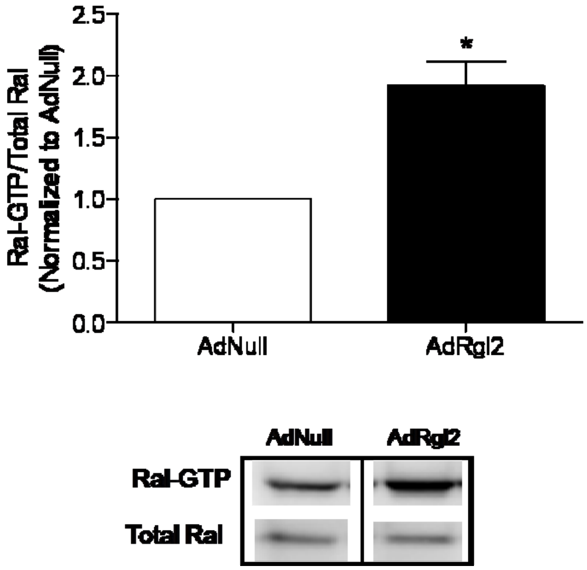

Increased Rgl2 expression induces Ral activation. Twenty-four hours after NRVMs were infected with 90 ifu/cell AdNull or AdRgl2, cell lysates were prepared and active Ral (Ral-GTP) was isolated from 500 µg of lysate protein by incubation with agarose coupled Ral-BP1-BD. Isolated (active) Ral and whole cell lysates (total protein) were resolved by SDS-PAGE and immunoblotted for RalA. Active Ral (Ral-GTP) values were then normalized to total Ral. The graph represents the ratio of these values normalized to AdNull. Significance was determined by one-sample t-test. Values are expressed as mean ± SEM, n=4. p=0.0091 vs. AdNull (*)

Figure 3.4

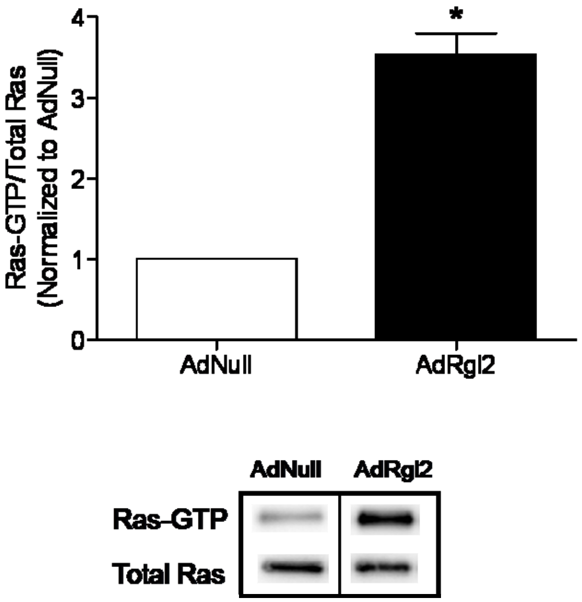

Increased Rgl2 expression induces Ras activation. Twenty-four hours after NRVMs were infected with 90 ifu/cell AdNull or AdRgl2, cell lysates were prepared and active Ras (Ras-GTP) was isolated from 500 μg of lysate protein by incubation with agarose coupled Raf-RBD. Isolated (active) Ras and whole cell lysates (total protein) were resolved by SDS-PAGE and immunoblotted for Ras. Active Ras (Ras-GTP) values were then normalized to total Ras. The graph represents the ratio of these values normalized to AdNull. Significance was determined by one-sample t-test. Values are expressed as mean ± SEM, n=3. p=0.0023 vs. AdNull (*)

Figure 3.5

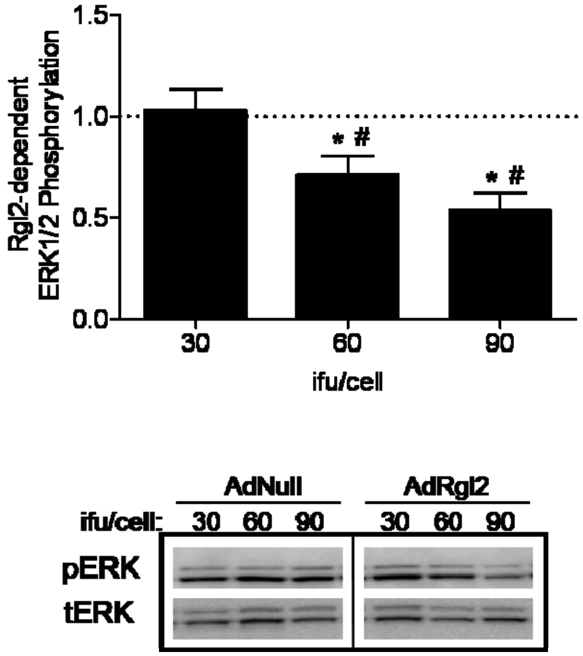

Increased Rgl2 expression inhibits ERK1/2 phophorylation in a titer dependent manner. Twenty-four hours after NRVMs were infected with increasing titers of AdNull or AdRgl2 (0-90 ifu/cell), cell lysates were prepared and resolved by SDS-PAGE followed by immunoblot analysis of kinase activation with the use of phospho-specific (Thr 202/Tyr 204) and total ERK1/2 antibodies. Phosphorylated ERK1/2 (pERK) values were normalized to total ERK1/2 (tERK) values and AdRgl2 values were subsequently normalized to the respective AdNull values. Significance was determined by wilcoxon sign-rank test for comparison to AdNull and one-way ANOVA for comparison of all other groups. Values are expressed as mean ± SEM, n=7-9. $p<0.05$ vs. AdNull (*), vs 30 ifu/cell AdRgl2 (#)

Figure 3.6

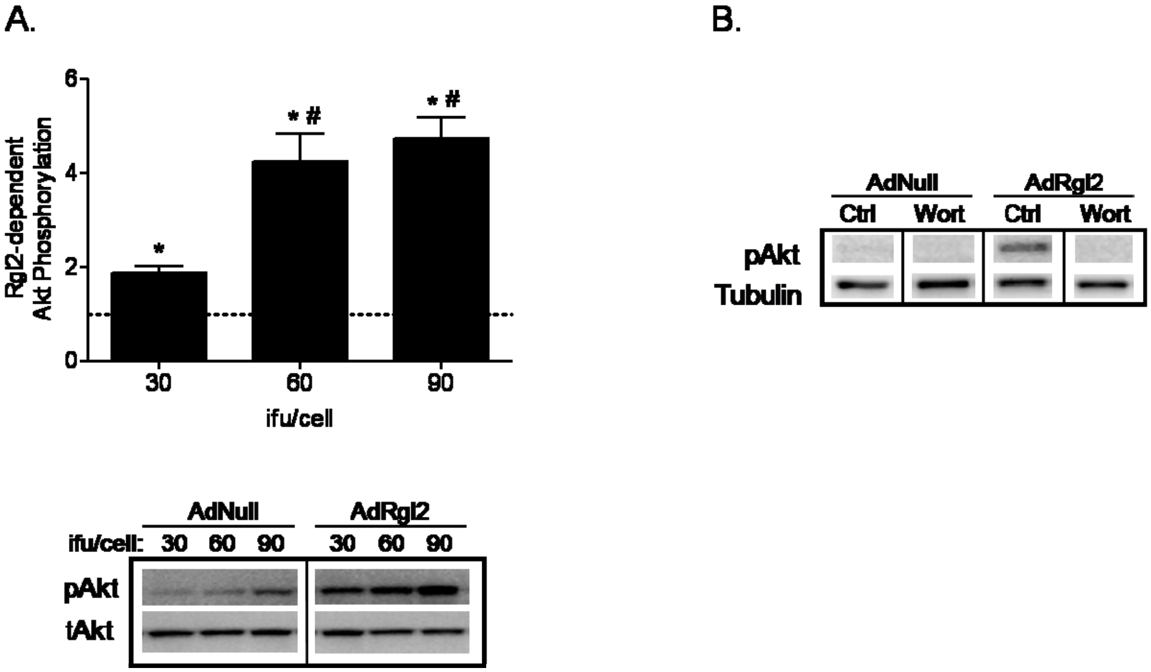

Increased Rgl2 expression enhances PI3-kinase activity. Panel A. Twenty-four hours after NRVMs were infected with increasing titers of AdNull or AdRgl2 (0-90 ifu/cell), cell lysates were prepared and resolved by SDS-PAGE followed by immunoblot analysis of kinase activation with the use of phospho-specific (Ser 473) and total Akt antibodies. Phosphorylated Akt (pAkt) values were normalized to total Akt (tAkt) values and AdRgl2 values were subsequently normalized to AdNull values. Significance was determined by wilcoxon sign-rank test for comparison to AdNull and one-way ANOVA for comparison of all other groups. Values are expressed as mean ± SEM, n=7-9. $p<0.05$ vs. AdNull (*), vs 30 ifu/cell AdRgl2 (#). **Panel B**. Twenty-four hours after infection with AdNull or AdRgl2 (90 ifu/cell), NRVMs were treated with 200 nM wortmannin (Wort) or vehicle for 30 minutes prior to lysate preparation. Lysates were prepared and kinase activation was assessed via immunoblotting with antibodies specific for pAkt (Ser 473) or tubulin. Western blots shown are representative of 3 independent experiments.

Figure 3.7

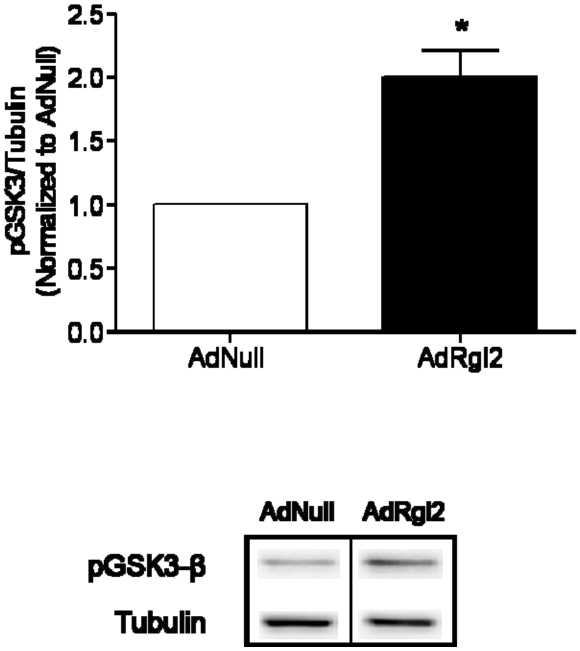

Increased Rgl2 expression enhances Akt activity. Twenty-four hours after infecting NRVMs with AdNull or AdRgl2 (90 ifu/cell), lysates were prepared and resolved by SDS-PAGE followed by immunoblot analysis of kinase activation with the use of antibodies specific for phospho-GSK3-β (Ser 9) and tubulin (a protein loading control). Phosphorylated GSK3-β (pGSK3-β) values were normalized to tubulin and AdRgl2 values were subsequently normalized to AdNull values. Significance was determined by one-sample t-test. Values are expressed as mean ± SEM, n=3. p=0.0168 vs. AdNull (*)

Figure 3.8

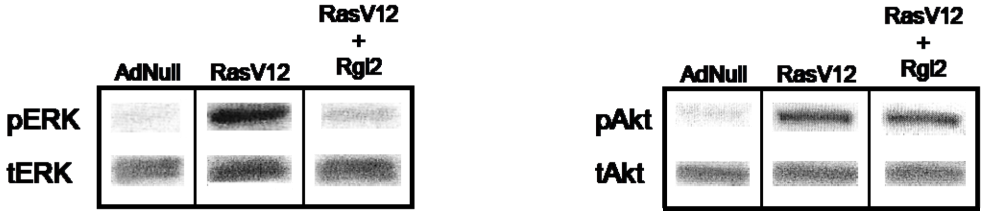
AdNull
RasV12
RasV12 + Rgl2
pERK
tERK
AdNull
RasV12
RasV12 + Rgl2
pAkt
tAkt

Rgl2 differentially regulates Ras-induced signaling. Twenty-four hours post-infection, lysates were prepared from NRVMs infected with AdNull, AdNull combined with AdRasV12, or AdRgl2 combined with AdRasV12. Proteins were resolved by SDS-PAGE and kinase activation was assessed by immunoblotting with antibodies specific for the following: pERK1/2 (Thr 202/Tyr 204), tERK1/2, pAkt (Ser 473), and tAkt. Western blots shown are representative of 8 independent experiments.

Figure 3.9

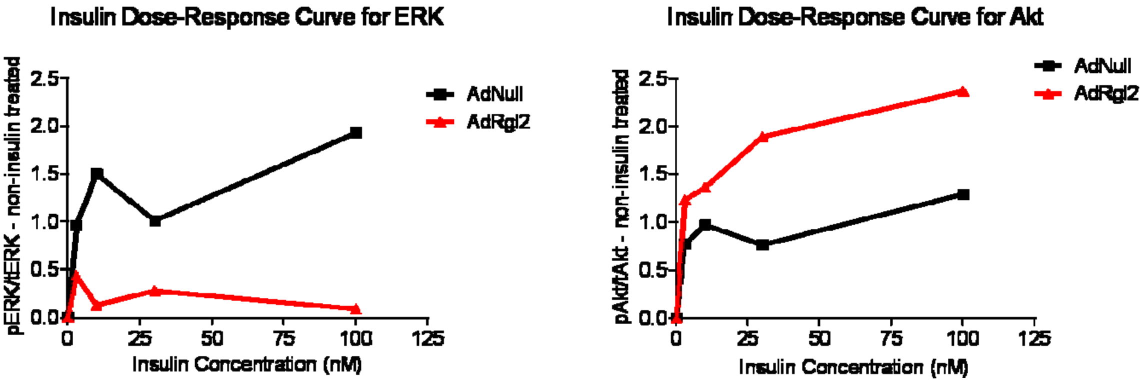

Dose-dependence of Rgl2-mediated changes in insulin signaling. Twenty-four hours after infection with AdNull or AdRgl2, NRVMs were treated with increasing concentrations of insulin (Ins; 0-100 nM) for 10 minutes. Lysates were prepared and kinase activation was assessed via immunoblotting with antibodies specific for the following: pERK1/2 (Thr 202/Tyr 204), tERK1/2, pAkt (Ser 473), and tAkt. Phosphorylated kinase was normalized to total kinase and the matching control (non-insulin treated) sample value was subtracted. Graphs represent results of a single experiment and are representative of 6 independent experiments.

Figure 3.10

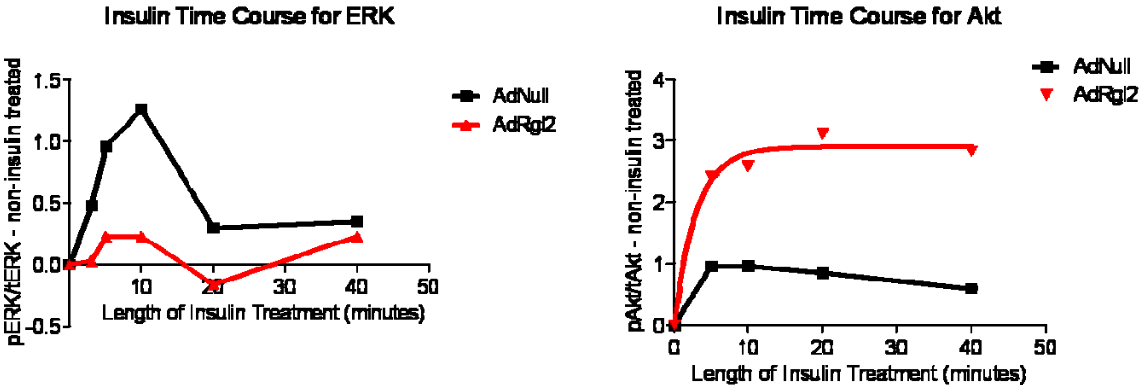

Time-dependence of Rgl2-mediated changes in insulin signaling. Twenty-four hours after infection with AdNull or AdRgl2, NRVMs were treated with 100 nM insulin (Ins) for increasing times (0-40 minutes). Lysates were prepared and kinase activation was assessed via immunoblotting with antibodies specific for the following: pERK1/2 (Thr 202/Tyr 204), tERK1/2, pAkt (Ser 473), and tAkt. Phosphorylated kinase was normalized to total kinase and the matching control (non-insulin treated) sample value was subtracted. Graphs represent results of a single experiment and are representative of 6 independent experiments.

Figure 3.11

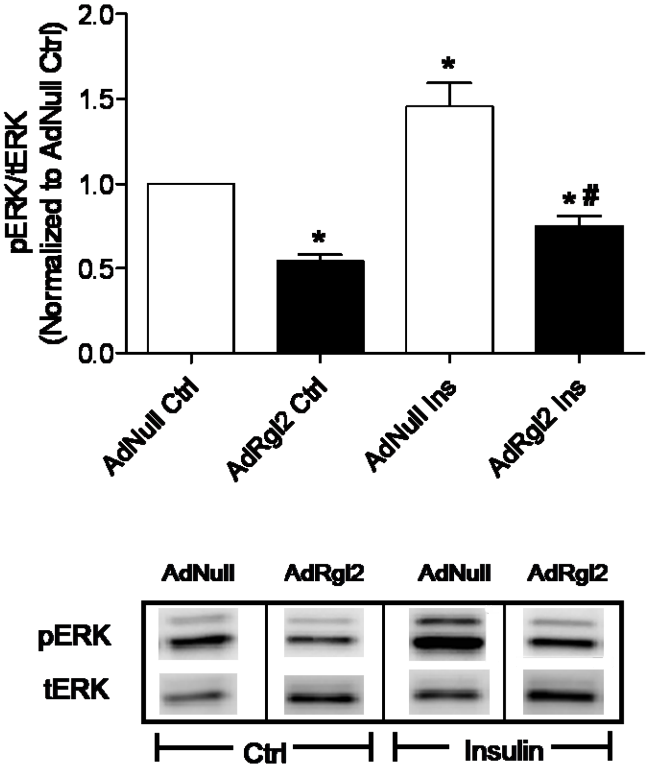

Rgl2 inhibits insulin-induced ERK1/2 phosphorylation. Twenty-four hours after infection with AdNull or AdRgl2, NRVMs were treated with 100 nM insulin (Ins) for 10 minutes or vehicle as control. Lysates were prepared and kinase activation was assessed via immunoblotting with antibodies specific for pERK1/2 (Thr 202/Tyr 204) or tERK1/2. Phosphorylated kinase was normalized to total kinase and all values were subsequently normalized to AdNull control. Significance was determined by wilcoxon sign-rank test for comparison to AdNull and one-way ANOVA for comparison of all other groups. Values are expressed as mean ± SEM, n=6. $p<0.05$ vs. AdNull control (*), $p<0.0001$vs insulin treated AdNull (#)

Figure 3.12

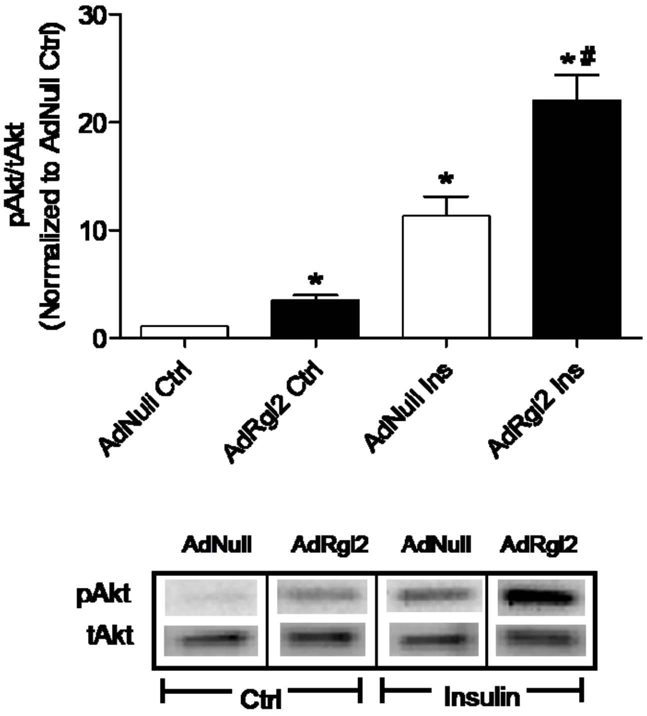

Rgl2 enhances insulin-induced PI3-kinase activity. Twenty-four hours after infection with AdNull or AdRgl2, NRVMs were treated with 100 nM insulin (Ins) for 10 minutes or vehicle as control. Lysates were prepared and kinase activation was assessed via immunoblotting with antibodies specific for pAkt (Ser 473) or tAkt. Phosphorylated kinase was normalized to total kinase and all values were subsequently normalized to AdNull control. Significance was determined by wilcoxon sign-rank test for comparison to AdNull and one-way ANOVA for comparison of all other groups. Values are expressed as mean ± SEM, n=6. p=0.0156 vs. AdNull control (*), p<0.0001 vs insulin treated AdNull (#)

Figure 3.13

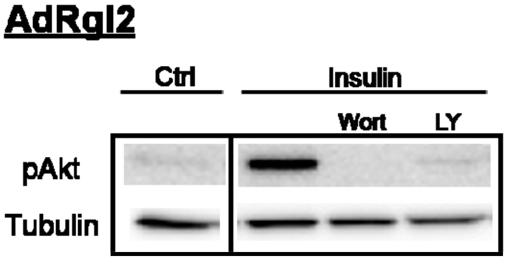

Rgl2-mediated enhancement of insulin-induced Akt phosphorylation is PI3-kinase-dependent. Twenty-four hours after infection with AdNull or AdRgl2, NRVMs were treated with 200 nM wortmannin (Wort), 50 μM LY-294002, or vehicle for 30 minutes prior to insulin treatment. NRVMs were then treated with 100 nM insulin (Ins) for 10 minutes or vehicle as control. Lysates were prepared and kinase activation was assessed via immunoblotting with antibodies specific for pAkt (Ser 473) or tubulin. Western blots shown are representative of 3 independent experiments.

Figure 3.14

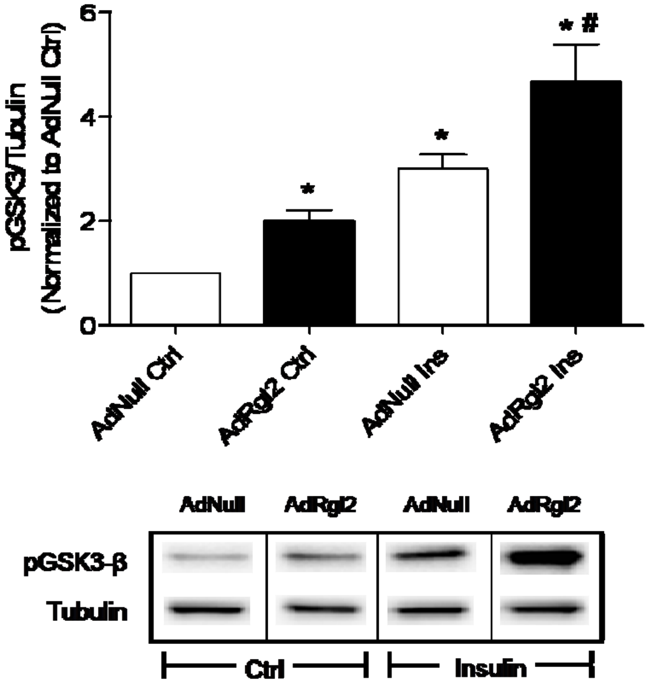

Rgl2 enhances insulin-induced Akt activity. Twenty-four hours after infection with AdNull or AdRgl2, NRVMs were treated with 100 nM insulin (Ins) for 10 minutes or vehicle as control. Lysates were prepared and kinase activation was assessed via immunoblotting with antibodies specific for pGSK3-β (Ser 9) or tubulin (protein loading control). Phosphorylated GSK3-β was normalized to tubulin and all values were subsequently normalized to AdNull control. Significance was determined by wilcoxon sign-rank test for comparison to AdNull and one-way ANOVA for comparison of all other groups. Values are expressed as mean ± SEM, n=4. $p<0.05$ vs. AdNull control (*), $p<0.05$vs insulin treated AdNull (#)

Figure 3.15

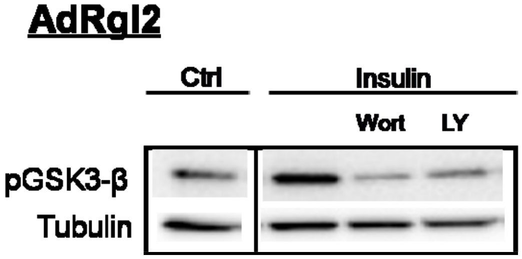

Rgl2-mediated enhancement of insulin-induced GSK3-β phosphorylation is PI3-kinase-dependent. Twenty-four hours after infection with AdNull or AdRgl2, NRVMs were treated with 200 nM wortmannin (Wort), 50 µM LY-294002, or vehicle for 30 minutes prior to insulin treatment. NRVMs were then treated with 100 nM insulin (Ins) for 10 minutes or vehicle as control. Lysates were prepared and kinase activation was assessed via immunoblotting with antibodies specific for pGSK3-β (Ser 9) or tubulin (protein loading control). Western blots shown are representative of 3 independent experiments.

Figure 3.16

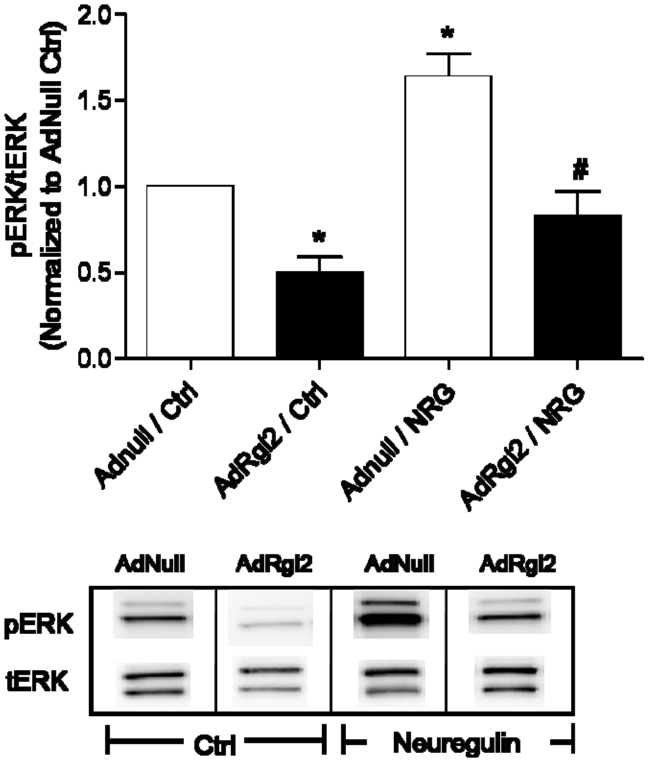

Rgl2 inhibits neuregulin-induced ERK1/2 phosphorylation. Twenty-four hours after infection with AdNull or AdRgl2, NRVMs were treated with 10 nM neuregulin-1 (NRG) for 10 minutes or vehicle as control. Lysates were prepared and kinase activation was assessed via immunoblotting with antibodies specific for pERK1/2 (Thr 202/Tyr 204) or tERK1/2. Phosphorylated kinase was normalized to total kinase and all values were subsequently normalized to AdNull control. Significance was determined by wilcoxon sign-rank test for comparison to AdNull and one-way ANOVA for comparison of all other groups. Values are expressed as mean ± SEM, n=5. p=0.0313 vs. AdNull control (*), p<0.0001 vs neuregulin treated AdNull (#)

Figure 3.17

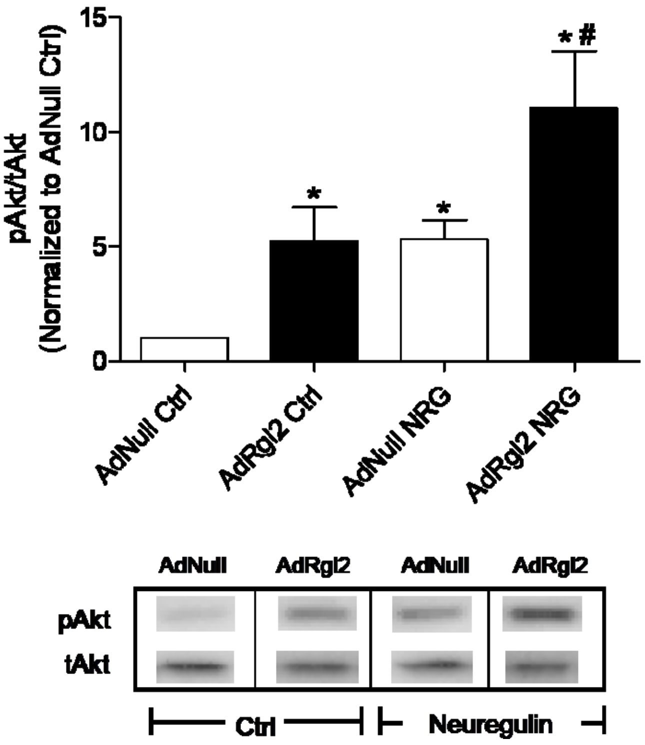

Rgl2 enhances neuregulin-induced PI3-kinase activity. Twenty-four hours after infection with AdNull or AdRgl2, NRVMs were treated with 10 nM neuregulin-1 (NRG) for 10 minutes or vehicle as control. Lysates were prepared and kinase activation was assessed via immunoblotting with antibodies specific for pAkt (Ser 473) or tAkt. Phosphorylated kinase was normalized to total kinase and all values were subsequently normalized to AdNull control. Significance was determined by wilcoxon sign-rank test for comparison to AdNull and one-way ANOVA for comparison of all other groups. Values are expressed as mean ± SEM, n=8. p<0.05 vs. AdNull control (*), vs neuregulin treated AdNull (#)

Figure 3.18

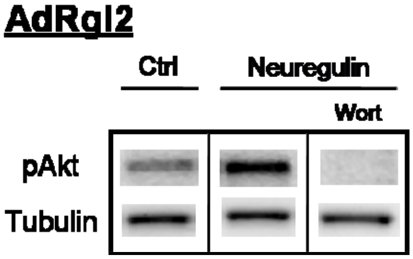

Rgl2-mediated enhancement of neuregulin-induced Akt phosphorylation is PI3-kinase-dependent. Twenty-four hours after infection with AdNull or AdRgl2, NRVMs were treated with 200 nM wortmannin (Wort) or vehicle for 30 minutes prior to insulin treatment. NRVMs were then treated with 10 nM neuregulin (NRG) for 10 minutes or vehicle as control. Lysates were prepared and kinase activation was assessed via immunoblotting with antibodies specific for pAkt (Ser 473) or tubulin. Western blots shown are representative of 3 independent experiments.

Figure 3.19

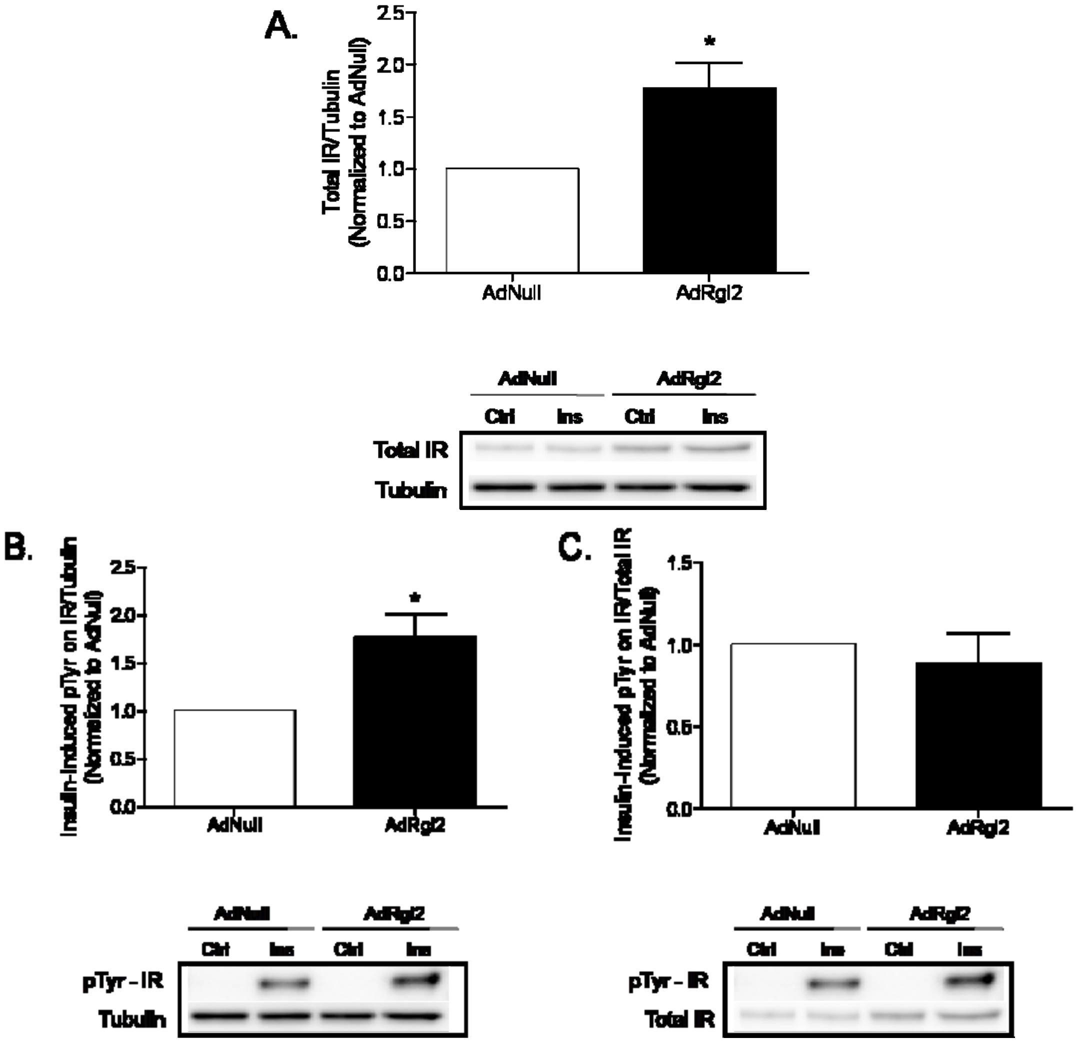

Rgl2 Increases IR-β Expression and Activation. Twenty-four hours after infection with AdNull or AdRgl2, NRVMs were treated with 100 nM insulin (Ins) for 3 minutes or vehicle as control. Lysates were prepared and proteins containing phosphorylated tyrosine residues (pTyr) were isolated from 500 µg of lysate protein by incubation with agarose conjugated anti-pTyr antibody. Isolated proteins (containing pTyr) were resolved by SDS-PAGE and immunoblotted for IR-β and pTyr. Whole cell lysates were also resolved by SDS-PAGE and immunoblotted for IR-β and tubulin. IR expression was assessed by normalizing IR-β from whole cell lysates to tubulin (**A**). IR activation was assessed by normalizing IR-β from pTyr isolated samples to either tubulin (**B**) or IR-β from whole cell lysates (**C**). All values were subsequently normalized to insulin treated AdNull values. Significance was determined by one-sample t-test. Values are expressed as mean ± SEM, n=5. p=0.032 vs. AdNull (*)

Figure 3.20

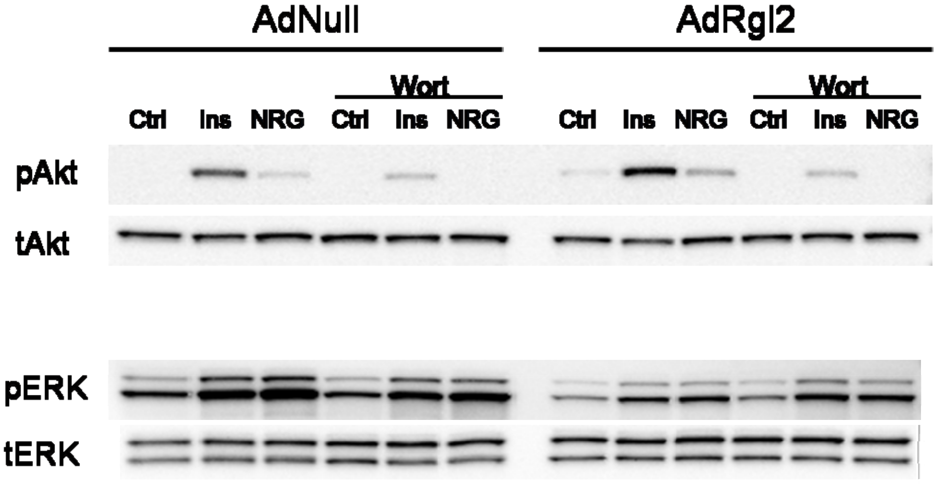
AdNull
AdRgl2
Wort
Wort
Ctrl
Ins
NRG
Ctrl
Ins
NRG
Ctrl
Ins
NRG
Ctrl
Ins
NRG
pAkt
tAkt
pERK
tERK

Enhanced Akt phosphorylation does not inhibit ERK1/2 phosphorylation in cardiomyocytes. NRVMs infected with AdNull or AdRgl2 were treated with 200 nM wortmannin (Wort) or vehicle for 30 minutes prior to agonist treatment. NRVMs were then treated with 100 nM insulin (Ins), 10 nM neuregulin-1 (NRG), or vehicle for 10 minutes. Lysates were prepared, protein resolved by SDS-PAGE, and kinase activation assessed by immunoblotting with the following antibodies: pERK1/2 (Thr 202/Tyr 204), tERK1/2, pAkt (Ser 473), and tAkt. Western blots shown are representative of 3 independent experiments.

Figure 3.21

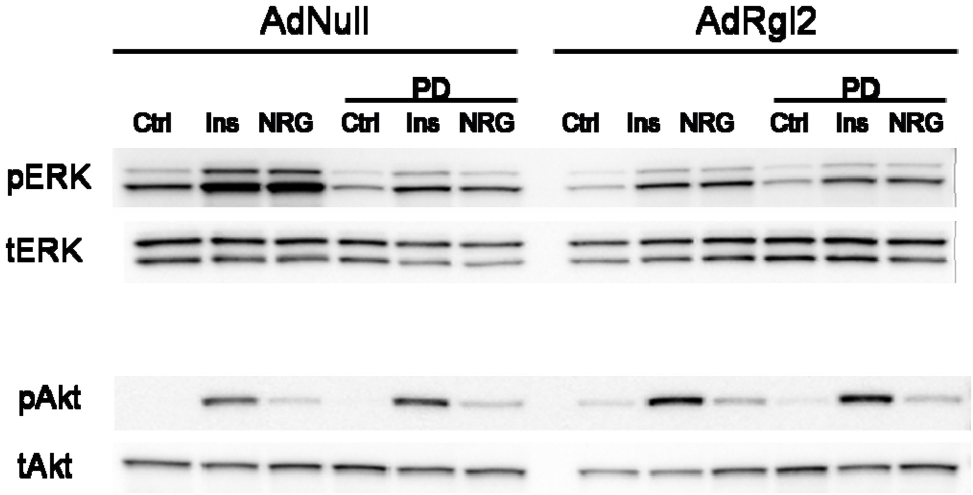

AdNull
AdRgl2
PD
PD
Ctrl
Ins
NRG
Ctrl
Ins
NRG
Ctrl
Ins
NRG
Ctrl
Ins
NRG
pERK
tERK
pAkt
tAkt

ERK1/2 inhibition does not enhance Akt phosphorylation in cardiomyocytes. NRVMs infected with AdNull or AdRgl2 were treated with 10 μM PD-98059 or vehicle for 30 minutes prior to agonist treatment. NRVMs were then treated with 100 nM insulin (Ins), 10 nM neuregulin-1 (NRG), or vehicle for 10 minutes. Lysates were prepared, protein resolved by SDS-PAGE, and kinase activation assessed by immunoblotting with the following antibodies: pERK1/2 (Thr 202/Tyr 204), tERK1/2, pAkt (Ser 473), and tAkt. Western blots shown are representative of 3 independent experiments.

Figure 3.22

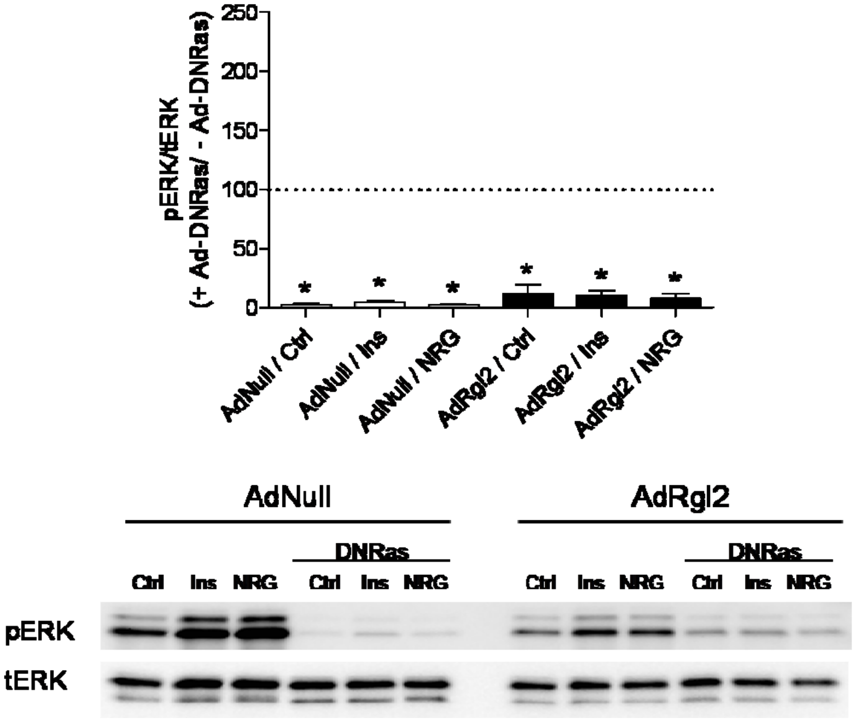

Dominant negative Ras (DNRas) mimics Rgl2-mediated inhibition of ERK1/2. NRVMs were infected with AdNull, AdNull combined with Ad-DNRas, AdNull combined with AdRgl2, or AdRgl2 combined with Ad-DNRas. Twenty-four hours post-infection, NRVMs were treated with 100 nM insulin (Ins), 10 nM neuregulin-1 (NRG), or vehicle for 10 minutes. Lysates were prepared, protein resolved by SDS-PAGE, and kinase activation assessed by immunoblotting with antibodies specific for pERK1/2 (Thr 202/Tyr 204) or tERK1/2. Phosphorylated kinase was normalized to total kinase and all values were then normalized to the appropriate samples not infected with Ad-DNRas (i.e. Adnull + Ad-DNRas treated with insulin was normalized to Adnull alone treated with insulin). Significance was determined by wilcoxon sign-rank test for comparison to samples not treated with AdDNRas and one-way ANOVA for comparison of all other groups. Values are expressed as mean ± SEM, n=4. p<0.0001 vs. corresponding sample not infected with Ad-DNRas (*)

Figure 3.23

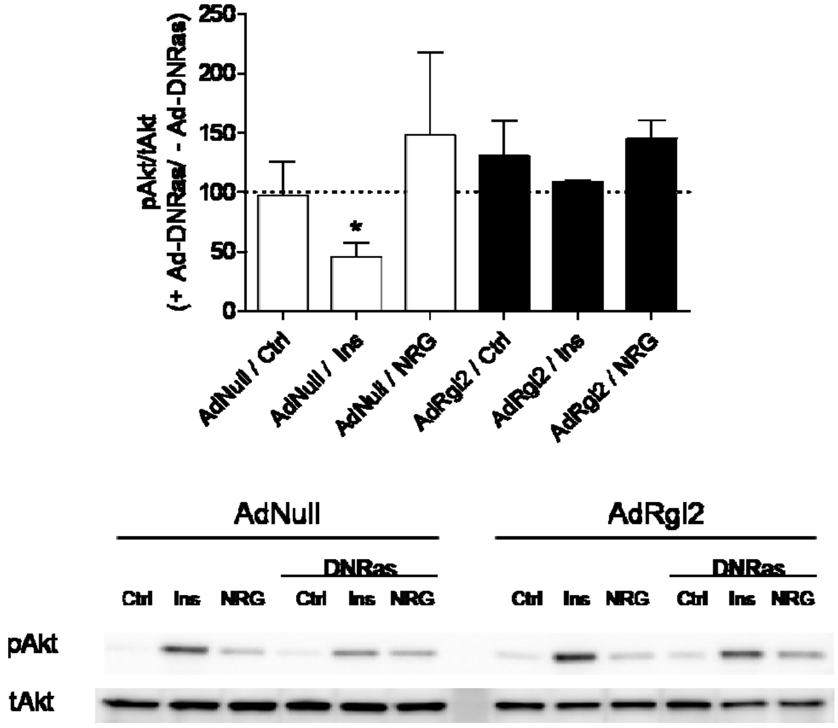

Rgl2-mediated Enhancement of Akt is not dependent on Ras. NRVMs were infected with AdNull, AdNull combined with Ad-DNRas, AdNull combined with AdRgl2, or AdRgl2 combined with Ad-DNRas. Twenty-four hours post-infection, NRVMs were treated with 100 nM insulin (Ins), 10 nM neuregulin-1 (NRG), or vehicle for 10 minutes. Lysates were prepared, protein resolved by SDS-PAGE, and kinase activation assessed by immunoblotting with antibodies specific for pAkt (Ser 473) or tAkt. Phosphorylated kinase was normalized to total kinase and all values were subsequently normalized to the appropriate samples not infected with Ad-DNRas (i.e. Adnull + Ad-DNRas treated with insulin was normalized to Adnull alone treated with insulin). Significance was determined by wilcoxon sign-rank test for comparison to samples not treated with AdDNRas and one-way ANOVA for comparison of all other groups. Values are expressed as mean ± SEM, n=4. p<0.05 vs. corresponding sample not infected with Ad-DNRas (*)

Figure 3.24

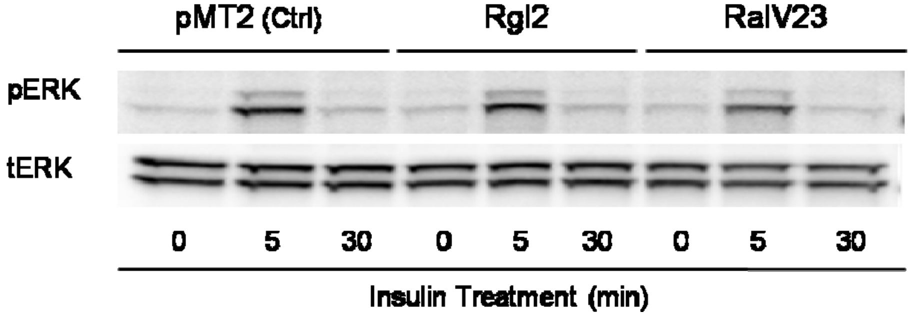
pMT2 (Ctrl)
Rgl2
RalV23
pERK
tERK
0
5
30
0
5
30
0
5
30
Insulin Treatment (min)

Rgl2 and Ral have no effect on ERK1/2 phosphorylation in transfected HEK-293 cells. After reaching 50% confluency, HEK-293 cells were transfected with cDNA encoding pMT2 (vector control), Rgl2, or RalV23. Forty-eight hours after transfection, cells were stimulated for 5 or 30 minutes with 100 nM insulin (Ins) or vehicle as control. Lysates were prepared, protein resolved by SDS-PAGE, and kinase activation assessed by immunoblotting with antibodies specific for pERK1/2 (Thr 202/Tyr 204) or tERK1/2. Western blots shown are representative of 4 independent experiments.

Figure 3.25

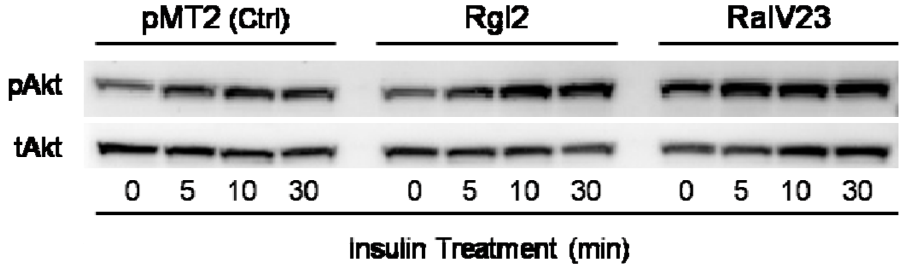

RalV23 mimics Rgl2-mediated enhancement of insulin-induced Akt phosphorylation in transfected HEK-293 cells. After reaching 50% confluency, HEK-293 cells were transfected with cDNA encoding pMT2 (vector control), Rgl2, or RalV23. Forty-eight hours after transfection, cells were stimulated for 5, 10, or 30 minutes with 100 nM insulin (Ins) or vehicle as control. Lysates were prepared, protein resolved by SDS-PAGE, and kinase activation assessed by immunoblotting with antibodies specific for pAkt (Ser 473) or tAkt. Phosphorylated kinase was normalized to total kinase and all values were subsequently normalized to pMT2 control. Western blots shown are representative of 4 independent experiments.

SECTION IV. DISCUSSION

A key component of cardiovascular signaling that is involved in both positive and negative regulation of cardiomyocyte function is the small molecular weight G-protein, Ras [44, 49]. Ras and its effectors have been extensively studied in other cell systems, but their roles in the myocardium continue to be elucidated [44, 97]. Using Ras as bait, a yeast-2-hybrid screen of a human heart cDNA library was performed to search for novel Ras interacting proteins in the myocardium. In this study, the only protein identified to interact with Ras was the RalGEF family member, Rgl2 [83]. Because of this specific Ras-Rgl2 interaction in the heart and the need for further study of G-protein signaling in the myocardium, the focus of my project was related to delineating the potential importance of Rgl2 in regulating cardiomyocyte signaling pathways.

I chose neonatal rat ventricular myocytes (NRVMs), a well-used model for studying cardiomyocyte signaling, to begin to elucidate the potential importance of Rgl2 in cardiomyocytes [84]. Adenoviral infection was used as the method of gene delivery because standard transfection approaches achieve only up to 10% efficiency in NRVMs [99]. Therefore, I used the AdRgl2 virus to increase Rgl2 expression in the cardiomyocytes as a gain-of-function model.

The first goal of my studies was to characterize the AdRgl2 virus so that the method could be optimized before studying the effect of Rgl2 on cardiomyocyte signaling. To this end, I varied the adenoviral titer to determine the concentration of virus needed to give maximal Rgl2 expression and to also determine the infection efficiency of the virus. Infection of NRVMs with AdRgl2 resulted in a titer-dependent increase in Rgl2 expression with the 60-90 ifu/cell titers achieving a maximal increase of 400-fold above control virus (AdNull) infected cells (**Figure 3.1**); no further increase was observed with viral titers greater than 90 ifu/cell. However, higher adenoviral titers induced observable toxicity which made quantification of Rgl2 levels by immunoblotting difficult. Biochemical analysis of signaling pathways using my approach requires that cells uniformly express the transgene. Therefore, I examined the percentage of NRVMs infected with AdRgl2 and discovered that 90 ifu/cell of the virus infected a majority (> 70%) of cardiomyocytes (**Figure 3.2**). Furthermore, co-localizing the transfected Rgl2 stain with a nonspecific membrane stain (WGA) allowed me to ascertain that a portion of the transfected Rgl2 is located at the plasma membrane where it may interact with its activator (Ras) and effector (Ral) as well as other molecules [76]. One limitation of this approach was that some WGA staining was observed in the cytosolic portion of the cell. This likely reflects WGA staining of glycosylated proteins located at other sites (i.e. endoplasmic reticulum or golgi) [100, 101]. It is currently unclear if Rgl2 localization to these intracellular membranes alters its function.

After determining the proper concentration of AdRgl2 to infect NRVMs, verifying protein expression, and finding that it was expressed in areas of the cell where it was likely to be active; I confirmed that the transduced protein was functionally active. The best characterized function of Rgl2 is the activation of the small molecular weight G-protein, Ral [76]. Therefore, the effect of Rgl2 on Ral activation was examined using a binding assay in which agarose-bound GST-RalBP1-BD was used to isolate active, GTP-bound Ral from cell lysates. As expected, Ral-GTP levels were increased in AdRgl2 infected NRVMs (**Figure 3.3**) confirming that the adenoviral-transduced Rgl2 was expressed and functional. The magnitude of Ral activation in AdRgl2 infected NRVMs (2-fold above AdNull) was similar to that reported by Kawai et. al. in which a hypertrophic agonist (cardiotrophin-1) was used to increase RalGDS mRNA levels by greater than 100-fold [82]. The findings that a large increase in RalGEF mRNA or protein yields approximately a 2-fold increase in Ral-GTP suggests that Ral expression may be the limiting factor for Ral-GTP formation. However, the time course of Rgl2-mediated Ral activation was not examined in my studies so I do not know if the 2-fold increase in Ral-GTP levels was representative of maximal Ral activation. Another potential explanation for the 2-fold increase in Ral activation by RalGEFs is that activators of RalGEFs (such as Ras) are limiting. Therefore, it is possible that not all expressed Rgl2 was activated in my experiments. To examine these possibilities, future studies should investigate the effect of increased Rgl2 expression on Ral-GTP formation over time and examine RalGEF activity (indexed by Ral-GTP formation) in RasV12 expressing cells.

Previous studies indicate that Rgl2 requires Ras-GTP for activation [75, 76]. The observation that Ral activation was increased in the AdRgl2 infected cardiomyocytes indicates that Rgl2 was active. Therefore, I examined whether Ras activation was altered in adenoviral-infected NRVMs with a method analogous to that used to assess Ral activation. My results demonstrate that increasing Rgl2 expression in NRVMs induced an increase in Ras-GTP levels (**Figure 3.4**). The increase in Ras activation cannot be explained by Rgl2-mediated guanine nucleotide exchange (GEF) on Ras as Wolthuis et. al. have previously demonstrated that Rgl2 only has GEF activity for Ral [76]. However, increased expression of RalGEF-RBD's has been shown to disrupt the interaction of a Ras inhibitor, (the RasGAP, NF1) with Ras [74]. Decreasing interaction of the GAP with Ras slowed Ras GTPase activity and induced an increase in Ras-GTP levels. Therefore, the increased Ras activation that I observed with increased Rgl2 expression could be indicative of Rgl2-mediated inhibition of Ras-RasGAP interaction.

Binding of GTP to Ras promotes Ras interaction with and activation of its effectors. The best characterized Ras effectors are Raf, PI3-kinase, and the RalGEFs [38]. Therefore, by enhancing Ras-GTP levels, Rgl2 could potentially increase activation of Raf-MEK-ERK as well as PI3-kinase-Akt pathways. To examine this possibility, I examined the effect of increased Rgl2 expression on ERK1/2 and Akt phosphorylation as indices of their respective activation. Results of these studies (**Figures 3.5, 3.6, and 3.7**) indicate that Rgl2 differentially regulates kinase signaling in a dose-dependent manner. Specifically, I found that increased Rgl2 expression inhibited Raf-MEK-ERK signaling (**Figure 3.5**), but enhanced PI3-kinase-Akt signaling (**Figure 3.6**). Although kinase phosphorylation is often used as an index of kinase activation, an increase in kinase phosphorylation does not always induce measurable changes in downstream effectors. Therefore, to confirm that the increase in Akt phosphorylation translated into an increased downstream effect, I examined the phosphorylation of a well characterized Akt substrate molecule, glycogen synthase kinase-3β (GSK3-β) [56]. GSK3-β is a serine/threonine kinase that was first identified as a regulator of glucose metabolism because it negatively regulates glycogen synthase to inhibit glycogen synthesis [88, 102]. However, it has more recently been implicated in the regulation of apoptosis, cardiac development, and pathological hypertrophy [89, 90, 103]. Akt negatively regulates GSK3-β by phosphorylation at the serine-9 residue which inhibits interaction of GSK3-β with its substrates [103]. When the effect of Rgl2 on GSK3-β serine-9 phosphorylation was analyzed, I found that GSK3-β phosphorylation was increased, indicating a decrease in GSK3-β activity (**Figure 3.7**). The parallel increase in Akt phosphorylation and GSK3-β phosphorylation indicates that activation of PI3-kinase-Akt induces measurable changes in downstream effectors. Moreover, these results are consistent with the possibility that Rgl2-mediated inhibition of GSK3-β via enhanced Akt phosphorylation could induce changes in cardiomyocyte metabolism, development, and survival [89, 90, 104].

Raf-MEK-ERK signaling is thought to regulate cardiomyocyte survival and function. For example, ERK1/2 is generally associated with anti-apoptotic cardiomyocyte signaling [69]. Studies of phenylephrine-induced cardiomyocyte hypertrophy have elucidated a role for ERK1/2 in regulating gene expression [105]. In contrast, ERK1/2 was not a component of Rgl2-mediated gene regulation. Interestingly, pharmacological MEK inhibition caused a small increase in Rgl2-induced ANF reporter gene expression [83]. ERK1/2 did not contribute to phenylephrine-induced reorganization of the actin cytoskeleton [105]. From this information, it is possible that Rgl2-mediated inhibition of ERK1/2 may alter cardiomyocyte survival. However, ongoing studies indicate that this is not the case. In addition, Rgl2-mediated inhibition of ERK1/2 could potentially alter cardiomyocyte gene expression, but would not be expected to regulate cytoskeletal changes. Therefore, further studies should assess the role of ERK inhibition in Rgl2-mediated changes in cardiomyocyte gene expression.

PI3-kinase-Akt signaling is implicated in the regulation of glucose metabolism due, in part, to Akt-mediated inhibition of GSK3-β as well as the regulation of cardiomyocyte survival and function (**Introduction Figure 1.5**) [56, 103]. Although acute activation of the PI3-kinase-Akt signaling cascade is cardioprotective, new evidence demonstrates that chronic Akt signaling can be detrimental to the myocardium. For example, transgenic mice expressing cardiac-specific, constitutively active Akt have increased damage due to ischemia-reperfusion-induced injury [106]. In addition, Akt activation is increased in the failing human heart [107]. Therefore, future studies must examine the time-dependent effects of Rgl2 so that the physiological outcome of Rgl2-mediated changes in cardiomyocyte signaling can be elucidated.

Given that increased Rgl2 expression promoted Ras-GTP, but differentially regulated ERK1/2 and Akt pathways, I determined whether Rgl2 would similarly regulate these pathways when Ras was specifically activated in NRVMs. To this end, constitutively active, GTPase deficient Ras (RasV12) was used to induce cardiomyocyte signaling in the presence or absence of increased Rgl2 expression. The results of these studies (**Figure 3.8**) yielded results similar to those obtained when Rgl2 was expressed alone. Specifically, Rgl2 inhibited Ras-induced ERK1/2 phosphorylation. RalGEF-RBDs have been shown to disrupt the interaction of Ras with Raf [73, 74, 96]. Therefore, a potential mechanism for Rgl2-mediated inhibition of ERK1/2 phosphorylation may involve the disruption of Ras-Raf interaction in a manner similar to that described for disrupting the Ras-RasGAP interaction.

Although Rgl2 effects on ERK1/2 phosphorylation were similar in unstimulated and AdRasV12 infected NRVMs, Rgl2 did not increase Ras-induced Akt phosphorylation as it did in unstimulated cells (**Figure 3.8**). One explanation for the lack of Rgl2-mediated

Akt stimulation in RasV12 expressing NRVMs is that RasV12 induced maximal Akt phosphorylation through the same signaling pathway induced by increased Rgl2 expression. This would prevent detection of any further increase by Rgl2. Because the use of RasV12 may have induced a “supraphysiologic” Akt response, I examined the effect of Rgl2 on Akt phosphorylation using a more physiological stimulus (i.e. growth factors). Although many growth factors are known to stimulate the phosphorylation of both Akt and ERK1/2, insulin is a physiologically important stimulator of Akt phosphorylation in humans [108]. When insulin signaling is reduced in conditions of insulin resistance, Akt phosphorylation is also reduced while ERK1/2 phosphorylation is maintained in some tissues [109-111]. Therefore, I chose to use insulin as a physiological stimulator of PI3-kinase-Akt and Raf-MEK-ERK signaling in the cardiomyocytes.

Initial studies were performed to determine the appropriate insulin concentration and length of stimulation to induce maximal Akt and ERK1/2 phosphorylation in the cardiomyocytes. These studies also investigated if Rgl2 regulated insulin-induced kinase signaling by changing the sensitivity of cells to insulin (i.e. insulin dose-dependence) or by changing the kinetics of insulin-induced activation/deactivation of signaling pathways. The concentration-dependent and time-dependent studies demonstrated that treating NRVMs with 100 nM treatment for 10 minutes induces a maximal plateau of both ERK1/2 and Akt phosphorylation (**Figures 3.9 and 3.10**). Furthermore, Akt phosphorylation was elevated at all time points and insulin concentrations in AdRgl2 infected NRVMs while ERK1/2 phosphorylation was inhibited. The finding that Rgl2 altered ERK1/2 and Akt phosphorylation at all time points and insulin concentrations indicates that these changes do not result from altering the interaction between insulin and its receptor nor from changes in the kinetics (activation/deactivation) of the signaling response.

The finding that Rgl2 increased insulin-induced, Akt phosphorylation (**Figure 3.12**) is similar to that of Hao et. al. who observed ablation of insulin-induced Akt phosphorylation in a mammary epithelial cell line (MCF-10A) expressing shRNA to inhibit RalGDS expression [112]. However, the mechanism proposed for RalGDS-induced Akt phosphorylation may differ from that of Rgl2. In the mechanism proposed by Hao, RalGDS mediated Akt phosphorylation via a PI3-kinase-independent mechanism that couples Akt to PDK through the scaffolding protein, JIP1. However, my data indicate that Rgl2-mediated Akt phosphorylation depends upon PI3-kinase (**Figure 3.13**). The coupling of Rgl2 to PI3-kinase-Akt signaling will need to be examined further to determine the mechanism for enhanced activation.

To determine the extent to which enhanced Akt phosphorylation was specific to insulin signaling, I determined if Rgl2 enhanced PI3-kinase-Akt signaling was induced by another RTK. For this, I treated cardiomyocytes with NRG to study the effect of Rgl2 on the signaling of another subfamily of RTKs (ErbB receptors). NRG is an epidermal growth factor ligand family member that functions in cardiac development and survival [113, 114]. NRG binding to ErbB3 and ErbB4 induces receptor dimerization, phosphorylation, and subsequent signaling [93, 115]. Of the different ErbB isoforms, only ErbB2 and ErbB4 are expressed in neonatal as well as adult cardiomyocytes. Once dimerized, the ErbB2/4 complex trans-autophosphorylates tyrosine residues within the cytoplasmic domain of the receptor and these phosphorylated residues allow the binding of SH2 domain containing effectors such as Src, Grb2/SOS, and PI3-kinase [91]. These effectors may then induce signaling within the cell. Like insulin, ErbB2/4-mediated activation of PI3-kinase-Akt signaling is shown to play a key role in cardioprotection [114, 116].

Similar to the insulin studies described above, initial studies with NRG were performed to determine the appropriate time and concentration to induce maximal ERK1/2 and Akt phosphorylation in cardiomyocytes. Results of these studies (unpublished results) demonstrated that a 10 nM NRG treatment for 10 minutes was sufficient to stimulate both Akt and ERK1/2 phosphorylation. Therefore, these conditions were used in all further studies. Importantly, my results demonstrate that increasing Rgl2 expression inhibits NRG-stimulated ERK1/2 phosphorylation to an extent that was also seen in insulin stimulated cells (**Figure 3.16**). In addition, Rgl2 enhanced NRG-induced Akt phosphorylation (**Figure 3.17**). However, the Rgl2-dependent increase in NRG-induced Akt phosphorylation appeared to be additive rather than synergistic as was the case for insulin. The lack of synergy between NRG/ErbB and Rgl2-induced Akt phosphorylation suggests that Rgl2 may have an effect on insulin-induced signaling that is receptor-specific.

Synergistic enhancement of insulin-induced PI3-kinase signaling in AdRgl2 infected NRVMs could result from an increase in IR expression and/or activation (tyrosine phosphorylation). Increased IR expression has previously been shown to regulate insulin signaling [117, 118]. To determine if the difference in the Rgl2-mediated regulation of NRG and insulin signaling occurred at the level of the receptor, I studied the effect of

Rgl2 on IR expression and activation. As hypothesized, Rgl2 increased IR expression with a parallel increase in IR activation (as indexed by tyrosine phosphorylation on the IR; **Figure 3.19**). The increase in IR expression and activation is consistent with the enhanced PI3-kinase-Akt signaling observed in the insulin time and dose-dependence experiments if the IR is limiting.

Rgl2 differentially regulated basal, Ras-induced, and RTK-induced ERK1/2 and PI3-kinase-Akt signaling in NRVMs. Therefore, my next goal was to study the mechanism by which Rgl2 alters kinase signaling within cardiomyocytes. I specifically tested the possibility that crosstalk between Raf-MEK-ERK and PI3-kinase-Akt pathway, Ras inhibition, or Ral activation could mediate the enhanced Akt phosphorylation and inhibited ERK1/2 phosphorylation observed with increased Rgl2 expression.

The PI3-kinase-Akt cascade and the Raf-MEK-ERK cascade have been shown to negatively regulate each other in non-cardiomyocyte cell systems [94, 95]. For example in an intestinal epithelial cell line (Caco-2/15 cells), increasing Akt activation either by adenoviral-mediated expression of constitutively active Akt or by increasing intracellular calcium decreased levels of phosphorylated ERK1/2 and MEK [94]. This Akt-mediated inhibition of ERK1/2 was ablated with the use of the pharmacological inhibitor of PI3-kinase, LY-294002. Conversely, inhibiting ERK1/2 phosphorylation by using pharmacological inhibition of MEK (U0126) conferred an increase in hydrogen peroxide-mediated Akt phosphorylation in primary cultures of rabbit renal proximal tubular cells [95]. Because the PI3-kinase-Akt cascade and the Raf-MEK-ERK cascade can negatively regulate each other, I examined the potential role for crosstalk between these two cascades in mediating the differential effects of Rgl2 on cardiomyocyte signaling.

When NRVMs were treated with the pharmacological inhibitor of PI3-kinase signaling, wortmannin (Wort), basal and RTK-induced Akt phosphorylation were inhibited as expected. However, **Figure 3.20** also illustrates that there was no effect of wortmannin on ERK1/2 phosphorylation which indicates that activation of PI3-kinase-Akt signaling does not mediate Rgl2-induced inhibition of either basal or RTK-induced ERK1/2 phosphorylation and argues against the possibility of regulating crosstalk between these two pathways. Conversely, ERK1/2 phosphorylation was ablated in NRVMs treated with the pharmacological inhibitor of MEK, PD-98059, while no change in Akt phosphorylation was observed (**Figure 3.21**). There was also no basal regulation of these pathways resulting from crosstalk. Thus, inhibition of Raf-MEK-ERK signaling does not appear to allow for the Rgl2-mediated enhancement of basal or RTK-induced

Akt phosphorylation. Furthermore, crosstalk between the Raf-MEK-ERK and PI3-kinase-Akt cascades does not appear to be the mechanism underlying differential regulation of these pathways by Rgl2.

The next potential mechanism for the differential regulation of ERK1/2 and Akt by Rgl2 that I explored was that the effects of Rgl2 expression might be mediated, in part, by inhibiting Ras-effector coupling and subsequent signaling. This mechanism is supported by my results showing that activation of the Raf-MEK-ERK cascade and RasV12-induced ERK1/2 phosphorylation were decreased in cardiomyocytes expressing increased Rgl2. Additional support for this hypothesis is derived from the finding that the RBDs of RalGEF molecules inhibit Ras-Raf interaction and subsequent Raf activation [74, 96]. Therefore, I determined the effect of Rgl2 on RTK-induced signaling when Ras-Ras effector coupling and activation was disrupted by co-infecting cardiomyocytes with adenoviruses encoding Rgl2 and dominant-negative Ras (DNRas). DNRas has a mutation that causes it to preferentially bind GDP so that it cannot interact with Ras effectors, but will inhibit endogenous Ras activation (and thereby prevent interaction with effectors) by competitively blocking its interaction with RasGEFs.

My results (**Figure 3.22**) demonstrate that DNRas prevented RTK-induced ERK1/2 phosphorylation in cardiomyocytes in both AdNull and AdRgl2 infected NRVMs. The ability of Rgl2 to mimic the effect of DNRas with regard to ERK1/2 phosphorylation is consistent with the possibility that Rgl2 uncouples Ras-Raf interaction. In contrast, expression of DNRas decreased insulin-induced Akt phosphorylation in NRVMs expressing endogenous levels of Rgl2, but not in NRVMs expressing increased Rgl2 (**Figure 3.23**). This indicates that Ras plays a role in insulin-induced Akt phosphorylation in cardiomyocytes. However, the finding that DNRas-induced inhibition of Akt phosphorylation was not observed in NRVMs expressing increased Rgl2 suggesting that Ras is not involved in Rgl2-mediated enhancement of Akt phosphorylation. Together, results using Ad-DNRas support the possibility that Rgl2 inhibits ERK1/2 phosphorylation by interfering with Ras-Raf interaction and that Ras mediates, in part, insulin-induced Akt phosphorylation. However, Rgl2-mediated activation of PI3-kinase-Akt signaling is independent of Ras or downstream of Ras.

The last potential mechanism for Rgl2-mediated regulation of ERK1/2 and Akt that I explored was the role of Ral in mediating Rgl2-induced regulation of kinase signaling in cardiomyocytes. An increase in Ral activation was observed in NRVMs expressing increased levels of Rgl2. Therefore, Rgl2-mediated activation of Ral may mediate the effects of Rgl2 on cardiomyocyte signaling. Because adenoviruses to induce expression of constitutively active Ral (RalV23) were not available, I used an alternative cell model system for this set of experiments. The human embryonic kidney-293 cell line (HEK-293) is frequently utilized to elucidate signaling mechanisms as it is easily maintained, amenable to transfection by a variety of methods which typically yield high transfection efficiencies, and yields highly reproducible results [119]. Therefore, HEK-293 cells were used to determine if Ral activation would mimic the effects of Rgl2 on kinase signaling.

My results demonstrate that Rgl2 and RalV23 did not affect insulin-induced ERK1/2 phosphorylation in HEK-293 cells (**Figure 3.24**). This contrasts with Rgl2-mediated inhibition of ERK1/2 phosphorylation in NRVMs. Because HEK-293 cells are a proliferative cell line, the mechanism by which ERK1/2 is activated in these cells may be different than the mechanism of activation in the non-proliferative NRVMs. An alternative, and more likely, explanation is that the transfection efficiency achieved was too low to detect a decrease in ERK1/2 phosphorylation in the HEK-293 cell population.

Similar to results obtained in NRVMs, both Rgl2 and RalV23 increased both basal and insulin-induced Akt phosphorylation in the HEK-293 cell line (**Figure 3.25**). The ability of RalV23 to mimic Rgl2 suggests that Ral-GTP may mediate Rgl2's enhancement of both insulin-induced and basal Akt phosphorylation. Additional studies need to be conducted in NRVMs using Ral adenoviruses to confirm the role of Ral in Rgl2-mediated enhancement of Akt phosphorylation. Similar to the studies performed with Ad-DNRas (**Figures 3.22 and 3.23**), a key experiment to determine which effects of Rgl2 are dependent upon Ral activity will be to induce expression of a dominant-negative Ral mutant (RalN28) in combination with increased Rgl2 expression in NRVMs.

Summary

Taken together, my results suggest a model (**Figure 4.1**) for Rgl2-mediated regulation of cardiomyocyte signaling. My model predicts that competition between the RBD of Rgl2 disrupts Ras-Raf and Ras-RasGAP interaction which results in decreased ERK phosphorylation and increased levels of Ras-GTP. Thus, downstream Ras signals may be regulated, in part, by altering the relative expression of Ras effectors as well as the co-localization of Ras with specific effector molecules. Rgl2 also most likely inhibits Ras interaction with PI3-kinase, but as the studies with Ad-DNRas demonstrated, Ras does not appear to be a major contributor to PI3-kinase-Akt signaling in cardiomyocytes. In addition to interacting with Ras, Rgl2 interacts with and activates Ral via its CDC25 domain. My results indicate that Ral activation promotes the PI3-kinase-dependent activation of Akt which increases phosphorylation of its downstream effector, GSK3-β. It is also likely that Ral activation regulates additional pathways (i.e. vesicular trafficking) that have yet to be studied.

The physiologic consequence of enhanced Rgl2 signaling is difficult to predict. However, some predictions can be made based upon what is known about Raf-MEK-ERK and PI3-kinase-Akt-GSK3-β signaling. ERK1/2 is thought to regulate cardiomyocyte apoptosis and gene expression. However, ERK1/2 is not required for cytoskeletal rearrangements in cardiomyocytes. Thus, I would predict that by inhibiting ERK1/2, Rgl2 would decrease gene expression without affecting the cytoskeleton. Enhanced activation of PI3-kinase-Akt signaling in cardiomyocytes increases cardiomyocyte size, metabolism, and survival. However, this may depend on the magnitude or duration of PI3-kinase-Akt activation as other studies show that chronic activation of Akt can be detrimental to the myocardium. Because AdRgl2 decreased susceptibility to apoptosis in both NRVMs and transgenic animals (mice with a cardiac-specific increase in Rgl2 expression), I predict that increased Rgl2-Ral activation would be cardioprotective and potentially a viable target in cardiovascular disease.

Diabetes is an important pathological setting in which insulin-induced PI3-kinase-Akt signaling is altered. Diabetic patients have many cardiovascular complications associated with increases in apoptotic signaling including increased myocardial damage during ischemic events and the onset of Diabetic Cardiomyopathy [120]. Therefore, by enhancing insulin-induced PI3-kinase-Akt signaling, Rgl2 may be able to protect against diabetes-associated cardiovascular dysfunction.

Limitations

A central limitation of my studies was that a gain-of-function (increased Rgl2 expression) approach was used to examine Rgl2 signaling. Increasing protein expression can sometimes promote interactions and effects that would not occur at physiological expression levels. Importantly, my results are consistent with other studies involving RalGDS, suggesting that Rgl2 may serve as the primary RalGEF family member in cardiomyocytes. Nonetheless, a gain-of-function model is the most commonly used method for studying proteins of unknown function and to which limited reagents are available. My goal was to study Rgl2 function in NRVMs, but the role of Rgl2 signaling in the myocardium is unknown and few Rgl2 specific reagents are available. Therefore, the most logical method for studying the effect of Rgl2 in cardiomyocytes was the gain-of-function model.

Another limitation is that the time at which transfected Rgl2 becomes activated is unknown and not subject to acute regulation. Thus, it is possible that increased Rgl2 expression and function results in compensatory secondary changes in NRVMs. To determine the time and consequence of Rgl2 activation, experiments to determine the time course for Rgl2-mediated changes in Akt phosphorylation, ERK1/2 phosphorylation, Ral activation, and Ras activation should be performed. If Ras and/or Ral activation occurs prior to the changes in Akt and ERK1/2, this could also give further evidence for the roles of Ras and Ral in Rgl2-mediated changes in cardiomyocyte signaling.

Because my studies were performed solely in isolated cells, an additional limitation is that the effect of Rgl2 cannot be directly extrapolated to the intact myocardium. However, the effect of increased Rgl2 expression in transgenic mice with a cardiac-specific increase in Rgl2 expression is currently being examined. These studies indicate that increased Rgl2 expression has no detrimental effects on the myocardium as the transgenic mice display no basal pathology. Furthermore, Rgl2 may have a protective effect in the myocardium as the Rgl2 transgenics appear to have decreased apoptosis and fibrosis in response to pressure-overload.

Future Studies

Future experiments should be designed to further investigate the roles of Ras, Ral, and Rap in Rgl2-mediated regulation of PI3-kinase-Akt and Raf-MEK-ERK signaling in cardiomyocytes as well as the physiological role of Rgl2 in the myocardium. The effect of Ral on PI3-kinase-Akt and Raf-MEK-ERK signaling in cardiomyocytes should be determined because Ral-mediated regulation of these cascades was examined in a non-cardiomyocyte cell system in my studies. I propose this be done with the use of adenoviruses to induce the expression of either a dominant-negative (RalN28) or constitutively active Ral mutant (RalV23). RalN28 would be used to determine if Ral is a necessary component of Rgl2-mediated regulation of Akt and ERK1/2. However, RalV23 would be used to determine if Ral activation alone is sufficient to induce changes in Akt and ERK1/2 phosphorylation and if the effect of RalV23 observed in the HEK293 cells was the same for NRVMs.

In addition to binding Ras, Rgl2 has high-affinity for binding another G-protein, Rap. Rap has been shown to negatively regulate Ras effector signaling [23]. Therefore, the role of Rap in mediating regulation of ERK1/2 and Akt by Rgl2 should also be examined. I propose that this be done by adenoviral-mediated expression of dominant negative and constitutively active Rap mutants (RapN17 and RapV12, respectively) as described for Ral above.

Another interesting avenue for future study would be the use of Rgl2 mutants that do not have the ability to interact with Ras or Ral to determine if interaction with these G-proteins is necessary for Rgl2-mediated regulation of ERK1/2 and Akt. To this end, the Rgl2-CAAX mutant that has a lipid binding CAAX-motif substituted for its RBD (Ras binding domain) could be used to determine if interaction with Ras is necessary for Rgl2 to regulate cardiomyocyte signaling [76]. Also, a Rgl2 mutant with disruption of the CDC25 (Ral activating) domain could be used to determine if Rgl2 interaction with Ral is necessary for Rgl2 to regulate cardiomyocyte signaling [15].

Decreased Rgl2 expression could help to elucidate the role of Rgl2 in physiology by determining the signaling cascades that require its activation. Studies of decreased Rgl2 signaling could be done with the use of shRNA against Rgl2 using viral constructs in cardiomyocytes or with the production of transgenic mice with a cardiac-specific decrease in Rgl2 expression (knock out). In addition, determining if Rgl2 expression is altered in human cardiovascular diseases could elucidate the role of Rgl2 in pathology. Together, these studies would give valuable information about the endogenous roles of Rgl2 in cardiovascular physiology and pathology.

Transgenic mice with cardiac-specific increases in Rgl2 expression have been developed and could, therefore, be used to elucidate the consequences of Rgl2-mediated changes in cardiomyocyte signaling. Rgl2 was shown to differentially regulate the signaling molecules ERK and Akt, which are implicated in the development of physiologic hypertrophy. Thus, it is possible that Rgl2 could be an important regulator of physiologic hypertrophy. To study this possibility, future studies should examine the effect of increased Rgl2 expression on the development of exercise-induced (physiologic) hypertrophy in the Rgl2 transgenic animals. In addition, PI3-kinase-Akt signaling is a key component of insulin signaling that is frequently downregulated in insulin resistance. Insulin resistant conditions, such as diabetes, are associated with increased myocardial apoptotic damage during ischemic events. Therefore, the effect of increased Rgl2 expression on ischemia-reperfusion-induced myocardial damage in the transgenic mice would also be an exciting area for future study, particularly if examined under insulin resistant conditions.

Copyright © Leah M. Allen 2008

Figure 4.1

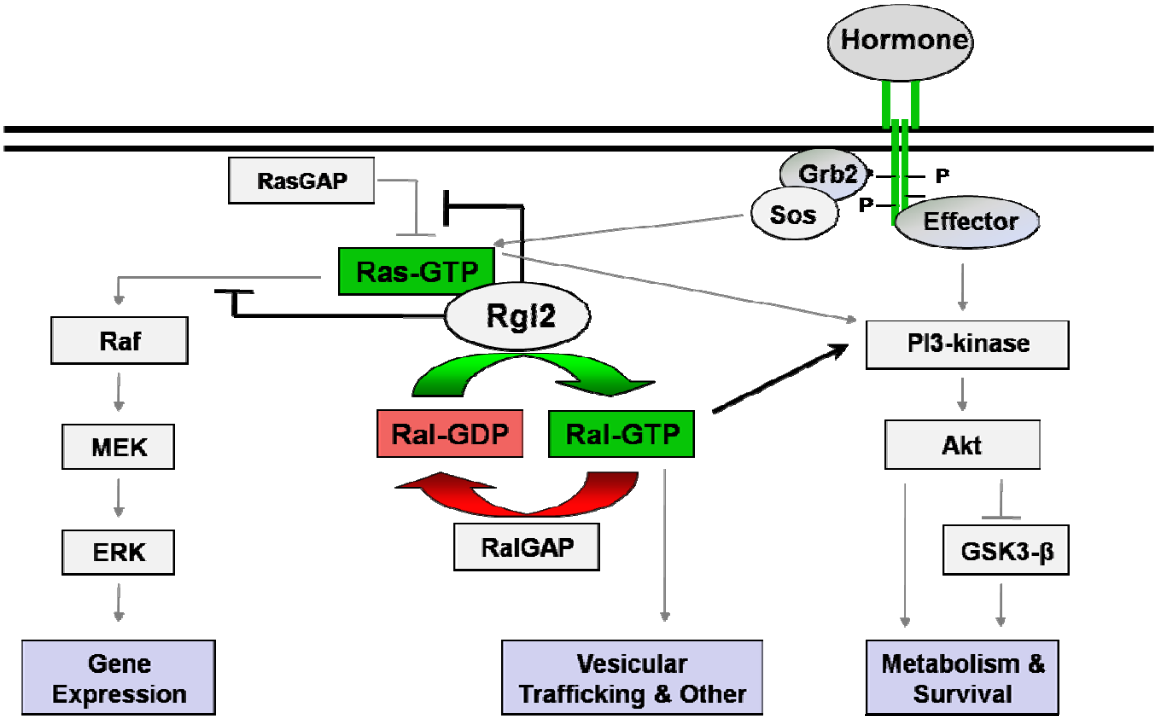
Hormone
Grb2
P
Sos
P
Effector
RasGAP
Ras-GTP
Rgl2
Raf
MEK
ERK
Gene Expression
Ral-GDP
Ral-GTP
RalGAP
Vesicular Trafficking & Other
PI3-kinase
Akt
GSK3-β
Metabolism & Survival

Model of Rgl2-mediated regulation of cardiomyocyte signaling. Rgl2 interacts with Ras via its RBD domain which localizes Rgl2 to the plasma membrane. RalGEF-RBD interaction with Ras has been shown to interfere with Raf and RasGAP binding to Ras. Therefore, Rgl2 may increase Ras activation by interfering with RasGAP binding to Ras. Rgl2 may also inhibit ERK phosphorylation by interfering with Ras-Raf interaction. The Rgl2-mediated inhibition of Raf-MEK-ERK signaling could alter expression of cardiomyocyte genes.

Localization at the plasma membrane places Rgl2 in close proximity to its effector, Ral, so that Rgl2 may activate Ral via its CDC25 domain. Ral then mediates Rgl2-induced enhancement of PI3-kinase-Akt-GSK3-β signaling which could induce increases in cardiomyocyte survival and function. However, Ral activation could have other effects in the myocardium that have not yet been studied as Ral activation is implicated in regulating vesicular trafficking.

SECTION V. REFERENCES

1. Hobbs, R.E., *Guidelines for the diagnosis and management of heart failure.* Am J Ther, 2004. **11**(6): p. 467-72.
2. Berenji, K., et al., *Does load-induced ventricular hypertrophy progress to systolic heart failure?* Am J Physiol Heart Circ Physiol, 2005. **289**(1): p. H8-H16.
3. Kannel, W.B., *Incidence and epidemiology of heart failure.* Heart Fail Rev, 2000. **5**(2): p. 167-73.
4. Nahorski, S.R., *Pharmacology of intracellular signalling pathways.* Br J Pharmacol, 2006. **147**(S1): p. S38-S45.
5. Rall, T.W., E.W. Sutherland, and J. Berthet, *The Relationship of Epinephrine and Glucagon to Liver Phosphorylase. IV. Effect of Epinephrine and Glucagon on the Reactivation of Phosphorylase in Liver Homogenates.* J. Biol. Chem., 1957. **224**(1): p. 463-475.
6. Sutherland, E.W., T.W. Rall, and T. Menon, *Adenyl Cyclase. I. Distribution, Preparation, and Properties.* J. Biol. Chem., 1962. **237**(4): p. 1220-1227.
7. Hunter, T., *The Croonian Lecture 1997. The phosphorylation of proteins on tyrosine: its role in cell growth and disease.* Philos Trans R Soc Lond B Biol Sci, 1998. **353**(1368): p. 583-605.
8. Hunter, T., *Signaling--2000 and beyond.* Cell, 2000. **100**(1): p. 113-27.
9. Johnston, C.A. and D.P. Siderovski, *Receptor-mediated activation of heterotrimeric G-proteins: current structural insights.* Mol Pharmacol, 2007. **72**(2): p. 219-30.
10. Takai, Y., T. Sasaki, and T. Matozaki, *Small GTP-Binding Proteins.* Physiol. Rev., 2001. **81**(1): p. 153-208.
11. Matozaki, T., H. Nakanishi, and Y. Takai, *Small G-protein networks: their crosstalk and signal cascades.* Cell Signal, 2000. **12**(8): p. 515-24.
12. Fidyk, N.J. and R.A. Cerione, *Understanding the catalytic mechanism of GTPase-activating proteins: demonstration of the importance of switch domain*

stabilization in the stimulation of GTP hydrolysis. Biochemistry, 2002. **41**(52): p. 15644-53.

13. Wolthuis, R.M.F. and J.L. Bos, *Ras caught in another affair: the exchange factors for Ral.* Current Opinion in Genetics & Development, 1999. **9**(1): p. 112-117.
14. Feig, L.A., T. Urano, and S. Cantor, *Evidence for a Ras/Ral signaling cascade.* Trends in Biochemical Sciences, 1996. **21**(11): p. 438-441.
15. Wolthuis, R.M., et al., *Ras-dependent activation of the small GTPase Ral.* Curr Biol, 1998. **8**(8): p. 471-4.
16. Hofer, F., et al., *Activated Ras interacts with the Ral guanine nucleotide dissociation stimulator.* Proc Natl Acad Sci U S A, 1994. **91**(23): p. 11089-93.
17. Jullien-Flores, V., et al., *Bridging Ral GTPase to Rho pathways. RLIP76, a Ral effector with CDC42/Rac GTPase-activating protein activity.* J Biol Chem, 1995. **270**(38): p. 22473-7.
18. Chien, U.H., et al., *Heteroduplex analysis of the sequence relationships between the genomes of Kirsten and Harvey sarcoma viruses, their respective parental murine leukemia viruses, and the rat endogenous 30S RNA.* J Virol, 1979. **31**(3): p. 752-60.
19. Shih, T.Y., et al., *Comparison of the genomic organization of Kirsten and Harvey sarcoma viruses.* J Virol, 1978. **27**(1): p. 45-55.
20. Der, C.J., T.G. Krontiris, and G.M. Cooper, *Transforming genes of human bladder and lung carcinoma cell lines are homologous to the ras genes of Harvey and Kirsten sarcoma viruses.* Proc Natl Acad Sci U S A, 1982. **79**(11): p. 3637-40.
21. Shimizu, K., et al., *Three human transforming genes are related to the viral ras oncogenes.* Proc Natl Acad Sci U S A, 1983. **80**(8): p. 2112-6.
22. Ancrile, B.B., K.M. O'Hayer, and C.M. Counter, *Oncogenic ras-induced expression of cytokines: a new target of anti-cancer therapeutics.* Mol Interv, 2008. **8**(1): p. 22-7.
23. Stork, P.J., *Does Rap1 deserve a bad Rap?* Trends Biochem Sci, 2003. **28**(5): p. 267-75.

24. Bos, J.L., J. de Rooij, and K.A. Reedquist, *Rap1 signalling: adhering to new models.* Nat Rev Mol Cell Biol, 2001. **2**(5): p. 369-77.

25. Ehrhardt, A., et al., *Ras and relatives--job sharing and networking keep an old family together.* Experimental Hematology, 2002. **30**(10): p. 1089-1106.

26. van Dam, E.M. and P.J. Robinson, *Ral: mediator of membrane trafficking.* Int J Biochem Cell Biol, 2006. **38**(11): p. 1841-7.

27. Sugden, P.H. and A. Clerk, *Activation of the Small GTP-binding Protein Ras in the Heart by Hypertrophic Agonists.* Trends in Cardiovascular Medicine, 2000. **10**(1): p. 1-8.

28. Gutkind, J.S., *The pathways connecting G protein-coupled receptors to the nucleus through divergent mitogen-activated protein kinase cascades.* J Biol Chem, 1998. **273**(4): p. 1839-42.

29. Luttrell, L.M., Y. Daaka, and R.J. Lefkowitz, *Regulation of tyrosine kinase cascades by G-protein-coupled receptors.* Curr Opin Cell Biol, 1999. **11**(2): p. 177-83.

30. Zwick, E., et al., *The EGF receptor as central transducer of heterologous signalling systems.* Trends Pharmacol Sci, 1999. **20**(10): p. 408-12.

31. Howes, A.L., et al., *Galphaq expression activates EGFR and induces Akt mediated cardiomyocyte survival: dissociation from Galphaq mediated hypertrophy.* J Mol Cell Cardiol, 2006. **40**(5): p. 597-604.

32. Bonfini, L., et al., *The Son of sevenless gene product: a putative activator of Ras.* Science, 1992. **255**(5044): p. 603-6.

33. Nimnual, A. and D. Bar-Sagi, *The two hats of SOS.* Sci STKE, 2002. **2002**(145): p. PE36.

34. Chardin, P., et al., *Human Sos1: a guanine nucleotide exchange factor for Ras that binds to GRB2.* Science, 1993. **260**(5112): p. 1338-43.

35. Innocenti, M., et al., *Mechanisms through which Sos-1 coordinates the activation of Ras and Rac.* J Cell Biol, 2002. **156**(1): p. 125-36.

36. Zhao, C., et al., *Phospholipase D2-generated phosphatidic acid couples EGFR stimulation to Ras activation by Sos.* Nat Cell Biol, 2007. **9**(6): p. 706-12.

37. Hancock, J.F., *PA promoted to manager.* Nat Cell Biol, 2007. **9**(6): p. 615-7.

38. Herrmann, C. and N. Nassar, *Ras and its effectors.* Prog Biophys Mol Biol, 1996. **66**(1): p. 1-41.

39. Herrmann, C., *Ras-effector interactions: after one decade.* Curr Opin Struct Biol, 2003. **13**(1): p. 122-9.

40. Stone, J.C., et al., *p21-ras effector domain mutants constructed by "cassette" mutagenesis.* Mol Cell Biol, 1988. **8**(8): p. 3565-9.

41. White, M.A., et al., *Multiple ras functions can contribute to mammalian cell transformation.* Cell, 1995. **80**(4): p. 533-541.

42. Parker, F., et al., *A Ras-GTPase-activating protein SH3-domain-binding protein.* Mol Cell Biol, 1996. **16**(6): p. 2561-9.

43. Sugden, P.H., *Ras, Akt, and Mechanotransduction in the Cardiac Myocyte.* Circ Res, 2003. **93**(12): p. 1179-1192.

44. Proud, C.G., *Ras, PI3-kinase and mTOR signaling in cardiac hypertrophy.* Cardiovasc Res, 2004. **63**(3): p. 403-13.

45. Ahuja, P., P. Sdek, and W.R. MacLellan, *Cardiac Myocyte Cell Cycle Control in Development, Disease, and Regeneration.* Physiol. Rev., 2007. **87**(2): p. 521-544.

46. Heineke, J. and J.D. Molkentin, *Regulation of cardiac hypertrophy by intracellular signalling pathways.* Nat Rev Mol Cell Biol, 2006. **7**(8): p. 589-600.

47. Fuller, S.J., J. Gillespie-Brown, and P.H. Sugden, *Oncogenic src, raf, and ras Stimulate a Hypertrophic Pattern of Gene Expression and Increase Cell Size in Neonatal Rat Ventricular Myocytes.* J. Biol. Chem., 1998. **273**(29): p. 18146-18152.

48. Thorburn, A., et al., *HRas-dependent pathways can activate morphological and genetic markers of cardiac muscle cell hypertrophy [published erratum appears in J Biol Chem 1993 Jul 25;268(21):16082].* J. Biol. Chem., 1993. **268**(3): p. 2244-2249.

49. Zheng, M., et al., *Sarcoplasmic reticulum calcium defect in Ras-induced hypertrophic cardiomyopathy heart.* Am J Physiol Heart Circ Physiol, 2004. **286**(1): p. H424-433.

50. Komuro, I., et al., *Expression of cellular oncogenes in the myocardium during the developmental stage and pressure-overloaded hypertrophy of the rat heart.* Circ Res, 1988. **62**(6): p. 1075-9.

51. Kai, H., et al., *Expression of Proto-oncogenes and Gene Mutation of Sarcomeric Proteins in Patients With Hypertrophic Cardiomyopathy.* Circ Res, 1998. **83**(6): p. 594-601.

52. Vanhaesebroeck, B., et al., *Signalling by PI3K isoforms: insights from gene-targeted mice.* Trends Biochem Sci, 2005. **30**(4): p. 194-204.

53. Wymann, M.P. and L. Pirola, *Structure and function of phosphoinositide 3-kinases.* Biochim Biophys Acta, 1998. **1436**(1-2): p. 127-150.

54. Klippel, A., et al., *Membrane localization of phosphatidylinositol 3-kinase is sufficient to activate multiple signal-transducing kinase pathways.* Mol Cell Biol, 1996. **16**(8): p. 4117-27.

55. Du, K. and P.N. Tsichlis, *Regulation of the Akt kinase by interacting proteins.* Oncogene, 2005. **24**(50): p. 7401-9.

56. Matsui, T. and A. Rosenzweig, *Convergent signal transduction pathways controlling cardiomyocyte survival and function: the role of PI 3-kinase and Akt.* J Mol Cell Cardiol, 2005. **38**(1): p. 63-71.

57. Shioi, T., et al., *The conserved phosphoinositide 3-kinase pathway determines heart size in mice.* Embo J, 2000. **19**(11): p. 2537-48.

58. McMullen, J.R., et al., *Phosphoinositide 3-kinase(p110alpha) plays a critical role for the induction of physiological, but not pathological, cardiac hypertrophy.* Proc Natl Acad Sci U S A, 2003. **100**(21): p. 12355-60.

59. Cho, H., et al., *Insulin resistance and a diabetes mellitus-like syndrome in mice lacking the protein kinase Akt2 (PKB beta).* Science, 2001. **292**(5522): p. 1728-31.

60. Chen, W.S., et al., *Growth retardation and increased apoptosis in mice with homozygous disruption of the Akt1 gene.* Genes Dev, 2001. **15**(17): p. 2203-8.

61. DeBosch, B., et al., *Akt1 is required for physiological cardiac growth.* Circulation, 2006. **113**(17): p. 2097-104.

62. Shiojima, I., et al., *Disruption of coordinated cardiac hypertrophy and angiogenesis contributes to the transition to heart failure.* J Clin Invest, 2005. **115**(8): p. 2108-18.

63. Dhillon, A.S. and W. Kolch, *Untying the regulation of the Raf-1 kinase.* Arch Biochem Biophys, 2002. **404**(1): p. 3-9.

64. Muslin, A.J., *Role of raf proteins in cardiac hypertrophy and cardiomyocyte survival.* Trends Cardiovasc Med, 2005. **15**(6): p. 225-9.

65. Avruch, J., et al., *Ras Activation of the Raf Kinase: Tyrosine Kinase Recruitment of the MAP Kinase Cascade.* Recent Prog Horm Res, 2001. **56**(1): p. 127-156.

66. Campbell, S.L., et al., *Increasing complexity of Ras signaling.* Oncogene, 1998. **17**(11 Reviews): p. 1395-413.

67. Ruwhof, C. and A. van der Laarse, *Mechanical stress-induced cardiac hypertrophy: mechanisms and signal transduction pathways.* Cardiovascular Research, 2000. **47**(1): p. 23-37.

68. Wang, L. and C.G. Proud, *Ras/Erk signaling is essential for activation of protein synthesis by Gq protein-coupled receptor agonists in adult cardiomyocytes.* Circ Res, 2002. **91**(9): p. 821-9.

69. Baines, C.P. and J.D. Molkentin, *STRESS signaling pathways that modulate cardiac myocyte apoptosis.* J Mol Cell Cardiol, 2005. **38**(1): p. 47-62.

70. Bueno, O.F., et al., *The MEK1-ERK1/2 signaling pathway promotes compensated cardiac hypertrophy in transgenic mice.* Embo J, 2000. **19**(23): p. 6341-50.

71. Harris, I.S., et al., *Raf-1 Kinase Is Required for Cardiac Hypertrophy and Cardiomyocyte Survival in Response to Pressure Overload.* Circulation, 2004. **110**(6): p. 718-723.

72. Yamaguchi, O., et al., *Cardiac-specific disruption of the c-raf-1 gene induces cardiac dysfunction and apoptosis.* J Clin Invest, 2004. **114**(7): p. 937-43.

73. Spaargaren, M. and J.R. Bischoff, *Identification of the Guanine Nucleotide Dissociation Stimulator for Ral as a Putative Effector Molecule of R-ras, H-ras, K-ras and Rap.* Proceedings of the National Academy of Sciences, 1994. **91**(26): p. 12609-12613.

74. Kikuchi, A., et al., *ralGDS family members interact with the effector loop of ras p21.* Mol Cell Biol, 1994. **14**(11): p. 7483-91.

75. Wolthuis, R.M., et al., *RalGDS-like factor (Rlf) is a novel Ras and Rap 1A-associating protein.* Oncogene, 1996. **13**(2): p. 353-62.

76. Wolthuis, R.M., et al., *Stimulation of gene induction and cell growth by the Ras effector Rlf.* Embo J, 1997. **16**(22): p. 6748-61.

77. Bos, J.L., *Ras-like GTPases.* Biochim Biophys Acta, 1997. **1333**(2): p. M19-31.

78. Feig, L.A., *Ral-GTPases: approaching their 15 minutes of fame.* Trends in Cell Biology, 2003. **13**(8): p. 419-425.

79. Nozawa, Y., *Roles of phospholipase D in apoptosis and pro-survival.* Biochim Biophys Acta, 2002. **1585**(2-3): p. 77-86.

80. Waselle, L., et al., *Role of Phosphoinositide Signaling in the Control of Insulin Exocytosis.* Mol Endocrinol, 2005. **19**(12): p. 3097-3106.

81. Humeau, Y., et al., *A role for phospholipase D1 in neurotransmitter release.* Proceedings of the National Academy of Sciences, 2001. **98**(26): p. 15300-15305.

82. Kawai, M., et al., *Ral GDP dissociation stimulator and Ral GTPase are involved in myocardial hypertrophy.* Hypertension, 2003. **41**(4): p. 956-62.

83. Post, G.R., et al., *Guanine nucleotide exchange factor-like factor (Rlf) induces gene expression and potentiates alpha 1-adrenergic receptor-induced transcriptional responses in neonatal rat ventricular myocytes.* J Biol Chem, 2002. **277**(18): p. 15286-92.

84. Morwinski, R., *The cultured myocardial cells as a model in cardiac research.* Biomed Biochim Acta, 1986. **45**(1-2): p. S237-40.

85. Cavanaugh, D.J., W.O. Berndt, and T.E. Smith, *Disassociation of Heart Cells by Collagenase.* Nature, 1963. **200**: p. 261-2.

86. Bian, D., et al., *Lysophosphatidic Acid Stimulates Ovarian Cancer Cell Migration via a Ras-MEK Kinase 1 Pathway.* Cancer Res, 2004. **64**(12): p. 4209-17.

87. Spencer, M.L., et al., *Nerve growth factor-dependent activation of the small GTPase Rin.* J Biol Chem, 2002. **277**(20): p. 17605-15.

88. Lee, J. and M.S. Kim, *The role of GSK3 in glucose homeostasis and the development of insulin resistance.* Diabetes Res Clin Pract, 2007. **77 Suppl 1**: p. S49-57.

89. Hardt, S.E. and J. Sadoshima, *Glycogen synthase kinase-3beta: a novel regulator of cardiac hypertrophy and development.* Circ Res, 2002. **90**(10): p. 1055-63.

90. Forde, J.E. and T.C. Dale, *Glycogen synthase kinase 3: a key regulator of cellular fate.* Cell Mol Life Sci, 2007. **64**(15): p. 1930-44.

91. Fuller, S.J., K. Sivarajah, and P.H. Sugden, *ErbB receptors, their ligands, and the consequences of their activation and inhibition in the myocardium.* Journal of Molecular and Cellular Cardiology, 2008. **44**(5): p. 831-854.

92. Garratt, A.N., C. Ozcelik, and C. Birchmeier, *ErbB2 pathways in heart and neural diseases.* Trends Cardiovasc Med, 2003. **13**(2): p. 80-6.

93. Garratt, A.N., *"To erb-B or not to erb-B..." Neuregulin-1/ErbB signaling in heart development and function.* Journal of Molecular and Cellular Cardiology, 2006. **41**(2): p. 215-218.

94. Laprise, P., et al., *Down-regulation of MEK/ERK signaling by E-cadherin-dependent PI3K/Akt pathway in differentiating intestinal epithelial cells.* J Cell Physiol, 2004. **199**(1): p. 32-9.

95. Zhuang, S., et al., *ERK promotes hydrogen peroxide-induced apoptosis through caspase-3 activation and inhibition of Akt in renal epithelial cells.* Am J Physiol Renal Physiol, 2007. **292**(1): p. F440-7.

96. Okazaki, M., et al., *Ras-interacting Domain of Ral GDP Dissociation Stimulator Like (RGL) Reverses v-Ras-induced Transformation and Raf-1 Activation in NIH3T3 Cells.* Cancer Res, 1996. **56**(10): p. 2387-2392.

97. Clerk, A. and P.H. Sugden, *Small Guanine Nucleotide-Binding Proteins and Myocardial Hypertrophy.* Circ Res, 2000. **86**(10): p. 1019-1023.

98. Herbert, T.P., et al., *Distinct signalling pathways mediate insulin and phorbol ester-stimulated eukaryotic initiation factor 4F assembly and protein synthesis in HEK 293 cells.* J Biol Chem, 2000. **275**(15): p. 11249-56.

99. Yamamoto, K., et al., *Induction of Tenascin-C in Cardiac Myocytes by Mechanical Deformation. ROLE OF REACTIVE OXYGEN SPECIES.* J. Biol. Chem., 1999. **274**(31): p. 21840-21846.

100. Geyer, H. and R. Geyer, *Strategies for analysis of glycoprotein glycosylation.* Biochimica et Biophysica Acta (BBA) **-** Proteins & Proteomics, 2006. **1764**(12): p. 1853-1869.

101. Mechref, Y., M. Madera, and M.V. Novotny, *Glycoprotein enrichment through lectin affinity techniques.* Methods Mol Biol, 2008. **424**: p. 373-96.

102. Embi, N., D.B. Rylatt, and P. Cohen, *Glycogen synthase kinase-3 from rabbit skeletal muscle. Separation from cyclic-AMP-dependent protein kinase and phosphorylase kinase.* Eur J Biochem, 1980. **107**(2): p. 519-27.

103. Kerkela, R., K. Woulfe, and T. Force, *Glycogen synthase kinase-3beta -- actively inhibiting hypertrophy.* Trends Cardiovasc Med, 2007. **17**(3): p. 91-6.

104. Sugden, P.H., et al., *Glycogen synthase kinase 3 (GSK3) in the heart: a point of integration in hypertrophic signalling and a therapeutic target? A critical analysis.* Br J Pharmacol, 2008. **153 Suppl 1**: p. S137-53.

105. Thorburn, J., J.A. Frost, and A. Thorburn, *Mitogen-activated protein kinases mediate changes in gene expression, but not cytoskeletal organization associated with cardiac muscle cell hypertrophy.* J. Cell Biol., 1994. **126**(6): p. 1565-1572.

106. Nagoshi, T., et al., *PI3K rescues the detrimental effects of chronic Akt activation in the heart during ischemia/reperfusion injury.* J Clin Invest, 2005. **115**(8): p. 2128-38.

107. Haq, S., et al., *Differential Activation of Signal Transduction Pathways in Human Hearts With Hypertrophy Versus Advanced Heart Failure.* Circulation, 2001. **103**(5): p. 670-677.

108. Cross, T.G., et al., *Serine/Threonine Protein Kinases and Apoptosis.* Experimental Cell Research, 2000. **256**(1): p. 34-41.

109. He, Z., et al., *Regulation of Vascular Endothelial Growth Factor Expression and Vascularization in the Myocardium by Insulin Receptor and PI3K/Akt Pathways in Insulin Resistance and Ischemia.* Arterioscler Thromb Vasc Biol, 2006. **26**(4): p. 787-793.

110. Araujo, E.P., et al., *Short-term in vivo inhibition of insulin receptor substrate-1 expression leads to insulin resistance, hyperinsulinemia, and increased adiposity.* Endocrinology, 2005. **146**(3): p. 1428-37.

111. Jiang, Z.Y., et al., *Characterization of selective resistance to insulin signaling in the vasculature of obese Zucker (fa/fa) rats.* J Clin Invest, 1999. **104**(4): p. 447-57.

112. Hao, Y., R. Wong, and L.A. Feig, *RalGDS Couples Growth Factor Signaling to Akt Activation.* Mol Cell Biol, 2008.

113. Zhao, Y.-y., et al., *Neuregulins Promote Survival and Growth of Cardiac Myocytes. PERSISTENCE OF ErbB2 AND ErbB4 EXPRESSION IN NEONATAL AND ADULT VENTRICULAR MYOCYTES.* J. Biol. Chem., 1998. **273**(17): p. 10261-10269.

114. Lemmens, K., K. Doggen, and G.W. De Keulenaer, *Role of Neuregulin-1/ErbB Signaling in Cardiovascular Physiology and Disease: Implications for Therapy of Heart Failure.* Circulation, 2007. **116**(8): p. 954-960.

115. Lemke, G., *Neuregulins in Development.* Molecular and Cellular Neuroscience, 1996. **7**(4): p. 247-262.

116. Fukazawa, R., et al., *Neuregulin-1 protects ventricular myocytes from anthracycline-induced apoptosis via erbB4-dependent activation of PI3-kinase/Akt.* Journal of Molecular and Cellular Cardiology, 2003. **35**(12): p. 1473-1479.

117. Brunetti, A., et al., *Human diabetes associated with defects in nuclear regulatory proteins for the insulin receptor gene.* J Clin Invest, 1996. **97**(1): p. 258-62.

118. Okamoto, H., et al., *Transgenic rescue of insulin receptor-deficient mice.* J Clin Invest, 2004. **114**(2): p. 214-23.

119. Thomas, P. and T.G. Smart, *HEK293 cell line: A vehicle for the expression of recombinant proteins.* Journal of Pharmacological and Toxicological Methods, 2005. **51**(3): p. 187-200.

120. Fang, Z.Y., J.B. Prins, and T.H. Marwick, *Diabetic Cardiomyopathy: Evidence, Mechanisms, and Therapeutic Implications.* Endocr Rev, 2004. **25**(4): p. 543-567.

SECTION VI. APPENDIX 1: PROTOCOLS

A. Preparation of Neonatal Rat Ventricular Myocytes (NRVMs)…………………..103
B. Adenoviral Purification……………………………………………………………108
C. Rapid Titer Test for Adenoviral Titration………………………………………...112
D. Adenoviral Infection of NRVMs…………………………………………………..115
E. Preparation of GST-fusion Proteins……………………………………………..116
F. G-protein Activation Assay in Adenoviral Infected NRVMs……………………...118
G. Immunoprecipitation to assess pTyr on IR-β……………………………………...120
H. Immunostaining NRVMs……………………………………………………………121
I. Criterion Western Blotting…………………………………………………………...122
J. Transfection of HEK-293 Cells……………………………………………………...123

A. Preparation of Neonatal Rat Ventricular Myocytes

Modified by Leah Allen 1-28-05 from Amaxa Biosystems and Dr Ginell Post's protocol
***This protocol should yield 1.0 x 10^6 to 1.8 x 10^6 myocytes/heart.

Reagents:

- Collagenase (Worthington Biochemical Corp. Cat. No. 4176)
  - Try 108Units/ml; amount added will vary according to lot #.
  - This should be optimized, start low and increase for best yield.
  - For example 108 U/ml (x 262 U/mg) = 0.41 mg/ml x #mls.

- Pancreatin (GibcoBRL #610-5725 or 25720-012)
  - Stock solution from Gibco is 25 mg/ml.
  - Aliquot into 3 mls and store @ -20°C.
  - This is light sensitive – keep out of light as much as possible.

- Serum:
  - FBS: Fetal Bovine Serum (100ml aliquots) (Gibco #16140-071)
  - HS: Equine Serum (5ml and 25ml aliquots) (Hyclone #APJ22102)

- Gelatin (Sigma; G-1890)
- Cell Culture Water (BioWhittaker; 17-724Q)
- DMEM; High Glucose + Hepes (GIBCO; 12430-054)
- Medium 199 (GIBCO; 12340-030)
- PBS Powder Packets (SIGMA; P-3813)

Stock Solutions:

- 10X Ads buffer (STOCK for 1X Ads dilution)
  For 125ml:
  - 8.5 g NaCl
  - 5.95 g HEPES (NO SODIUM SALT)
  - 0.1713 g $NaH_2PO_4 \cdot H_2O$
  - 1.25 g Glucose
  - 0.5 g KCl
  - 0.2463 g $MgSO_4$ (**0.985g $MgSO_4 \cdot 7H_2O$**)

  pH to 7.35 +/- 0.05 with NaOH
  (SLOW to react).
  Adjust volume to 125ml – Be sure to use Cell Culture Water.
  Filter through 0.22µM.

Autoclave:

Day before isolation: dissection tools (6), spin-flask, glass beakers (3), and 500ml glass bottle (1)
Day of isolation: 1% gelatin

Dissection Tools:

Gross Dissection: 1 lrg. scissors, 1 lrg. curved forcep, 1 med. straight scissors, 1 med. curved forcep
Trisector/Mincing Tools: 1 small forcep, 1 small scissors

On Day of Isolation:

Thaw: HS, FBS, PS (for media), Pancreatin (Pancreatin must be thawed @ room temperature)

Heat (37°C): 100ml Plating Media for 1 litter; Heat (37°C): 150ml Plating Media for 2 litters.

1. 1 x 250ml beaker with stir bar (to make 1X Ads and check pH)
2. 1 x 150ml beaker with stir bar (for enzyme solution)
3. 1 x 250ml beaker with 70% EtOH (for dissecting tools)
4. 1 x 1000ml beaker with 70% EtOH (for dipping neonates) – Ice Cold
5. 2 x 250ml filter units (for enzyme solution and fresh 1X Ads)
6. autoclaved dissection tools (autoclave on Friday)
7. thick paper towels
8. 2 x plastic bags for disposal of animals
9. Large weigh boats for neonates (10/boat)
10. Warm water bath + hook up pump to spin flask.
11. 1 x medium culture dish containing STERILE 1X PBS buffer (on ice) for collection of heart tissue
12. Prepare solutions
13. Warm to 37°C: Maintenance Media (containing FBS + HS)
14. Autoclave Gelatin and keep warm in water bath.

Preparation of Solutions (Day of Experiment):

Be sure to use autoclaved glassware.

- Plating Media (250 ml):
  - 170ml DMEM with Penicillin/Streptomycin (PS)
  - 42.5ml Medium 199 w/ PS
  - 25ml HS
  - 12.5ml FBS

  Sterile Filter (Gelman Sciences #12158)
  **Add 5ml PS for 500ml DMEM (or for 500ml M199)
  Heat: 100ml Plating Media for 1 litter; Heat: 150ml Plating Media for 2 litters.

- 1% Gelatin:
  - Example: 5g gelatin in 500ml Cell Culture Water.
  - Autoclave: small liquid cycle in pan containing a small layer of water.

  1-2 litters: 2g gelatin in 200ml Cell Culture Water

- 1X Ads buffer:
  1-2 litters:
  Make 200mls total by diluting 20ml 10X Ads Stock solution in 180ml Cell Culture Water. Check pH [pH to 7.35 +/- 0.05 with .01N NaOH (SLOW to react)].

- 1X Ads + 5% HS (Enzyme Stopping Solution):
  1-2 litters: 95 ml 1X Ads + 5 ml HS --- Filter

- Digestion Buffer / Enzyme Solution (See Below)

Preparation of Digestion Buffer/Enzyme Solution:
**See "Collagenase and Pancreatine Calculation Form" in Excel

Add collagenase to 1X Ads buffer and stir the enzyme solution gently for a minimum of 5 min.
Filter, add pancreatin, and leave solution @ room temperature.

For 1-2 litters: Will need 7-8mls/digestion (normally 8 digestions)
For >2 litters: Will need 0.3ml enzyme solution/heart/digestion (normally 8 digestions)

To calculate by hand:
Measure **Y**mls 1X Ads buffer into beaker
Y= .3ml enzyme buffer/heart/digestion (usually 8)

A. Weigh Collagenase❖
   (Need: 115Units/ml)(Stock: **X** Units/mg) = _______mg/ml

   _______mg/ml x _______ml (**Y**-value) = _____mg of Collagenase

B. Pancreatin❖❖
   Stock = 25mg/ml
   Final Concentration should be between 0.8 and 1.0 mg/ml

Dissections:

1. Count neonates (1-2 day old rats) and place in weigh boats.

2. Pick up neonate with large curved forceps and dip into ice cold 70% EtOH. Decapitate with large scissors and place neonate on its back. (Can do 5-7 at a time.)

3. Make a midline incision through the sternum, holding the body down with the large forceps. Press downward on ribs with the forceps to pop heart up through the incision.

4. Clip/pull the heart out with the small forceps and transfer to a medium culture dish (10cm^2) containing (calcium and magnesium free) PBS on ice.

5. As the hearts are being collected, the dissecting partner trims the atria, fat, and connective tissue. If no partner: the atria, fat, and connective tissue must be trimmed as quickly as possible after collecting all hearts (for 1-2 litters)

6. Mince hearts in dry culture dish lid (requires at minimal a trisection) and transfer to a 50ml conical tube containing approx. 12ml warm digest buffer/enzyme solution.

Collection of Cells:

1. While in cell culture hood, transfer cells (and digestion buffer) to water jacketed spin flask. Take care not to trap heart pieces below stir bar.

DO NOT PICK UP HEART PIECES VIA PIPETTE.

2. Connect spin flask to 37°C water bath and set on stir plate. The heart tissue should be stirred gently…just quick enough to avoid clumping.

3. Allow first digestion to incubate for 20min. Remove supernatant and discard ONLY for this first digestion. (Be sure to remove supernatant in the hood for each digestion.)

4. All other digestions should be incubated for 10min, collected, and added to 2mls of 1X Ads + 5% HS (for 1-2 litters).

5. Centrifuge each collection for 1min @ 340g. Resuspend in 2mls 1X Ads + 5% HS and monitor digestions #2-3 and #7-8 by combining 10μl trypan blue + 10 μl cell suspension. (Counting is not necessary – study cell viability.)

6. Place resuspended cells in incubator before monitoring viability!

7. After digestion is complete, combine digestion collections and centrifuge 1min @ 340g. Resuspend in 20 mls of plating media and place in cell culture flask. Incubate for 2 hrs @ 37°C. (This will purify myocytes by allowing fibroblasts to attach while myocytes remain free.)

8. Drain cells into 50ml conical tube and count as indicated below.

Counting Cells and Calculations:

1. Combine 20μl trypan blue + 20 μl cell suspension.
2. Make sure that cells are well suspended before adding to trypan blue.
3. Count 2X and Average
4. To calculate cells per ml: 2(average count / 4 grids) = "X" x 10^4 cells/ml
5. Convert to the value times 10^6 cells/ml.
6. Total Cells = (cells/ml)(cell suspension volume)
7. Cells per Heart = (Total Cells)/(Number of Neonates)
    a. Expected Yield = 1.0 x 10^6 to 1.8 x 10^6.

Plating:

10cm^2 plates use 3.0 x 10^6 cells/plate with a volume of 10ml/plate.
6 well plates use 0.3 x 10^6 to 0.5 x 10^6 cells/well with a volume of 2ml/well.
2 well chamber slides use 0.1 x 10^6 cells/well with a volume of 1ml/well.

B. Adenovirus Purification

Modified in 2006 from DeBeer and Kraner Lab Protocols by LA and CG

Supplies:

- Beckman Centrifuge Tubes (Polyallomer)
  25 x 89mm (#326823) & 14 x 89mm (#331372)
- Heavy CsCl **(See Below)** (Order from Sigma #C-4036)
- Light Cesium Chloride (CsCl) **(See Below)**
- Dry Ice / ethanol (EtOH) Bath
- Water Bath @ 37^{o}C
- Centrifuge
- 10mM Tris, pH8, sterile
- Ice Bucket with wet ice
- 15ml conical tubes
- 10DG BIO-RAD desalting column
- Sterile PBS (Gibco #14190-144)
- Sterile eppendorf tubes
- P20, P200, P1000 pipetmen
- Sterile Aerosol Barrier Tips (all sizes)
- Rack for Eppendorf Tubes
- Ring Stand with 2 clamps
- Beaker with 0.5% Bleach to catch waste
- 18 gauge needles (pink)
- Bleach

Reagents:

10mM Tris pH 8.0

	grams of CsCl	vol. of 10mM Tris pH 8.0
Heavy Cesium Chloride:	21.12 g	28.89 ml
(1.45g/ml)	42.23 g	57.70 ml
	211.15g	288.85 ml

	grams of CsCl	vol. of 10mM Tris pH 8.0
Light Cesium Chloride:	11.20 g	38.81 ml
(1.20g/ml)	22.39 g	77.61 ml
	111.95 g	388.05 ml

******Sterile filter all of the above solutions.******

Also, before beginning purification, be sure to sign up for DeBeer Lab centrifuge and rotors 1 week in advance.

Purification:

1. Place the SW28 rotor in the Beckman Centrifuge, turn on centrifuge, and cool. (Vacuum must be on to cool)

2. Harvested virus (frozen stock or fresh) must be freeze / thawed 3X using dry ice / EtOH bath and a 37°C water bath. If the virus is frozen, it must be thawed 3X and frozen 2X. Be sure that the virus has been completely frozen and thawed each time. Ideally the virus should be in 2 aliquots of equal volume.

    ***It is VERY important to keep the virus cool. Therefore, gently rotate 50ml conical tube containing partially thawed virus and listen for “clink” from ice hitting tube top/bottom. When a soft “clink” is heard, take virus out of bath and gently rotate tube @ room temp. until “clink” is gone.

3. After the 3rd thaw, centrifuge the lysate 1500 rpm @ 4°C for 10 min. Cellular membranes will be pelleted and removed from the virus containing supernatant.

4. While the lysate is spinning, prepare the CsCl gradient. Using 2 of the 25x89mm Beckman Centrifuge tubes (per 50-60 plate prep), first pipette 9ml of light CsCl into each tube. Then pull 9ml of heavy CsCl into a 10ml pipette and lower the pipette tip to the bottom of the tube. **Slowly** (think of tightening hand rather than pushing button) pipette the heavy CsCl into the bottom of the tube, being careful to keep the tip near the bottom of the tube. Once nearly all of the CsCl has been pipetted, gently bring pipette up out of the tube.

5. Remove the lysate from the centrifuge into hood. Remove supernatant from cell pellet into a fresh 50ml centrifuge tube. Take approx. half of supernatant and gently layer on top of the light CsCl. Hold the Beckman Centifuge Tube at an angle and pipette the supernatant gently along the side of the tube. A maximum of 20ml of supernatant may be loaded per tube.
   (Final composition ~ 9ml Light CsCl + 9ml Heavy CsCl + 10ml Virus/Supernatant + 10ml 10mM Tris pH8.)

6. Load the tubes into a Beckman SW28 rotor. Make sure that tubes are balanced! Centrifuge **20,000 rpm; 4°C; 2 hrs.** Use maximum acceleration and NO BRAKE for deceleration. (Total time ~ 3 hrs.) When finished, place the SW40Ti rotor into the centrifuge and start vacuum to cool it.

7. Remove the tubes from the centrifuge and clamp onto a ring stand above a beaker of bleach. The virus will appear as a narrow, opaque, white band 2/3 down the gradient. The lower band = live virus. The upper band = dead virus. When harvesting, only harvest the **lower** band.

8. To harvest the virus, puncture the bottom of the tube **at the seam** with an 18G needle. Finding the correct pressure to puncture the tube is difficult at first, but becomes easy with practice. Once the needle has entered the tube, gently move the needle so that the beveled edge is just inside the tube. The CsCl will begin to drip gently from the Leur end of the needle:

The needle can become easily clogged using these “soft” centrifuge tubes and therefore, may drip very slowly. If this is the case, you have 3 options: either allow the dripping to continue at a slow rate, use a syringe to suck the liquid through the needle, or remove the needle. If removing the needle, BE CAREFUL! The CsCl will flow quickly from the tube once the needle has been removed. Therefore, be prepared to catch the virus band in a matter of seconds. If the needle is completely clogged, then either remove it, or puncture the tube with a 2nd needle. Do NOT use a 2nd needle if the 1st is dripping, as it will be difficult to collect the band.

9. Collect only the bottom virus band into a 15ml conical tube. Do NOT collect any bands above it. The tube should look similar to the diagram at the end of the protocol. Once the band has been collected, the virus should be stored on wet ice while continuing.

10. Dilute the collected band with an equal volume of 10mM Tris pH8.

11. Prepare the CsCl gradient. Using 2 of the 14x89mm Beckman Centrifuge Tubes (per 50-60 plate prep), first pipette 3.5ml of light CsCl into each tube. Then pull 3.5ml heavy CsCl into a 5ml pipette and lower the pipette tip to the bottom of the tube. Slowly pipette the heavy CsCl into the bottom of the tube, being careful to keep the pipette tip near the bottom of the tube. Once nearly all of the CsCl has been pipetted, gently bring pipette up out of the tube.

12. Gently layer the diluted virus on top of the light CsCl. Hold the Beckman Centrifuge Tube at an angle and pipette the supernatant gently along the side of the tube. A maximum of 4ml of virus may be loaded per tube. Be sure that tubes are almost completely filled…if not, fill the remainder of tube (carefully) with 10mM Tris pH8.

13. Load the tubes into a Beckman SW 40Ti rotor, being sure that the tubes are balanced and properly hooked on to rotor. Centrifuge **20,000 rpm; 4°C; overnight.**

14. Clamp a 10DG desalting column onto a ring stand above a beaker. Wash 2X with 10ml sterile PBS. This will take approx. 15min. Should be done before stopping the centrifuge.

15. Set up a test tube rack with 6 sterile 1.5ml microfuge tubes. These will be used to collect the virus from the column.

16. Remove the tubes from the centrifuge and clamp onto a ring stand above a beaker containing bleach. The virus will appear as a narrow, opaque, white band 2/3 down the gradient. Sometimes there are “hairs” (white strands that run vertically) visible in the tube. These should be removed gently with a pipette before harvesting the band.

17. Harvest bottom band following the same procedure as before (step #7).

18. Collect only the bottom band into a 15ml conical tube. Do NOT collect any bands above it!!!! The gradient should look similar to the diagram at the end of

the protocol. Once the band has been collected, the virus should be stored on wet ice while continuing.

19. Load the collected bands onto the desalting column (should already be washed 2X with PBS).

> The column does not flow until dry (liquid remains in it at all times). It only flows until the volume placed on top of the column has entered it. It is also possible to use a stopcock on the column. The stopcock would be recommended if there is more than 2.5ml of volume for the collected bands to avoid losing some of the virus before the PBS is added.

Once the column has stopped flowing, load 10ml sterile PBS onto the column. **Be sure that 6 x 1.5ml centrifuge tubes are ready for the collection prior to adding the PBS.** Begin collecting small fractions in the microfuge tubes for a minimum of 5ml. If the band was easily visible before collection, then it may be possible to see the virus exit the column. (Watch for drips to become cloudy…similar to what is done for collecting the band out of the gradient.) Try to obtain the most concentrated fraction in 1 or 2 tubes. *With practice, it is possible to collect fewer tubes and to contain the most concentrated virus in 1or 2 tubes.*

20. Do 1:50 dilutions of each fraction and read at OD_{260}. (i.e. 490µl PBS + 10µl virus) **Don't forget the Blank (500µl PBS).**

OD_{260} x Dilution Factor x 10^{12} particles/ml = Concentration (pt/ml)

To read the OD on the DeBeer lab machine:

- Turn on machine in the back under the paper roll and wait for it to warm up.
- Select dsDNA; hit ENTER.
- Scroll down to Positioner; ENTER.
- In the pop up window, select "1 cell platform"; ENTER.
- Run test.
- Read Blank.
- Read Sample.
- After reading fractions, return to our lab and combine the fractions with the highest readings (usually 0.2 to 0.6 is good).
- Return to DeBeer lab and read the final/combined virus.
- When finished, don't forget to print out readings and clean area near machine with bleach.
- Go to spreadsheet and determine how to aliquot the virus.

5e11pt/tube = stock for 50 plate amplification of virus.
5e10pt/tube = for cell culture.
1e11pt/tube = for cell culture.
2e11pt/tube = for cell culture.

21. Add autoclaved glycerol to 10%. (i.e. for 1ml virus, add 100µl of glycerol.)

22. Make desired aliquots and freeze at -70oC. It is recommended to make atleast 2 aliquots of 5e^{11}pt/tube of virus for the next purification.

C. Rapid Titer Test for Adenoviral Titration

1-27-05 (Revised from Dr. Reto Asmis's kit-free protocol)

Day 1: Seed Plates

- Use HEK-293 cells.
- Plate 2 x 12 well plates @ 0.1 x 10^6 cells/well.
- Maintain in 1ml/well Growth medium: DMEM + 10% FBS
- FALCON Multiwell # 353225: 12 well plates.

Day 3: Infect Cells

1. Cells should be approx. 0.5 x 10^6 cells/well.

2. Use the following viruses:______________________________.

3. Using serum containing medium as diluent, prepare 10-fold serial dilutions of viral samples from 10^{-2} to 10^{-6}ml as follows.

   Well #1 = Blank (negative control)
   Well #2 = 10µl viral stock in 900µl diluent = 10^{-2} ml
   Well #3 = 100µl of 10^{-2} dilution in 900µl diluent = 10^{-3} ml
   Well #4 = 100µl of 10^{-3} dilution in 900µl diluent = 10^{-4} ml
   Well #5 = 100µl of 10^{-4} dilution in 900µl diluent = 10^{-5} ml
   Well #6 = 100µl of 10^{-5} dilution in 900µl diluent = 10^{-6} ml

4. Add 100µl of each dilution dropwise into each well. This should be performed in duplicate to ensure accuracy.

5. Incubate cells @ 37°C in 5% CO_2 for 48 hrs.

Day 5: Fix Cells and Add Antibodies

1. PREPARE IN ADVANCE: a minimum of 140ml/plate of PBS + 1%BSA solution (sterile filtered) and a minimum of 13ml/plate PBS.

2. Aspirate medium. Allow cells to dry in hood for 5 min.

3. Fix cells by VERY GENTLY adding 1 ml -20°C 100% methanol **(Place in the Freezer on Thursday)** to each well.
   Take care – cells will come off plate easily during this step. Also, perform this in the hood.

4. Incubate the plate @ -20°C for 10 min.

5. Remove methanol. Gently rinse 3 times with 1 ml PBS + 1% BSA @ Room Temp. Dissolve 5g BSA (from Sigma #A-3803) in 500ml 1X PBS and sterile filter.

6. Prepare Antibodies:
   1° antibody (1:500)= Biogenesis Adenovirus (anti-hexon): goat anti-Ig #0151-9004
   2° antibody (1:500)= Jackson Rabbit Anti-Goat IgG (H+L) #305-035-003
   Vortex. Centrifuge @ 14,000 rpm for 5-10 min @ 4°C. Then place on ice.

7. Dilute 1° antibody **(stored at -20°C)** 1:500 in 1X PBS + 1% BSA.

8. Aspirate final rinse from the wells. Then add 1 ml of 1° antibody dilution to each well. Incubate 1 hr @ 37°C.

9. Remove 1° antibody, then GENTLY rinse the wells 3X with 1 ml 1X PBS + 1% BSA.

10. Dilute 2° antibody **(stored at -20°C)** 1:500 in 1X PBS + 1% BSA.

11. Aspirate final rinse from the wells. Then add 1 ml of 2° antibody dilution to each well. Incubate 1 hr @ 37°C and shake by hand each 10-15 min.

12. Prior to removing the 2° antibody, prepare DAB working solution **(stored at -20°C)** from Sigma #D-4418. 1 DAB tablet + 1 Urea tablet dissolved in 15ml H_2O. Mix well and be sure to KEEP in the DARK.

13. Aspirate 2° antibody. Then GENTLY rinse each well 3X with 1 ml 1X PBS + 1% BSA.

Day 5 (cont'd): Develop Color and Quantify

1. After removing the final 1X PBS + 1% BSA rinse; add 1 ml DAB working solution to each well. Incubate at Room Temp for 10 min.

2. Aspirate DAB working solution and add 1 ml 1X PBS to each well.

3. Count a minimum of four fields of brown/black positive cells using a microscope with a 20X objective lens. **Count dilutions with 10% or fewer POSITIVE cells.** Calculate the mean # of positive cells in each well.

4. DON'T FORGET to count the negative control so that the BACKGROUND can be subtracted.

5. Calculate the infectious units (ifu) per ml for each well as follows:

[(infected cells/field) x (573 fields)] / [viral volume (ml)] x (dilution factor)

Example: ifu/ml = (44+36+45+46+40+42+53+35) / 8
= 40.357 x 573
= 23134.875 / 0.1ml
= 231348.75 x 10^{-5}
= 2.3 x 10^{10}
2.3 x 10^{10} ifu/ml

Reagents:

- FALCON Multiwell # 353225: 12 well plates.
- Sigma #A-3803: BSA
- 1° Antibody: Biogenesis Adenovirus (anti-hexon) #0151-9004; goat anti-Ig
- 2° Antibody: Jackson Rabbit Anti-Goat IgG (H+L) #305-035-003
- Sigma #D-4418: DAB Working Solution

D. Adenoviral Infection of NRVMs (2 days after plating cells)

1. Record name, date, and purpose of experiment.

2. Change media to serum free media (SFM) 2 hours prior to infection.

3. Get viruses from the -80°C freezer and leave on ice.
   - AdNull (STOCK = 2.8 x 10^{10} pt/µl = 4.78 x 10^{8} ifu/µl) - Made 3-1-06
   - AdRgl2 (STOCK = 9.68 x 10^{9} pt/µl = 2.34 x 10^{8} ifu/µl) - Made 2-1-06

4. Dilute the virus from stock as follows:
   - Dilute AdNull (1:4) by adding 2µl of Adnull Stock to 6µl of SFM (4°C). The AdNull virus is now at 1.195 x 10^{8} ifu/µl.
   - Dilute AdRgl2 (1:2) by adding 3µl of AdRlf Stock to 3µl of SFM (4°C). The AdRgl2 virus is now at 1.17 x 10^{8} ifu/µl.

5. Add virus to larger volumes sufficient to infect plates (see example below):
   - AdNull (**90ifu/cell**): Add 1.98µl **03/06 Diluted Adnull** to 15mls SFM (1 plate).
   - AdRgl2 (**90ifu/cell**): Add 2.02µl **02/06 Diluted Rlf** to 15mls SFM (1 plate).
   - Add 2mls per NRVM well.

6. 3 hours post-infection, add 1% FBS (20µl in 2ml) to the infected cells.

E. Preparation of GST-fusion proteins

Modified from Dr. Ginell Post's Protocol with the help of the Gong Lab on 5-30-06 by LA

Day 1:

Transform BL21 (DE) Competent Cells (from Invitrogen or Stratagene) with the fusion protein before this step or use transformed bacteria from glycerol stocks. Streak transformant onto LB/ampicillin plates and allow to grow overnight at 37°C ~ 12 hours. ***This bacteria is used because it lacks proteases. Therefore, giving a higher protein yield.

Day 2:

Inoculate a single purified transformant colony into 4mls of LB containing 50µg/ml ampicillin (STOCK = 50mg/ml) and thoroughly mix. Then add 1ml to 4 tubes containing 5ml of LB/amp and grow overnight at 37°C.

Make LB/0.4% glucose (2g into 500ml) and autoclave (in 1L flasks from the Gong lab) to sterilize.

Day 3:

1. Add the overnight cultures to 1L (4 x 250ml) of LB/**amp**/0.4% glucose and grow @ 37°C with shaking until $O.D._{600} \leq 0.4$ (1.5-2hrs).

2. After the correct O.D. is reached, add 100µl of 1M IPTG (0.2mM final; for every 500ml of growth media) and grow for a minimum of 6 hrs at 30°C.

3. Centrifuge for 10min @ 5000rpm at room temp. Freeze pellets @ -20°C overnight in a frost-free freezer.

Day 4:

1. Resuspend each pellet in ice-cold NETN lysis buffer - a total of 10 to 20mls should be used. Add 1mg/ml lysozyme stock (200µl for 10ml) and incubate for 1 hour on ice. ****To make lysozyme, dilute in TBS.

2. While tubes incubate, wash beads (0.75ml of suspended beads per 10ml supernatant): use 15ml conical tube, with 1ml lysis buffer, centrifuge 30sec @ 4°C @ 2,000rpm, take of liquid (top layer), repeat 2X.

3. Transfer supernatant from step 1 to 50ml centrifuge tube.

4. Sonicate on ice in 10sec bursts with 10sec pauses for 2min – Use Gong Lab sonicator, medium sized probe.

5. Centrifuge @ 16,500rpm for 15min @ 4°C. Transfer 10ml supernatant to 15ml conical tubes.

6. Incubate cell lysate with 0.75ml of suspended, prewashed GSH-agarose beads and nutate in the cold room for 1hr.

7. Centrifuge 30sec @ 2,000rpm @ 4°C and wash 4X with 10ml NETN buffer. Transfer beads to a single 15ml conical tube.

8. To elute, add 2X bead volume (1.5ml) of fresh 20mM Glutathione (GSH) in 100mM Tris, pH8. Nutate 20min in the cold room. Centrifuge as before to collect supernatant. Transfer supernatant to a new tube.

9. Repeat elution of beads a second time and add supernatant to first.

10. Dialyze eluate for 2hrs in the cold room against 500ml dialysis buffer in a slide-a-lyzer (the entire 3mls should fit into one unit).

11. Measure protein using Bradford Assay with dialysis buffer and assay protein by PAGE. Dilute 1:2, 1:4, 1:8, 1:16, 1:32, and 1:64.

Reagents:

- **NETN Buffer: 300ml**

20mM Tris, pH 7.4	0.7268g – pH to 7.4
100mM NaCl	1.753g
2mM EDTA	0.223g
0.5% Ipegal	1.5ml
**1mM DTT (add FRESH)	1µl of 1M Stock/1ml as needed.
**Protease Inhibitors (add FRESH)	100X (10µl/ml)

- **GSH: 15ml**

  15ml of 100mM Tris, pH 8.
  0.092g GSH
  (Make 100mM Tris by adding 0.2428g to 20ml dH$_2$O and pH to 8.)

- **Dialysis Buffer: 1L**

Tris, pH 7.4	6.057g – pH to 7.4
150mM NaCl	8.766g
5mM MgCl	5ml of 1M Stock
10% glycerol (sterile)	100ml
**1mM DTT (add FRESH)	1ml of 1M Stock (from Gong Lab)

  Note: Save ~15ml dialysis buffer for Bradford Assay.

- **Ampicillin Stock (50mg/ml): 3ml**

  3ml dH$_2$O
  0.15g Ampicillin
  Filter w/ 0.22µm.
  Use at 50µg/ml. (1µl/1ml)

- **Glycerol Stocks: 1ml**

  0.5ml sterile glycerol
  0.5ml transformed bacteria in LB broth
  Mix thoroughly and freeze @ -80°C.

F. G-protein Activation Assay in Infected NRVMs

Day 1: Isolate and Plate Myocytes

- Plate myocytes on 10 cm plates @ 3 x 10^6 cells/plate.

Day 2:

- Rinse myocytes 2X (to remove dead cells) and place back into serum containing media.

Day 3: Infection

- Wash cells 3X with serum-free media 2 hours prior to infection.
- Infect cells w/ 90ifu/cell.
- Three hours post-infection add 1% FBS (to help minimize cell death).

Day 4: Cell Treatment and Ral Assay

1. Prepare G-protein Buffer with protease inhibitors (See Below).
2. On ice, wash plates 1X with ice cold PBS.
3. Lyse cells in 750 µl G-protein Buffer and scrape into eppendorf tubes.
4. Incubate on ice for 15 min.
5. Clear lysates by centrifugation @ 10,000 rpm for 10 min @ 4°C.
6. Transfer supernatant to a fresh eppendorf tube.
7. Perform Lowry Protein Assay and aliquot 500 to 650µg of each sample to a fresh tube for the G-protein Activation Assay.
8. Add 40 µl of GST-RalBP1-BD or GST-Raf-RBD pre-coupled beads to the aliquoted protein (See Protocol for Pre-coupling Below).
9. Incubate with gentle agitation in cold room for 1 hour.
10. Wash beads 4X with 1 ml G-protein Buffer.
11. Resuspend beads in 30 µl loading dye (21µl G-protein Buffer + 7.5µl XT loading dye + 1.5µl reducing agent).

    Samples can be stored @ -20°C or experiment continued:

12. Boil samples, spin down beads and run 30 µl on 12% SDS-PAGE.
13. Transfer to PVDF membrane and probe with monoclonal anti-Ral A (Transduction Labs) or monoclonal anti-Ras (BD Bioscience), respectively.

Pre-coupling GST-RalBP1-BD or GST-Raf-RBD to Glutathione Beads:

Modified from Dr. Ginell Post's protocol by LA on 1-27-05

1. Wash GSH-glutathione beads (Pharmacia): Shake the bottle to resuspend the mix. Pipette 1 ml into 15 ml conical tube. Sediment beads by centrifugation @ 2000 rpm for 30 sec. Wash beads 2X with 2 ml ice cold G-protein Buffer.
2. Resuspend in 0.75ml G-protein Buffer.
3. Mix 4µg of GST-RalBP1-BD or GST-Raf-RBD for every 1µl of washed GSH-sepharose bead slurry. Incubate with gentle rocking in cold room for 1 hr. Sediment beads by centrifugation 2000 rpm for 30 sec.
4. Wash beads 5X with ice cold G-protein Buffer.
5. Resuspend in 0.5µl G-protein Buffer for every 1µl of bead slurry incubated with GST-RalBP1-BD or GST-Raf-RBD. Store @ 4°C. Beads are now, approximately, 4µg/µl. Use 40µl per sample.

   GST-RalBP1-BD from Ginell Post's lab in the -70° is aliquoted at 250 µg/tube.

G. Immunoprecipitation (IP) to assess pTyr on IR-β

pTyr = phosphorylated tyrosine residues

Use 6 wells of a 6-well plate or a $10cm^2$ plate for each treatment because a minimum of 500μg (recommended by Upstate) of protein is required for IP.

Collecting Cell Lysates (24 hours post-infection):

- Treat cells with 100nM insulin for 3 minutes or leave untreated as control.
- Aspirate media and rinse cells with ice-cold PBS.
- Aspirate PBS and add 600μl/plate ice-cold 1X **RIPA** Lysis Buffer containing protease and phosphatase inhibitors.
- Allow plate to sit on ice for 2 - 3min.
- Scrape cells, transfer to eppendorf tube, incubate on ice for 1 hour, and sonicate (on ice).
- Centrifuge @ 10,000rpm for 5 min @ 4^0C; transfer supernatant to a fresh tube, perform Lowry protein assay (with fresh standards) and begin IP.

Immunoprecipitation Using Anti-pTyr Agarose Conjugate (Cell Signaling #9419 – stored @ -20°C):

- Before IP, aliquot **500μg (minimum)** of cell lysate (at a concentration of 1μg/1μl) to a fresh centrifuge tube.
- Resuspend beads to a 50% slurry by gentle inversion or pipette. (Placing on ice for 5min will lower buffer viscosity.)
- Add 1μl of the 50% slurry of Anti-pTyr Agarose Conjugate for every 10μl of cell lysate.
- Gently rock the reaction mixture @ 4^0C overnight.

The following day: Collect agarose beads by pulsing (45 seconds in the microcentrifuge @ 2,500rpm @ 4^0C) and remove the supernatant.
Save supernatant for immunoblotting control.

- Wash the beads 3X with ice-cold RIPA buffer.
- Resuspend the agarose beads in 30μl 2X electrophoresis sample buffer (21λ RIPA Buffer + 9λ Dye) and boil for immediate analysis via SDS-PAGE and immunoblotting.
- Immunoblot for IR-β and p-Tyr.
- Whole Cell Lysates: immunoblot for IR-β, pERK, tERK, pAkt, tAkt, Rlf, and loading control (Tubulin or Actin).

H. Immunostaining NRVMs

Detection of: HA-Rgl2, Wheat Germ Agglutinin (WGA), and DAPI in NRVMs infected with AdRgl2 or AdNull

1. Wash 2x 2 min with 1.0 mL warm Serum Free DMEM+P/S without phenol red.
2. Fix with PFA, add 1.0 mL/well of *2 chambered slide* and incubate 30 min at room temperature.
3. Pour off PFA, wash 1x 5 min with warm Serun Free DMEM, 1.0 mL/well.
4. Permeabilize the cells: 0.1% Triton X-100 in PBS, incubate for 8 min. (mix 5mL 0.2% Triton X-100 with 5ml PBS).
5. Wash 1x 5 min with 1.0mL warm Serum Free DMEM.
6. Block with 1% BSA in wash solution for 30 min (.25 grams in 25mL DMEM).
7. For HA-tag: dilute 1:200, incubate 60 min at RT (25µL in 5mL DMEM w/ BSA) (.80mL/well).
    - Wash once with DMEM.
    - **In the dark**, add 2ºAb: Alexa Fluor 568 Goat anti-rabbit IgG (red) for 30 min, at 5µl/ml dilution (25µL in 5mL). To this, add WGA (green) at 1:100 (50µL in 5mL).
8. Wash 1x 5 min with 0.5 mL warm Serum Free DMEM without phenol red.
9. Add 0.8 ml of DAPI nuclear stain (blue) to each chamber, and incubate for 5 min. (2uL in 6 mL).
10. Wash 2x 5 min with 1.4 mL warm Serum Free DMEM without phenol red.
11. Keep moist, remove chambers, add 25uL of mowiol nonfluorescent mounting media to each well, mount clean coverslip.
12. Store level at 4°C overnight in the dark and cold.
13. View with confocal.

I. Criterion Western Blotting

1. Turn heater on to 100°C and prepare **1x Transfer Buffer**:
   - 800mL dH20
   - 100mL 10X Transfer Buffer
   - 100mL MeOH
     Chill to 4°C

2. Prepare **1X MOPS Running buffer** :
   - 950mL dH2O
   - 50mL 20X MOPS Buffer

3. How much XT Sample Dye / MBST-OG / RIPA / Pull Down Lysis Buffer were the lysates collected in? ______________

4. Obtain 12% Criterion Tris gel (Exp. Date:________) and rinse with water. Then remove comb and tape at bottom of gel and place in chamber -Add 1X MOPS Running Buffer.

   pre-run 15 min-150V - Current:______________

5. Load sample: 30µL max /lane

Run 150-200V:

___150___ V ____10____ min ____________amps

___200___ V ____50____ min ____________amps

TRANSFER:

1. Wet Immobilon PVDF membrane in methanol and filter papers in 1X Transfer Buffer.

2. Wet everything in 1X Transfer Buffer before adding to sandwich.

3. Prepare sandwich black-filter-gel-pvdf-filter-red

4. place in chamber black side to black, red to red

5. Fill chamber with ice packet and transfer buffer with stirbar - Add ice tray to bottom and run 100V for 35 min changing ice as needed. KEEP COLD.
   Current:_____________________amps

6. Allow PVDF to dry a minimum of 15 minutes after rinsing with methonal.
7. Block with 5% BSA in TBS/Tween (2g BSA/40mLTBS/T) for at least 1 hour – or dry overnight

8. Incubate with 1° Ab OVERNIGHT- 4°C – or the next day.

J. Transfection of HEK-293 Cells

Record the date and purpose of the experiment.

Cell Plating:

Use 3 wells (in 6-well plates) for each transfection.

Typically need a minimum of 2 x 6-well plates of HEK-293 cells plated @ 0.2 x 10^6 cells/well.

Transfection (Typically 2 days post-plating):

The cells are ~50% confluent (50-70% is recommended).

_Trans_IT-293 Reagent/DNA Complex Formation:

- In a sterile, plastic 12 x 75mm tube, add 57.6µl of *Trans*IT-293 Transfection Reagent (2-12µl / µg of DNA = 18µl x 3.2 wells) dropwise to 640µl of serum free media – do 1 tube for each plasmid.
- Mix thoroughly by gentle pipetting.
- Incubate @ RT for 20 minutes.
- Add 3µg (x 3.2 wells = 9.6µg) pMT2 DNA to tube "1", 3µg (x 3.2 wells = 9.6µg) HA-Rgl2(wt) DNA to tube "2", and 3µg (x 3.2 wells = 9.6µg) HA-RalV23 DNA to tube "3".
- Mix thoroughly by gentle pipetting.
- Incubate @ RT for 20 minutes.

Tube	**Serum Free Media/well**	*Trans*IT-293 Transfection Reagent/well	**DNA/well**	**DNA volume**
1	200µl	18µl	3µg pMT2	3.5µl
2	200µl	18µl	3µg HA-Rgl2 (wt)	6.2µl
3	200µl	18µl	3µg HA-RalV23	5.1µl

*****Everything was multiplied by 0.2x what was needed to ensure that the correct volume of transfection mix was added to each well.**

- Add 200µl *Trans*IT-293 Reagent/DNA complex mixture prepared above dropwise to the cells and gently rock dish side to side to distribute complexes evenly.
- Incubate ~ 48 hours.

Treat Transfected HEKs with Agonists 48hrs Post Transfection:
*****Serum Starve for 4 hrs prior to agonist treatment and lysate collection**

- Use non-dilute agonist (straight from STOCK tube).
- 100μM Insulin Stock made in .01N HCl by LA

ID	Agonist	Volume Added	Length of Insulin Stimulation	Agonist Add Time
1	Ctrl	X	N/A	0:00
2	100nM Ins	2λ	5min	0:05
3	100nM Ins	2λ	30min	0:30

A = pMT2; B = Rlf; C = RalV23

Collecting Cell Lysates:

- Place cell plates on ice.
- Aspirate media and rinse cells with ice-cold PBS.
- Aspirate PBS and add 150μl/well ice-cold 1X **MBST/OG Lysis Buffer** containing protease and **phosphatase** inhibitors.
- Allow plate to sit on ice for 2 minutes.
- Scrape cells, transfer to eppendorf tube, and incubate on ice for 30 minutes.
- Centrifuge @ 13,000rpm for 10 min @ 4^0C.
- Transfer supernatant to a fresh tube and perform Lowry protein assay.
- Verify expression of transfected protein and assess changes in insulin signaling via western blot.

Notes:

The Mirus protocol for transfecting HEK-293 cells can be modified. Their protocol is setup for transfection of cells plated in 35mm diameter wells. However, if we have plated the cells in 75cm^2 area flasks, we must scale up the protocol by 7.8 due to the following math:

35mm diameter = 17.5mm radius
Area of a circle = πr^2
Plating area of 35mm diameter well = $\pi(17.5)^2$ = 962mm^2 = 9.62cm^2

75cm^2/9.62cm^2 = 7.8

The 75cm^2 flasks have a plating area that is 7.8x larger than the wells in the protocol, therefore, all volumes in the protocol were multiplied by 7.8.

SECTION VII. VITA

Leah Allen

Date of Birth: September 11, 1980

Birthplace: Murray, KY

Education

Bachelor of Science *2003*
University of Kentucky; Lexington, KY
Biological Sciences

High School Graduate *1998*
Nelson County High School; Bardstown, KY
Honors

Honors & Awards

Kentucky Young Scientist Summer Research Fellowship (KYSS) *Summer 2001*
University of Kentucky; Dr. Ginell Post's Lab

Undergraduate Research Program in Pharmaceutical Science *Summer 2002*
University of Kentucky; Dr. Ginell Post's Lab

ASPET Travel Award *Spring 2006*
Experimental Biology Conference 2006
San Francisco, CA

American Heart Association Pre-doctoral Fellowship *July 2006 – June 2008*
Ohio Valley Affiliate #0615085B

Professional Memberships

American Heart Association *2004 - 2006*
American Society for Pharmacology and Experimental Therapeutics (ASPET) *2005 - 2006*

Community Service & Volunteer Work

Pharmacology Laboratory *Fall 1999 – Spring 2000*
University of Kentucky
Dr. Myron Jacobson, Pharmaceutical Sciences
Objective: To develop laboratory skills including pipette use and protein assays.

Pharmacology Laboratory *Fall 2000 – Spring 2001*
University of Kentucky
Dr. Ginell Post, Pharmaceutical Sciences
Objective: To further my development of laboratory skills including protein assays, western blotting, and tissue culture.

"Girls in Science" Mentor *2004 - 2006*
University of Kentucky
Program Coordinator: Sondra Floyd, Behavioral Sciences
Objective: Encourage middle school girls to pursue careers in science.

Science Fair Judge, *Lexington, KY* *2004 - 2005*
Glendover Elementary School

Science Fair Judge, *Lexington, KY* *2006 - 2008*
Fayette County Science Fair

"Winged Women" Member, *Lexington, Kentucky* *2006 - Present*
Coordinator: Fran Morris Mandel
Objective: Make beaded women with wings that are sold to raise money for local women's and children's charities.

Science Fair Judge, *Eastern Kentucky University* *2007 - 2008*
Kentucky State Science Fair

Experience

Pharmacology Laboratory, *University of KY* *May 2001 – June 2003*
Laboratory Assistant
Dr. Ginell Post, Pharmaceutical Sciences

BIO 151, *University of Kentucky* *Spring 2003*
Teaching Assistant
Dr. Alma Ferrier, Biological Sciences

PHR 931, *University of Kentucky* *Fall 2003*
Teaching Assistant
Dr. Jim Pauly, Pharmaceutical Sciences

PHR 941, *University of Kentucky* *Spring 2004*
Teaching Assistant
Dr. Todd Porter, Pharmaceutical Sciences

Translating Research to Youth through Information and Technology (TRY-IT!), *University of Kentucky* *Summer 2007*
Instructor
Sondra Floyd, Behavioral Sciences
NIH Grant; Science Education Partnership
Award #1R25RR023304-01

BIO 139, *Kentucky Community and Tech. College System* *Fall 2007*
Adjunct Faculty
Dr. Deborah Sullivan-Davis & Dr. Jean Jackson,
Biological Sciences

Translating Research to Youth through Information and Technology (TRY-IT!), *University of Kentucky* *Summer 2008*
Instructor
Stacie Wojciechowski, Behavioral Sciences
NIH Grant; Science Education Partnership
Award #1R25RR023304-01

Research Activities

Presentations:

- *Fall 2004 Poster Session*, Gill Heart Institute Cardiovascular Research Day "The Ras-interacting Protein Rlf Specifically Enhances Insulin Induced AKT Phosphorylation in Cardiomyocytes"
- *Fall 2005 Poster Session*, Gill Heart Institute Cardiovascular Research Day "The Ras-interacting Protein Rlf Regulates Insulin Signaling in Cardiomyocytes"
- *Spring 2006 Poster Session*, Experimental Biology Conference "The Ras Interacting Protein Rlf Selectively Regulates Insulin Signaling in Cardiomyocytes"
- *Fall 2006 Poster Session*, Gill Heart Institute Cardiovascular Research Day "The Ras-interacting Protein Rlf Enhances Insulin-mediated Cardioprotective Signaling"

- *Fall 2007 Poster Session*, Gill Heart Institute Cardiovascular Research Day “Rgl2 differentially regulates insulin signaling in cardiomyocytes and selectively restores PI3-kinase-Akt activation in insulin-desensitized cardiomyocytes”

Abstracts (for unpublished work):

- Post, G.R., Swiderski, C., **Allen, L.**, Webb, N., Wolthius, R.M.F., and Mochizuki, N.
  Ral Guanine Nucleotide Exchange Factor-mediated signaling in neonatal rat ventricular myocytes (2001) Gill Heart Institute Research Day, Lexington, KY.
- **Allen-Klee, L.**, Post, G.R., and Post, S.R.
  The Ras-interacting Protein Rlf Specifically Enhances Insulin Induced AKT Phosphorylation in Cardiomyocytes (2004) Gill Heart Institute Research Day, Lexington, KY.
- Scotland, R., **Allen-Klee, L.**, Post, G., and Post, S.
  The Ras Interacting Protein Rlf Differentially Regulates Hypertrophic Signaling Pathways in Cardiomyocytes (2004) Gill Heart Institute Research Day, Lexington, KY.
- Scotland, R., **Allen-Klee, L.**, Post, G., and Post, S.
  The Ras Interacting Protein Rlf Differentially Regulates Hypertrophic Signaling Pathways in Cardiomyocytes (2005) 2nd Annual Symposium of the AHA Council on Basic Cardiovascular Sciences-Targeting Heart Failure, Keystone, CO.
- **Allen-Klee, L.**, Post, G.R., and Post, S.R.
  The Ras Interacting Protein Rlf Regulates Insulin Signaling in Cardiomyocytes (2005) Gill Heart Institute Research Day, Lexington, KY.
- Scotland, R., **Allen-Klee, L.**, Post, G., and Post, S.
  The Ras Effector Rlf Protects from Maladaptive Hypertrophic Signaling (2005) Gill Heart Institute Research Day, Lexington, KY.
- Scotland, R.L., Schroder, E.A., **Allen-Klee, L.**, Satin, J., Post, G.R., and Post, S.R.
  The Ras Interacting Protein Rlf Differentially Regulates Hypertrophic Signaling Pathways in Cardiomyocytes (2005) American Heart Association Scientific Sessions, Dallas, TX.
- **Allen-Klee, L.**, Post, G.R., and Post, S.R.
  The Ras Interacting Protein Rlf Selectively Regulates Insulin Signaling in Cardiomyocytes (2006) American Society of Pharmacology and Experimental Therapeutics Experimental Biology, San Francisco, CA.
- Scotland, R.L., Schroder, E.A., **Allen-Klee, L.**, Satin, J., Post, G.R., and Post, S.R. Inhibition of Maladaptive Cardiac Hypertrophy by the Ras Effector Protein Rlf (2006) American

Society of Pharmacology and Experimental Therapeutics Experimental Biology, San Francisco, CA.

- **Allen, L.**, Blunt, B.C., Post, G.R., and Post, S.R.
  The Ras-interacting Protein Rlf Enhances Insulin-mediated Cardioprotective Signaling (2006) Gill Heart Institute Research Day, Lexington, KY.
- **Allen, L.**, Blunt, B.C., Post, G.R., and Post, S.R.
  Rgl2 differentially regulates insulin signaling in cardiomyocytes and selectively restores PI3-kinase-Akt activation in insulin-desensitized cardiomyocytes (2007) Gill Heart Institute Research Day, Lexington, KY.
- Blunt, B.C., **Allen, L.**, Scotland, R.L., Post, G.R., and Post, S.R.
  The Ras-interacting protein Rgl2 reduces apoptosis in cardiomyocytes (2007) Gill Heart Institute Research Day, Lexington, KY.

Publications:

- Blunt, B.C., Scotland, R.L., **Allen, L.**, Post, G.R., and Post, S.R.
  The Ras-interacting protein Rgl2 differentially regulates kinase activation and reduces apoptosis in cardiomyocytes – *In Progress*
- **Allen, L.**, Blunt, B.C., Post, G.R., and Post, S.R.
  Rgl2 selectively regulates receptor tyrosine kinase signaling in cardiomyocytes. – *In Progress*